UNIVERSITA' DEGLI STUDI DI NAPOLI FEDERICO II

PhD in

MODEL ORGANISMS IN BIOMEDICAL AND VETERINARY RESEARCH

XXVII CICLO

PhD THESIS

Study of evolution, expression and function of Nitric Oxide Synthases in the cephalochordate *Branchiostoma lanceolatum*

Coordinator:
Prof. Paolo De Girolamo

Co - Tutor:
Dr. Salvatore D'Aniello

Tutor
Prof Paolo De Girolamo

Author:
Giovanni Annona

To you

and my family

Index

Abbreviation list ..... *IV*

Abstract ..... *VIII*

Chapter 1 - Introduction *1*

1.2 The cephalochordates Amphioxus 12

1.2.1 Discovery of Amphioxus 12

1.2.2 Amphioxus a link between past and present 16

1.2.2 Phylogeny 19

1.2.3 The model system: Amphioxus 21

1.2.4 Development and larval anatomy 25

1.2.5 Larval nervous system 32

1.3 NO/NOS Amphioxus *36*

Chapter 2 - Material and Methods *40*

2.1 Animal's culture and embryos collection 41

2.1.1 Adult *B. lanceolatum* sampling 41

2.1.2 *B. lanceolatum* facility 44

2.1.3 *B. lanceolatum* spawning 45

2.1.4 Embryo collection 48

2.2 Biomolecular techniques 49

2.2.1 RNA Extraction and purification 49

2.2.2 Reverse transcription 49

2.2.3 Polymerase Chain Reaction(PCR) 50

2.2.4 DNA/RNA gel electrophoresis 50

2.2.5 Molecular Cloning 51

2.2.6 PCR colony screening 52
2.2.7 DNA sequencing 52
2.2.8 Riboprobe synthesis 53
2.2.9 Riboprobe quantification 54
2.3 Primers for WISH and qPCR design 55
2.4 Whole mount *in situ* hybridization (WISH) 56
2.5 Quantitative PCR(qPCR) 57
2.6 NO quantization: Griess assay and DAN assay 58
2.6.1 Bradford protein assay 58
2.6.3 DAN assay 58
2.6.4 Griess assay 59
2.7 NO detection: DAF-FA DA assay 60
2.8 Variation of NO endogenous levels during development 61
2.9 NOS phylogenetic analysis 62
2.9.1 Cephalochordate evolutionary study 62
2.9.2 Bony fishes and chondrichthyes evolutionary study 62
2.9.3 Sequences analysis 65
Chapter 3 - Results *66*
3.1 NOS phylogeny 67
3.1.1 Cephalochordates NOS phylogeny 67
3.1.2 Bony fishes and chondrichthyes NOS phylogeny 69
3.2 Characterization of the expression levels of NOS genes in development .. 71
3.2.1 *B. lanceolatum* NOS-A gene expression levels 71
3.2.2 *B. lanceolatum* NOS-B gene expression level 72
3.2.3 *B. lanceolatum* NOS-C gene expression levels 73
3.3 Characterization of the expression profile of NOS genes in development 74

3.3.1 *B. lanceolatum* NOS-A gene expression 74
3.3.2 *B. lanceolatum* NOS-B gene expression 74
3.3.3 *B. lanceolatum* NOS-C gene expression 75
3.3.4 *B. lanceolatum* SoxB1 gene expression 76
3.4 Endogenous NO level duringdevelopment 78
3.4.1 Griess assay 78
3.4.2 DAN assay 79
3.5 NO localization 80
3.6 Role of NO during the development 81
Chapter 4 - Discussion *83*
Conclusion *91*
Acknowledgment *93*
Collaborative project *96*
Bibliography 99

Abbreviation list

aa	Aminoacids
ADH3	Alcohol dehydrogenase class III
AP	Alkaline Phosphatase
ASSEMB	Association of European Marine Biological Laboratories
BH_4	Tetrahydrobiopterin cofactor
BR	Blocking Reagent
BSA	Bovine Serum Albumine
CaM	Calmodulin
Ca^{2+}	Calcium ion
Cys	Cysteine
cDNA	complementar DNA
CNS	Central Nervous System
DAF-FM-DA	diaminofluorophore 4-amino-5-methylamino-2′-7′-difluorofluorescein diacetate
DAN	Diamino compound 2,3-diaminonaphthalene
DC	Dorsal Compartment motoneurons
DDAH	dimethylarginine-dimethylaminohydrolase
DEPC	Diethylpyrocarbonate
DIG	Digoxigenin
DNA	Deoxyribonucleic Acid
dNTP	deoxyribose nucleoside triphosphate
ERR	Estrogen-related receptor gamma
Et-OH	Ethanol
eNOS	endothelial NOS
FAD	Flavin Adenine Dinucleotide
FMN	Flavin Mononucleotide
FSW	Filtered Sea Water
GAD	Glutamic Acid Decarboxylase

Gbx	Gastrulation brain homeobox
Gly	Glycine
GTP	Guanosine triphosphate
HB	Hybridization Buffer
Hox	Homeotic gene
iNOS	inducible NOS
LB	Luria Bertani
L-NA	L-Nω-Nitroarginine
L-NAME	L-Nω-Nitroarginine Methyl Ester
LPS	Large Paired Neurons
L-32	Ribosomal protein L32
miniprep	Plasmid DNA mini preparation
NED	N-naphthyl-ethylenediamine
NO	Nitric Oxide
NOS	Nitric Oxide Synthase
nNOS	neuronal NOS
ON	Over Night
Otx	Orthodenticle (Drosophila) homolog
PFA	Paraformaldehyde
PMC	Primary Motor Center
PNS	Peripheral nervous system
PP	Phosphate
MOPS	3-(N-morpholino)propanesulfonic acid
NADPH	nicotinamide adenine dinucleotide phosphate
NaR	Nitrate Reductase
PCR	Polymerase Chain Reaction
qPCR	Quantitative PCR

RNA	Ribonucleic acid
SA	Sulfanilamide
sGC	Soluble Guanylate Cyclase
SEM	Scanning Electron Microscopy
SoxB1	HMG transcription factor SoxB1
SZN	Stazione Zoologica Anton Dohrn
VC	Ventral Compartment motoneurons
VGAT	Vesicular GABA/Glycine transporter
VGLUT	Vesicular Glutamate Transporter
WB	Wash buffer
WS	Wash Solution
WISH	Whole mount *in situ* hybridization
Anatomy	
ap	anterior process of first somite
ba	branchial anlage
c	neurenteric canal
cv	celebral vesicle
ch	notochord
dkk	intestinal opening of the club-shaped gland
Fb	Forebrain
g	gut cavity
Hb	Hindbrain
hkk	cutaneous opening of the club-shaped gland
i	intestine
kk	the club-shaped gland
ko	first gill pouch
ld	left anterior gut diverticulum
lp	left postoral papilla
m	mouth
Mb	Midbrain

md	midventral line of intestine
mes	mesoderm
mh	ventral median line of epidermis
n	nerve chord
nc	neurocoel
np	neuropore
o	ovary
op	unpaired papilla
po	preoral pit
rp	right papilla
spc	splanchnocoel (body cavity)
s1	mesodermal somites 1
s2	mesodermal somites 2
th	endostyle
t	testis
Developmental stage	
G	Gastrula
N	Neurula
PM	Pre-mouth larva
L 3 dpf	Larva 3 days post fertilization
L 5 dpf	Larva 5days post fertilization
SA	Small Adult

Abstract

Nitric oxide (NO) is a highly reactive, diffusible gas, essential for many physiological functions including neurotransmission, learning and memory, cardiovascular homeostasis, angiogenesis, host defense through immune response, cell migration, and apoptosis.

In vertebrates, NO is produced by the enzymatic conversion of L-arginine by three distinct Nitric Oxide Synthase (NOS) that have been identified as products of different genes with distinct expression patterns, cellular localization, regulation, catalytic properties and inhibitor sensitivity.

The pathway of NO formation is one of the oldest bioregulatory systems, highly conserved in metazoan. Comparative studies in different model systems using non-vertebrate organisms, especially basal chordates, are very useful. Because it is likely that the basic primary roles will be evolutionary conserved, the chordate amphioxus is the best available stand-in for the ancestor of the vertebrates. Importantly, amphioxus has a body plan, central nervous system, circulatory system and genome that are *vertebrate-like,* but simpler. In addition, in comparison to vertebrates, amphioxus has the same spectrum of gene families, but has markedly fewer genes per family (Holland et al., 2008; Putnam et al., 2008).

This relative genomic simplicity makes amphioxus an especially favorable prospect for functional studies of signaling networks and other physiological processes.

Amphioxus has 3 NOS genes although evolutionary analysis has shown that there is no a direct relationship between the 3 amphioxus NOS and vertebrate eNOS, nNOS and iNOS genes (Andreakis et al., 2011). This indicates that, despite its high conservation, NOS evolution has also been very dynamic in some respects, with recurrent episodes of lineage-specific gene duplications. The study of amphioxus NOS will help to understand the acquisition of new functions of NOS enzymes, but also might illustrate convergent evolution events during NOS evolution.

The following thesis project is designed to accomplish the first complete and detailed study of NOS during development. Although much has been published

on NOS expression and function in many different organisms, very little is known about its role during the first stages of animal development.

Chapter 1 - Introduction

Annona Giovanni, PhD

1.1 NOS/NO evolution: structure, biosynthesis and conservation

Nitric Oxide (NO) was identified and described for the first time in 1989 and in 1992 it was entitled as the "Molecule of the year" by the journal *Science* (Koshland, 1992). In 1998 three north American scientists, Dr. Robert F. Furchgott, Dr. Louis J. Ignarro and Dr. Ferid Murad, received the Nobel Prize for Physiology and Medicine for the discovery of nitric oxide's role in the cardiovascular and nervous systems (SoRelle, 1998). In an unrelated way this researchers discovered how a colourless and odourless gas could act as a signaling molecule in crucial biological processes, such as regulation of blood pressure and maintenance of vascular tone. Twenty years later over 86.000 papers on NO were published with different aims and model organisms, from bacteria to mammals (Bryan et al., 2009). The NO is a high reactive molecule, although potentially toxic, it is involved in a wide spectrum of physiological processes. It has been proposed that NO is involved in defence mechanisms of primitive microorganisms at the time of origin of life (Feelisch and Martin, 1995) and is very well known that it is necessary in the first phases of life, as in male gametes development and for egg activation after the fertilization (Kuo et al., 2000), later in development (Gouge et al., 1998) and during the metamorphosis (Bishop and Brandhorst, 2003; Comes et al., 2007; Leise et al., 2001). NO acts as an inter- and intracellular signaling molecule in such diverse tissues as the vascular system, the immune system, and neural communication in several biological systems.

Nitric oxide is a free radical, lipophilic, diatomic gas under atmospheric conditions. Its small Stokes' radius (diffusion index) and neutral charge allows rapid membrane diffusion (Goretski and Hollocher, 1988; Stamler et al., 1992). These main properties make this molecule an extremely versatile messenger in cellular communication. NO is a retrograde neurotransmitter, it is released from the postsynaptic neuron and diffuses to the presynaptic area where it activates several targets, or it is involved in synaptic transmission (Regehr et al., 2009) (Figure 1.1).

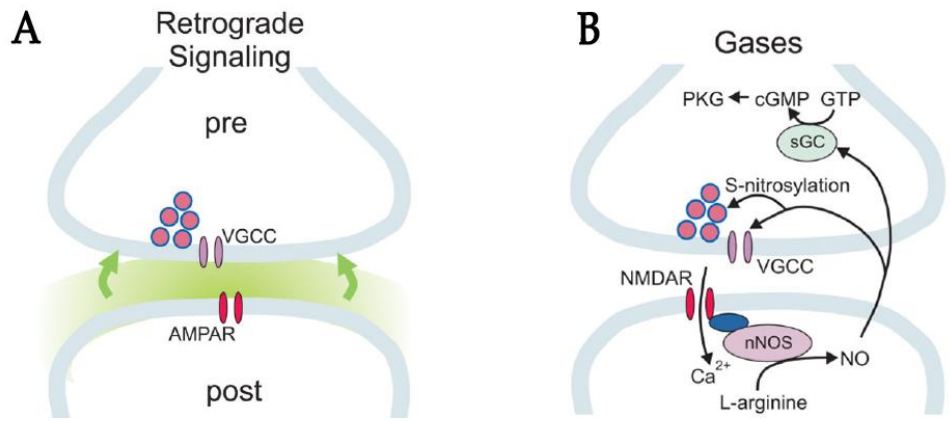

Figure 1.1 -*Representation of retrograde signaling systems. (A) General representation. (B) Retrograde signaling mediated by NO gaseous messenger (Regehr et al., 2009).*

Because of its free radical nature, NO is a very unstable molecule and its role as a direct signal mediator is limited to a short time window after its production (Martínez-Ruiz and Lamas, 2009). This signaling molecule can be involved in two different pathway indicated as "*classic*" or "*non-classic*". In the *classic* signaling the NO requires a fundamental effector molecule, which is considered its natural ligand: the soluble enzyme Guanylate Cyclase (sGC). NO induces the rupture of the His-Fe (II) bond within the heme of sGC that induces a conformational change in the His ligand (pentacoordinate NO complex), resulting in the conversion of GTP to cGMP plus Phosphate (PP) (Martínez-Ruiz and Lamas, 2009; Snyder and Bredt, 1992). This second messenger, cGMP, is involved in the regulation of several kinase proteins and in the control of ion-channels and phosphodiesterases (Ahern et al., 2002). In the *non-classic* pathway, also named "cGMP-independent", NO interact with other molecules such as oxygen, oxygen-derived free radicals, glutathione, and specific protein residues (mainly cysteine and tyrosine), producing several types of post-translational modifications in target proteins, as the S-Nitrosylation, S-Thiolation or Tyrosine Nitration (Martínez-Ruiz and Lamas, 2009) (Figure 1.2).

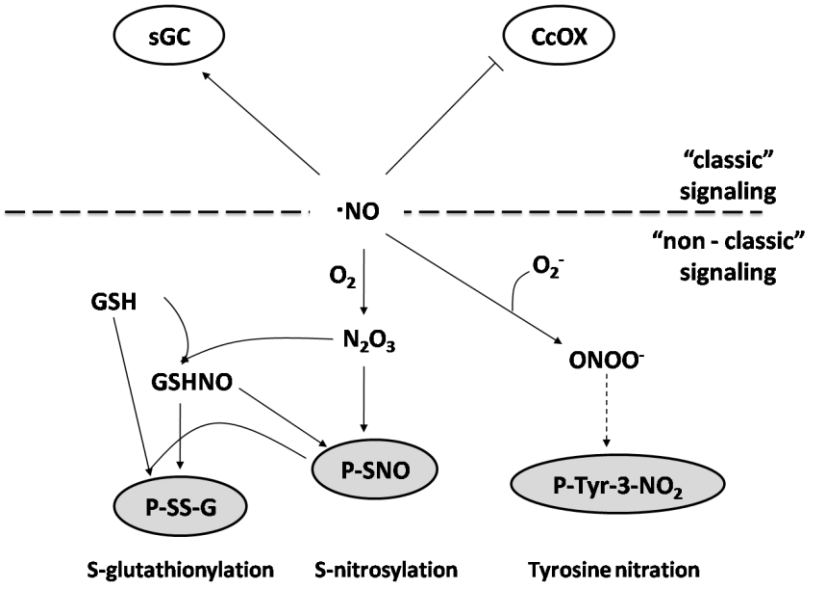

Figure 1.2 -*Direct effect of NO and indirect effect mediated by different post-traslational modifications (Martínez-Ruiz and Lamas, 2009).*

The biosynthesis of Nitric Oxide is catalysed by the Nitric Oxide Synthase (NOS) enzymes through oxidation of a guanidino nitrogen of L-Arginine to L-Citrulline. The oxidation of L-Arginine, the substrate of the reaction, occurs via two successive mono-oxygenation reactions, producing N^Ghydroxy-L-Arginine as an intermediate and NO as a secondary product (Bryan et al., 2009) (Figure 1.3). For each reaction, two moles of O_2 and 1.5 moles of nicotinamide adenine dinucleotide phosphate (NADPH), co-substrate of the reaction, are consumed per mole of NO produced (Liu and Gross, 1996).

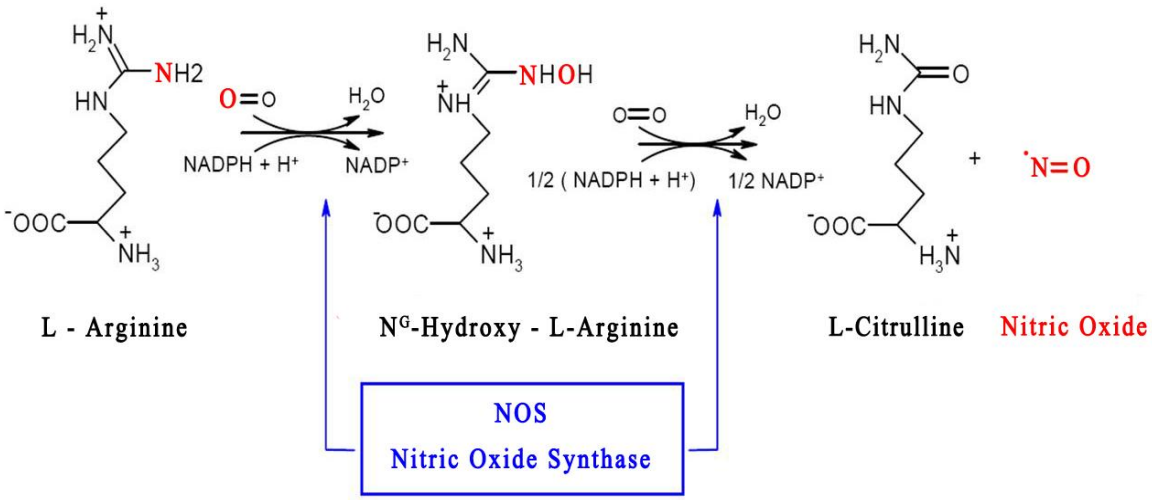

Figure 1.3 -*Biosynthesis of NO.*

The eukaryotes' NOSs are composed by the fusion of two very large monomers (133 - 161 kD), exhibiting a homodimeric structure with the C-terminal reductase domain linked to the N-terminal oxygenase domain. The reductase domain contains binding sites for the flavin adenine dinucleotide (FAD), the flavin mononucleotide (FMN) and the reduced NADPH, while the oxygenase domain contains binding site for the heme, the cofactor tetrahydrobiopterin (BH_4) and L-Arginine (Alderton et al., 2001; Andrew and Mayer, 1999) (Figure 1.4).

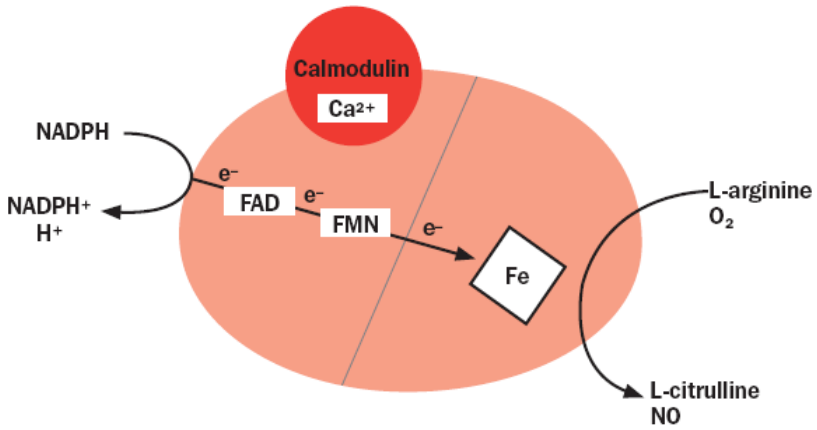

Figure 1.4 -*Nitric Oxide Synthase structure (Alderton et al., 2001).*

A functional NOS transfers electrons from NADPH, via the FAD and FMN flavins in the carboxy-terminal reductase domain, to the heme in the amino-terminal

oxygenase domain. At the heme site, the electrons are used to reduce and activate O_2 and to oxidize L-Arginine to L-Citrulline, producing NO. The two dimers are connected by a calmodulin (CaM) binding domain that enhances the electron transfer within the reductase domain (Förstermann and Sessa, 2012; Piazza et al., 2012) (Figure 1.5).

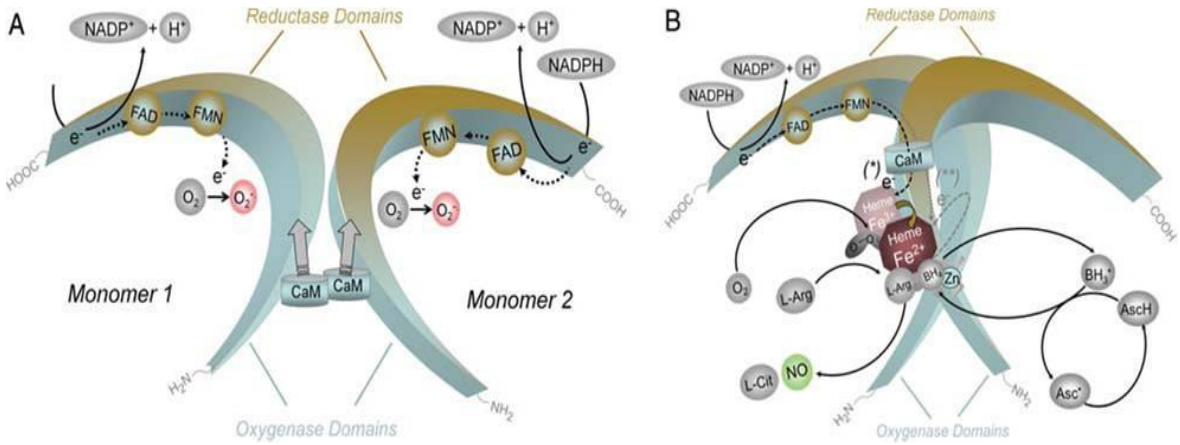

Figure 1.5 -*Structure and catalytic mechanisms of functional NOS. (A) Inactive form, (B) Functional dimers with binding of heme group (Förstermann and Sessa, 2012).*

Nitric Oxide Synthases are ubiquitous in living organisms, including bacteria (Crane et al., 2010) and plants (Crawford, 2006; Foresi et al., 2010). It is known that, during the evolution an ancestral proto-NOS was recurrently duplicated in different animal lineages, acquiring new structural configurations through gains and losses of protein motifs (Andreakis et al., 2011). In vertebrates, three distinct NOSs have been identified, showing specific expression profiles, cellular and subcellular localization, regulation, catalytic property, and inhibitor sensitivity (Alderton et al., 2001; Andreakis et al., 2011; Griffith and Stuehr, 1995). The three genes were referred to as neuronal, endothelial and macrophage inducible following the cell-type from which they were isolated for the first time (i.e. neurons, vascular endothelium, and immunoactivated macrophage cell lines). However, it is now clear that each of these enzymes is produced in more than a single cell type or tissue. Unfortunately, the nomenclature used in literature is confusing, in fact these three genes are indicated with different acronyms: nNOS,

NOS1, NOSI (for the neuronal gene), eNOS, NOS3, NosIII (forthe endothelial gene) and iNOS, NOS2, NOSII (for the inducible gene).

Neuronal NOS (nNOS) is expressed in specific neurons of the central nervous system (CNS) and peripheral nervous system (PNS). In CNS it is implicated in the neurogenesis, synaptic plasticity, learning and memory (Zhou and Zhu, 2009). In PNS structures as the spinal cord, symphatetic ganglia, peripheral nitrergic nerves, epithelial cells of various organs and vascular smooth muscle, the nNOS is involved in the control of body pressure, relaxing of the cells involved in gut peristalsis and vasodilatation (Fange, 2005; Förstermann et al., 1994; Förstermann and Sessa, 2012). The expression of the inducible NOS (iNOS), although primarily identified in macrophages, can be virtually stimulated in any cell type or tissue. It is essential for the control of intracellular bacteria or parasites, in fact the iNOS is involved in various types of inflammatory processes (Förstermann and Sessa, 2012). The product of this enzyme can directly interfere with the DNA of target cells, causing strand breaks and fragmentation (Fehsel et al., 1993; Wink et al., 1991). Endothelial NOS (eNOS), the best characterized for its actions in the vascular system, is mostly expressed in endothelial cells but has also been detected in cardiac myocytes, platelets and some neurons of the brain (Förstermann and Sessa, 2012). Nitric Oxide, derived from eNOS, is a homeostatic regulator of numerous essential cardiovascular functions, in fact it is involved in vasodilatation, inhibition of platelet aggregation and adhesion to the vascular wall (thus avoiding problems of thrombosis), control of vascular smooth muscle proliferation and inhibition of vascular inflammation (Förstermann and Sessa, 2012).

For all the three enzymes a conformational change, associated with Calmodulin binding (Calcium-modulated protein, CaM), is required for the electron transfer (Ghosh and Salerno, 2003). This link, and consequently the enzyme activity, is regulated by specific stimuli and conditions. Both neuronal and endothelial proteins are constitutively expressed. For the reversible binding of CaM it is necessary an increase in the levels of free intracellular calcium, Ca^{2+}, up to specific micromolar concentrations. Conversely, the inducible NOS, thanks to a greater

affinity, carry a permanently bound molecule of CaM, which does not dissociate even at low Ca^{2+} concentrations (Cho et al., 1992); so the iNOS expression is not regulated by intracellular $Ca^{2+}$and, in basal conditions, its activity is very low. The iNOS expression is regulated at the transcriptional level by bacterial products (for example lipopolysaccharides) or cytokines, generating high and sustained amounts of NO (Förstermann and Sessa, 2012). From a structural point of view the NOSs are very big proteins (more than 1000 aminoacids [aa]) and even though the three enzymes, show a very high degree of sequence identity among them, specific characteristics exist for each of them (Figure 1.6).

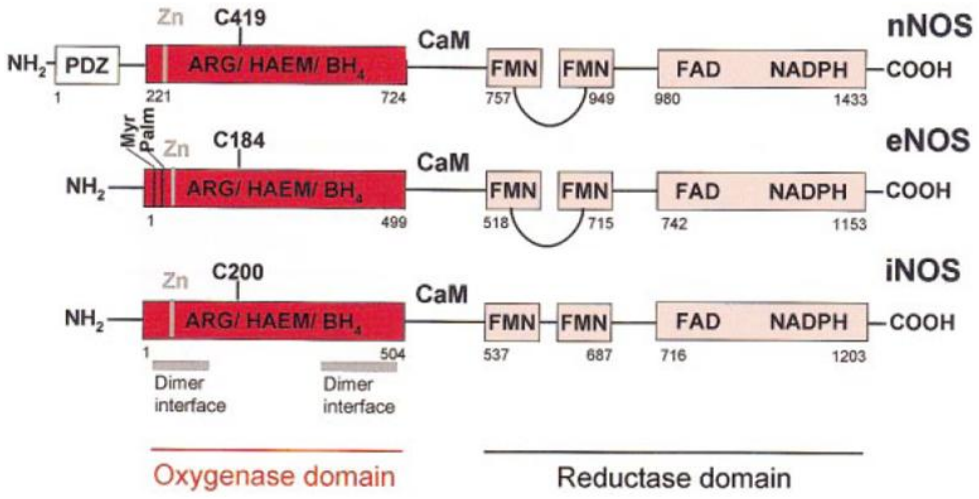

Figure 1.6 -*Human neuronal nitric oxide synthase (nNOS), endothelial NOS (eNOS) and inducible NOS (iNOS) domain structure (Alderton et al., 2001).*

The constitutive nNOS and eNOS are characterized by the presence of the so called 'autoinhibitory loop', that is responsible of the Ca^{2+} dependence interfering with the binding of CaM. This element inhibits intradomain electron transfer but at specific Ca^{2+} concentrations CaM acts by displacing the autoinhibitory element allowing the enzymatic activity (Nishida and Ortiz de Montellano, 1999). The autoinhibitory loop is about 52-55 aa long and is situated within the FMN binding domain located approximately 80 aa residues at 3' of the CaM binding sequence. The constitutive NOSs moreover show other specific characteristics. The N-terminal sequence of nNOS is approximately 300 aa longer than other NOS.

This region contains the PDZ domain that mediates specific protein-protein interactions. It is involved in the recognition and binding to the carboxyl-terminus of various proteins, as receptors or ion channels (Lee and Zheng, 2010; Stricker et al., 1997; Titheradge et al., 1998). The N-terminal sequence of eNOS, like for nNOS, serves to localize the enzyme to membranes, through two post-translational modifications: the N-myristoylation and palmitoylation. In N-myristoylation, after removal of the N-terminal methionine residue, myristic acid is attached via amide formation to the amino group of glycine in positions 2 (Gly-2) of the endothelial NOS protein. Whereas in palmitoylation, palmitic acids is added through an N-amide bond to residues of cysteine in position 15 and 26 (Cys-15 and Cys-26) of the endothelial NOS molecule. Amide linkage of N-myristoylation is highly stable and generally irreversible under physiological conditions. In contrast, palmitoylation is a reversible post-translational modification in which the fatty acid is covalently attached to protein cysteine residues by thioester formation. Myristoylation allows weak protein-protein and protein-lipid interactions and plays an essential role in membrane targeting; palmitoylation, instead, enhances the hydrophobicity of proteins, contributing to protein-membrane interactions (Robinson and Michel, 1995; Titheradge et al., 1998). As mentioned before, the NOS genes have a similar genomic structure, suggesting a common ancestral NOS gene and for long time monomeric prokaryotic gene have been considered to be the precursors of metazoan NOS, which originated during evolution by the fusion of a bacterial oxygenase domain to a reductase domain (Alderton et al., 2001). Recently, it has been reported that the NOS isolated from the bacterium *Sorangium cellulosum* contains a covalently attached unique NOS-like reductase domain, but the different arrangement of the domains in the bacterial and metazoan enzymes suggests independent events in prokaryotic and eukaryotic lineages (Agapie et al., 2009). All animal NOS genes and their protein products share several features. This conservation has been maintained over more than 800 Million of years of evolution (Gu, 1998; Wray et al., 1996), and it is currently observable at different levels. The aminoacid sequence is highly conserved, except for the N-terminal region (i.e., PDZ) and an internal segment in the FMN-binding domain (inhibitory

loop). In addition, intron positions and phases are highly preserved in animal NOS genes. At least 24 introns, in fact, are in the same position from placozoans to mammals, suggesting that these introns were already present in the ancestor NOS gene of Metazoa (Andreakis et al., 2011) (Figure 1.7).

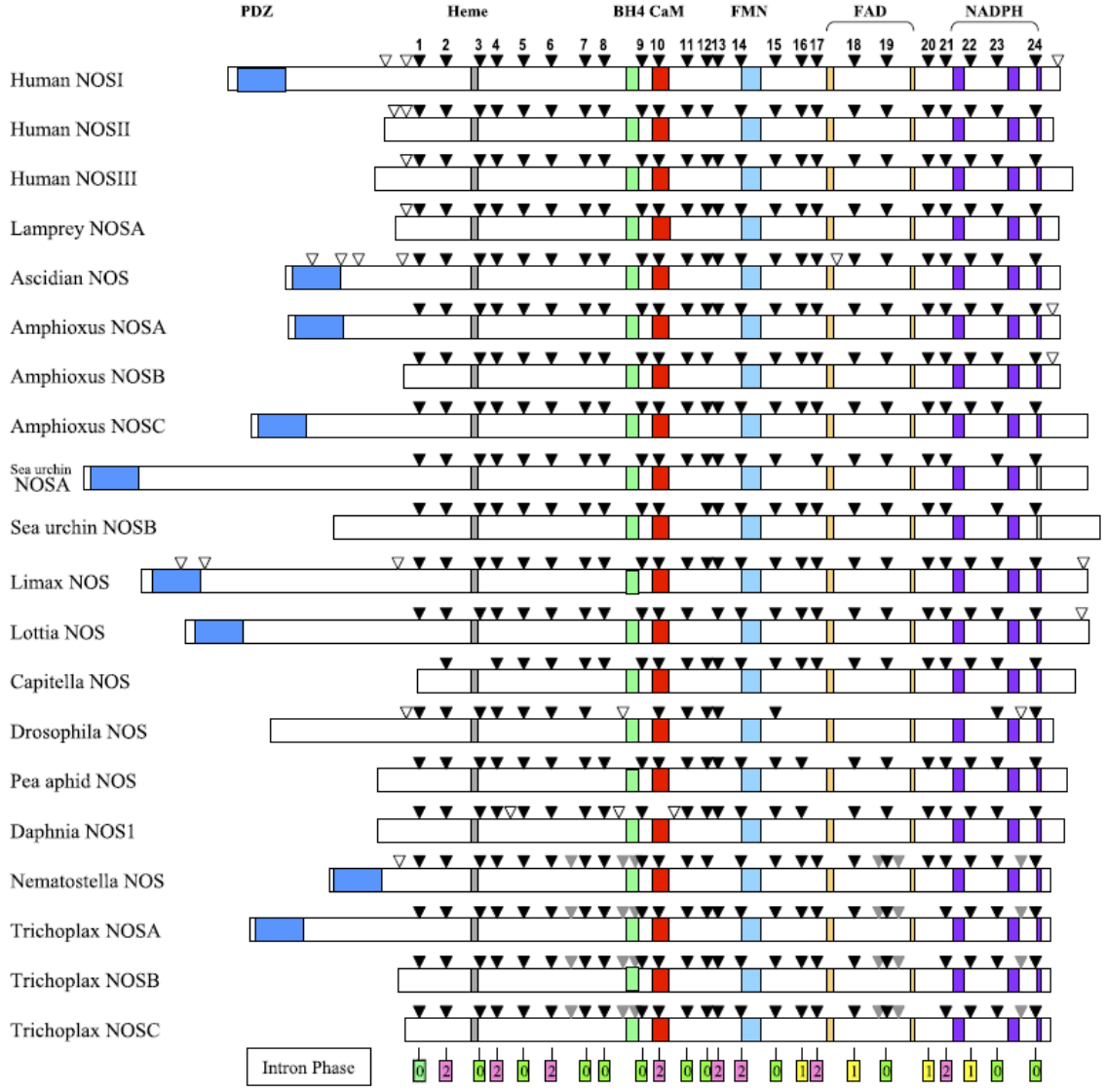

Figure 1.7 -*Schematic representation of 20 animal NOS. Functional domains in the protein are shown as colored boxes. The positions of the introns relative to the protein structure are depicted by arrowheads. Black arrowheads indicate overall conserved intron positions, numbered 1–24. Gray arrowheads denote intron positions conserved in non bilaterian phyla. White arrowheads denote lineage-specific introns (Andreakis et al., 2011).*

Table 1.1 -*Structural features of NOS from different species.*

Species	Gene Name	Gene Size[a] (kb)	Exons/ Introns	Protein (aa)	PDZ Domain	My/ Palm	Heme	BH_4	CaM	FMN	Inhibitory Loop	FAD	NADPH
Homo sapiens	*Nos*I	113.0	27/26	1434	Yes	No	Yes	Yes	Yes	Yes	Yes	Yes	Yes
	*Nos*III	20.4	26/25	1203	No	Yes	Yes	Yes	Yes	Yes	Yes	Yes	Yes
	*Nos*II	41.6	26/25	1153	No	No	Yes	Yes	Yes	Yes	No	Yes	Yes
Gallus gallus	*Nos*I	27.3	29/28	1609	Yes	No	Yes	Yes	Yes	Yes	Yes	Yes	Yes
	*Nos*II	16.8	26/25	1136	No	No	Yes	No	Yes	Yes	Yes	Yes	Yes
Anolis carolinensis	*Nos*I[b]	36.1	20/19	1354	No	No	Yes	Yes	Yes	Yes	Yes	Yes	Yes
	*Nos*III[b]	33.9	30/29	1399	No	No	Yes	Yes	Yes	Yes	Yes	Yes	Yes
	*Nos*II[b]	43.0	30/29	1232	No	No	Yes	Yes	Yes	Yes	No	—	—
Xenopus tropicalis	*Nos*I	36.4	27/26	1416	Yes	No	Yes	Yes	Yes	Yes	Yes	Yes	Yes
	*Nos*III	19.4	24/23	1107	No	—	Yes	Yes	Yes	Yes	Yes	Yes	Yes
	*Nos*II	20.6	25/24	1116	No	No	Yes	Yes	Yes	Yes	No	Yes	Yes
Danio rerio	*Nos*I	118.3	27/26	1431	Yes	No	Yes	Yes	Yes	Yes	Yes	Yes	Yes
	*Nos*IIa	12.3	22/21	1010	No	No	Yes	Yes	Yes	Yes	No	Yes	Yes
	*Nos*IIb	23.4	25/24	1077	No	Yes/No	Yes	Yes	Yes	Yes	No	Yes	Yes
Callorhinchus milii	*Nos*			304	—	—	Yes	Yes	—	—	—	—	—
Scyliorhinus canicula	*Nos*			1125	No	No	Yes	Yes	Yes	Yes	No	Yes	Yes
Squalus acanthias	*Nos*			212	—	—	—	—	Yes	Yes	Yes	—	—
Petromyzon marinus	*Nos*A	53.4	26/25	1146	No	No	Yes	Yes	Yes	Yes	Yes	Yes	Yes
	*Nos*B			589	No	Yes/No	Yes	Yes	Yes	Partial	—	—	—
Branchiostoma floridae	*Nos*A	10.2	26/25	1329	Yes	No	Yes	Yes	Yes	Yes	Yes	Yes	Yes
	*Nos*B[b]	15.2	25/24	1131	No	No	Yes	Yes	Yes	Yes	No	Yes	Yes
	*Nos*C	40.9	25/24	1441	Yes	No	Yes	Yes	Yes	Yes	Yes	Yes	Yes
Ciona intenstinalis	*Nos*			1396	Yes	No	Yes	Yes	Yes	Yes	Yes	Yes	Yes
Ciona savignyi	*Nos*[b]	27.6	30/29	1336	Yes	No	Yes	Yes	Yes	Yes	Yes	Yes	Yes
Saccoglossus kowalevskii	*Nos*			207	—	—	—	—	—	Yes	No	—	—
Strongylocentrotus	*Nos*A[b]	51.6	23/22	1729	Yes	No	Yes	Yes	Yes	Yes	Yes	Yes	Yes
purpuratus	*Nos*B[b]	28.4	23/22	1322	No	No	Yes	Yes	Yes	Yes	Yes	Yes	Yes
Aplysia californica	*Nos*			1387	No	No	Yes	Yes	Yes	Yes	Yes	Yes	Yes
	*Nos*2			1175	No	No	Yes	Yes	Yes	Yes	Yes	Yes	Yes
Lehmannia valentiana	*Nos*			1632	Yes	No	Yes	Yes	Yes	Yes	Yes	Yes	Yes
Lottia gigantea	*Nos*[b]	19.6	25/24	1558	Yes	No	Yes	Yes	Yes	Yes	Yes	Yes	Yes
Lymnaea stagnalis	*Nos*1			1153	No	No	Yes	Yes	Yes	Yes	Yes	Yes	Yes
	*Nos*2			1218	No	No	Yes	Yes	Yes	Yes	Yes	Yes	Yes
Sepia officinalis	*Nos*b			1132	No	No	Yes	Yes	Yes	Yes	Yes	Yes	Yes
Capitella capitata	*Nos*[b]	7.3	23/22	1135	No	No	Yes	Yes	Yes	Yes	Yes	Yes	Yes
Aedes aegypti	*Nos*			1112	No	No	Yes	Yes	Yes	Yes	Yes	Yes	Yes
Anopheles gambiae	*Nos*			1113	—	—	Yes	Yes	Yes	Yes	Yes	Yes	Yes
Anopheles stephensi	*Nos*			1247	No	No	Yes	Yes	Yes	Yes	Yes	Yes	Yes
Apis mellifera	*Nos*			1143	No	No	Yes	Yes	Yes	Yes	Yes	Yes	Yes
Acyrthosiphon pisum	*Nos*	71.6	24/23	1189	No	No	Yes	Yes	Yes	Yes	Yes	Yes	Yes
Bombyx mori	*Nos*			1209	No	No	Yes	Yes	Yes	Yes	Yes	Yes	Yes
	Nos-like			1097	No	No	Yes	Yes	Yes	Yes	Yes	Yes	Yes
Daphnia pulex	*Nos*1	13.3	26/25	1184	No	No	Yes	Yes	Yes	Yes	Yes	Yes	Yes
	*Nos*2[b]			1091	No	No	Yes	Yes	Yes	Yes	No	Yes	Yes
Daphnia magna	*Nos*1			1182	No	No	Yes	Yes	Yes	Yes	Yes	Yes	Yes
	*Nos*2			1083	No	No	Yes	Yes	Yes	Yes	No	Yes	Yes
Drosophila melanogaster	*Nos*			1349	No	No	Yes	Yes	Yes	Yes	Yes	Yes	Yes
Drosophila pseudoscura	*Nos*			1348	No	No	Yes	Yes	Yes	Yes	Yes	Yes	Yes
Gecarcinus lateralis	*Nos*			1199	No	No	Yes	Yes	Yes	Yes	Yes	Yes	Yes
Gryllus bimaculatus	*Nos*			1163	No	No	Yes	Yes	Yes	Yes	Yes	Yes	Yes
Luciola cruciata	*Nos*			1136	No	No	Yes	Yes	Yes	Yes	Yes	Yes	Yes
Luciola lateralis	*Nos*			1133	No	No	Yes	Yes	Yes	Yes	Yes	Yes	Yes
Manduca sexta	*Nos*			1206	No	No	Yes	Yes	Yes	Yes	Yes	Yes	Yes
Rhodnius prolixus	*Nos*			1174	No	No	Yes	Yes	Yes	Yes	Yes	Yes	Yes
Tribolium castaneum	*Nos*			1105	No	No	Yes	Yes	Yes	Yes	Yes	Yes	Yes
Discosoma striata	*Nos*			1115	No	No	Yes	Yes	Yes	Yes	No	Yes	Yes
Nematostella vectensis	*Nos*[b]	20.3	31/30	1242	Yes	No	Yes	Yes	Yes	Yes	No	Yes	Yes
Pleurobrachia pileus	*Nos*			288	—	—	—	—	—	Yes	No	Yes	—
Oscarella carmela	*Nos*			210	—	—	—	—	—	Yes	Yes	—	—
Trichoplax adhaerens	*Nos*A	8.4	30/29	1380	Yes	No	Yes	Yes	Yes	Yes	Yes	Yes	Yes
	*Nos*B	9.2	30/29	1124	No	No	Yes	Yes	Yes	Yes	Yes	Yes	Yes
	*Nos*C	9.6	30/29	1112	No	No	Yes	Yes	Yes	Yes	Yes	Yes	Yes

[a] Locus size.
[b] Predicted genes manually corrected.

Most species have a single NOS gene; in some species as *Ciona intestinalis* it appears to encode for a constitutive neuronal NOS for the presence of the PDZ (Comes et al., 2007), but other as the cnidarian *Discosoma striata* lacks the element responsible for calcium dependence typical of constitutive NOS (Moroz et al., 2007). On the other hand in the insect *Bombyx mori* posses two NOS genes, a neuronal-like and an inducible one (Imamura et al., 2002).

In tetrapods three NOS have been identified, nevertheless many bony fishes posses only one neuronal NOS (Andreakis et al., 2011; Gonzalez-Domenech and Munoz-Chapuli, 2010; Martínez-Ruiz and Lamas, 2009); it is evident that the number of NOS present in different species is not directly linked to the degree of animal complexity.

In the basal chordate amphioxus, three different NOS genes have been found, two neuronal and one inducible. Evolutionary analysis showed that there is not a direct relationship between the three amphioxus NOS and the vertebrate eNOS, nNOS and iNOS (Andreakis et al., 2011). Very few is known about the expression profile of NOS genes in this key animal and the role of NO during its development.

1.2 The cephalochordates Amphioxus

1.2.1 Discovery of Amphioxus

Amphioxus made its appearance in the scientific world for the first with Peter Simon Pallas in 1774 (Pallas, 1774). The young German zoologist in his work "*Spicilegia Zoologica, quibus novae imprimus et obscurae animalium species iconibus, descriptionibu. Tomus I*", described for the first time this animal as a gastropod mollusk, that he named "*Limax lanceolatus*", having a streamlined body plan with both ends spear-shaped, characterized by transparent body and showing internal compartmentalized musculature. Few years after the death of Pallas, amphioxus specimens have been found in several places. In Cornwall, Dr. Jonathan Couch, during one of his walks on the beach after a storm found in a small pool left by the tide a small, alive, very active, transparent animal. After a preliminary microscopy examination, Dr. Couch sent it to the expert Dr. William Yarrell in London for a deeper analysis.

In Väderöarna, a Western Sweden archipelago, several amphioxus specimens were found, by two medical students and by Dr. Sundevall (Fange, 2005). Some years later, on the same beaches, Dr. Bengt Fries found a big colony of amphioxus during his research on marine animals. Unfortunately none of these animals were never further studied (Fange, 2005).

A very big population of amphioxus was found near capo Posillipo in the north-west of the gulf of Naples (Bone, 1958; Haberling, 1924). Here amphioxus was "re-discovered" by the natural history Professor of the University of Naples Federico II, Prof. Oronzo Gabriele Costa (Costa, 1834). Prof. Costa observed a sort of vertebral column, assuming that amphioxus was not a snail but it resembled a very simple fish, belonging probably at same genus of lamprey.

In his book Prof. Costa described amphioxus as an atypical fish without eyes, nasal neither gill openings. He believed, wrongly, that the structures surrounding the mouth (oral cirri) were gills, therefore baptizing the animal as *Branchiostoma lubricum*. Two years later, in 1836, Dr. William Yarrell described for the first time the defining morphological trait of chordates, the notochord, as a flexible cartilaginous column (Yarrell, 1841) naming it *Amphioxus lanceolatus* (amphioxus

from the Greek stay for "both [ends] pointed," in reference to their shape). The scientific community, years later, adopted *Branchiostoma* (Costa) *lanceolatum* (Pallas) as the definitive name of the specie, while amphioxus is still used as a common name. In 1866, in Naples (Italy) another distinguished embryologist, Professor Alexander Kovalevsky, used amphioxus as model system in his studies (Ulett, 2010). Looking at amphioxus and ascidian embryos he identified features common to all chordates, as the notochord, dorsal nerve cord, and metameric muscle, as well as common developmental mechanisms. In fact, he was able to recognize the formation of the archenteron by invagination during amphioxus gastrulation and the development of the nerve chord from neural folds. Kovalevsky also recognized such anatomical similarities as the possession of gill slits in embryonic vertebrates and in adult amphioxus. Therefore, he classified amphioxus and ascidians as chordates, and this represent one of his most important contributions to the chordate developmental biology. A large part of these early conclusions continue to appear to be true today and our understanding that chordates develop from a bilayered gastrula can be traced to this fundamental work, which revolutionized embryology and zoology (Hecht et al., 1998). For the importance of his discoveries in the embryology field, not only in chordates, nowadays Kowalevsky is remembered within annual prize, the Alexander Kowalevsky Medal, awarded by the 147-year-old Saint Petersburg Society of Naturalists (SPSN) in Russia.

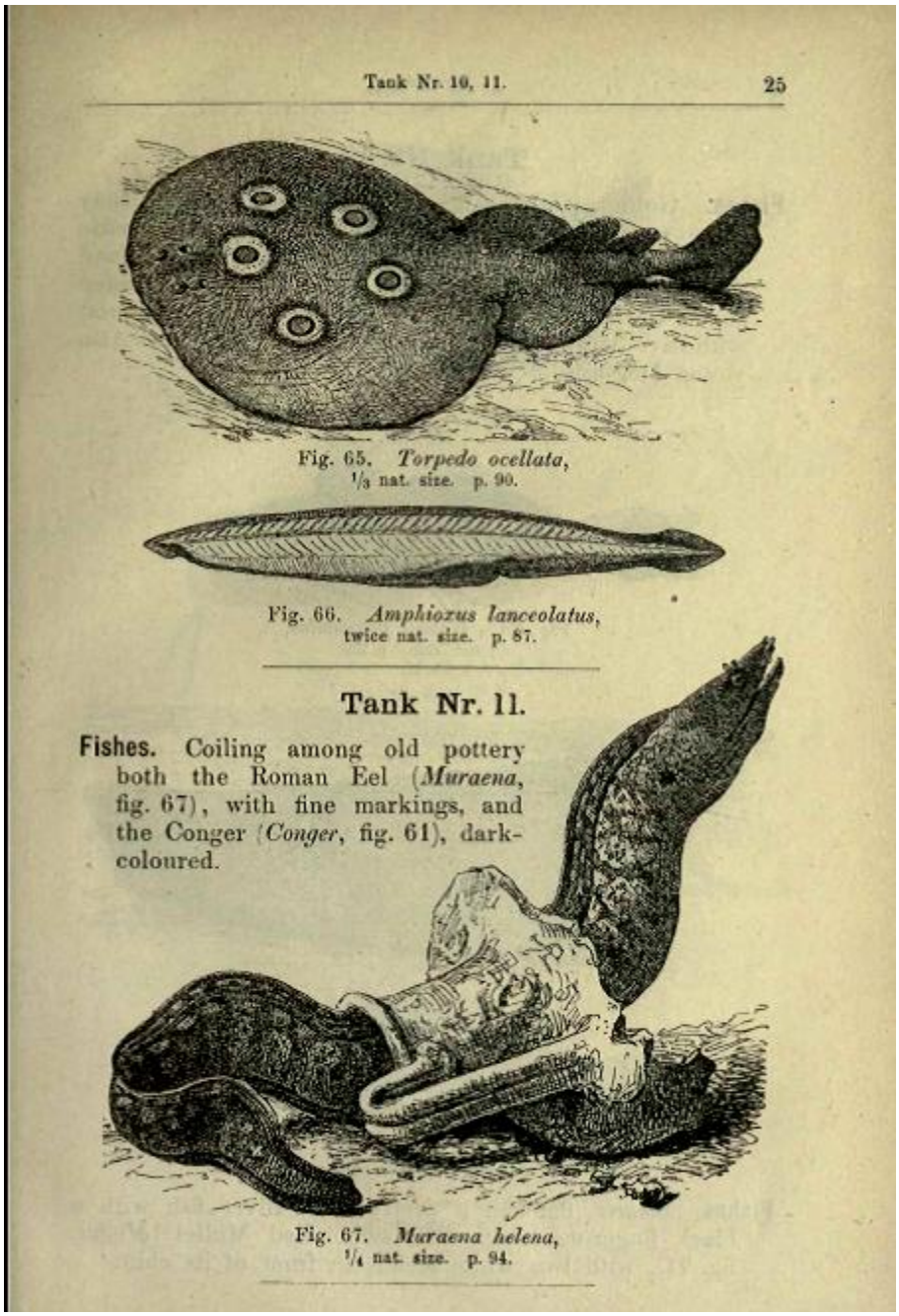

Tank Nr. 10, 11. 25

Fig. 65. *Torpedo ocellata*, 1/3 nat. size. p. 90.

Fig. 66. *Amphioxus lanceolatus*, twice nat. size. p. 87.

Tank Nr. 11.

Fishes. Coiling among old pottery both the Roman Eel (*Muraena*, fig. 67), with fine markings, and the Conger (*Conger*, fig. 61), dark-coloured.

Fig. 67. *Muraena helena*, 1/4 nat. size. p. 94.

Figure 1.8 -*A page of the "Guide to the aquarium at Zoological Station at Naples" of the 1896 in which it is reported the presences of Amphioxus specimens in the thank number 11*

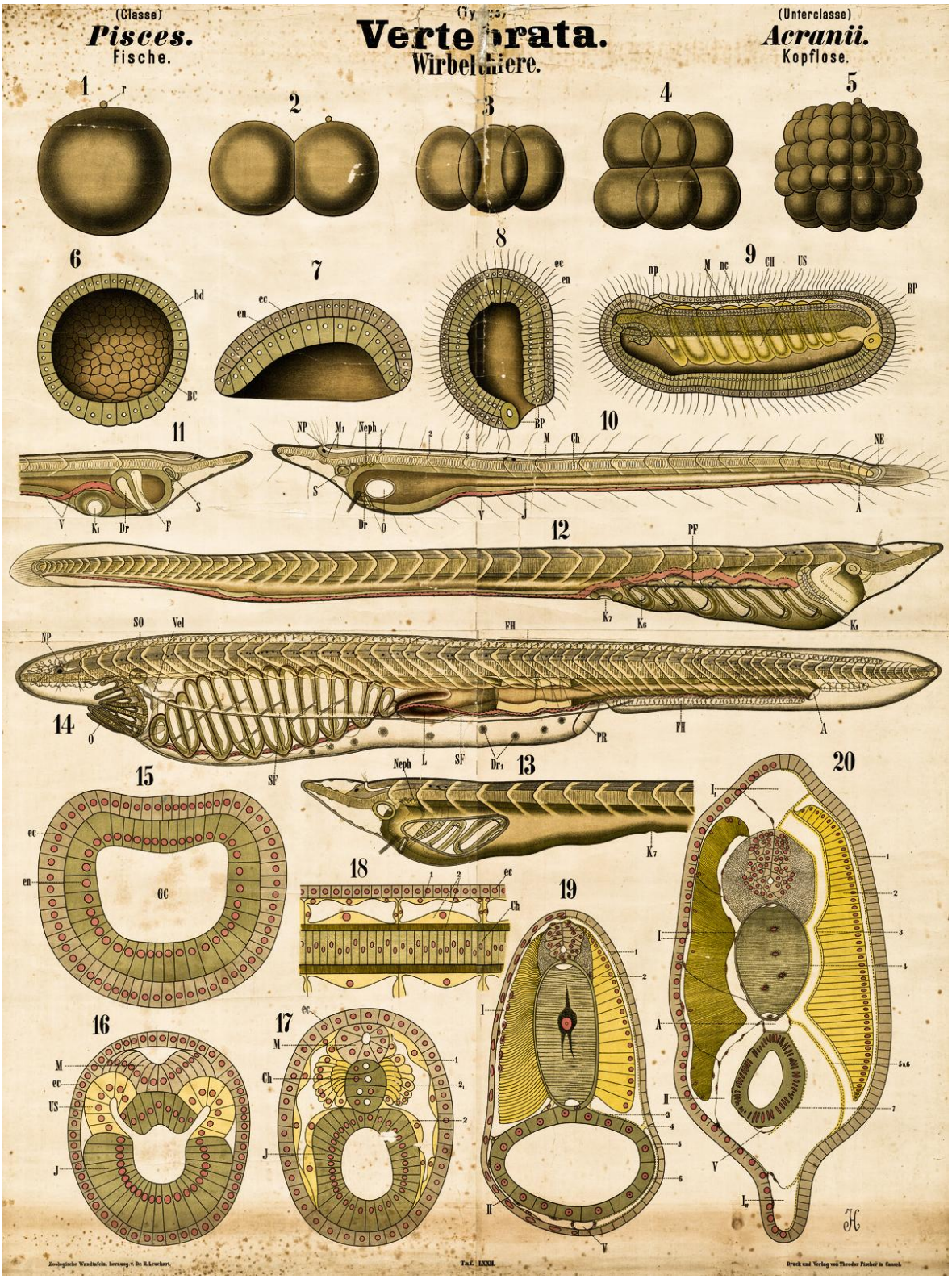

Figure 1.9 -*Wall chart from a Karl Georg Friedrich Rudolf Leuckart collection, the famous German zoologist and parasitologist (1822 - 1898). This Chart shows stages through development (1–12) with tissue derived from the ectoderm coloured grey, from the endoderm coloured grey-green and the mesoderm coloured yellow. Using the longitudinal section of the adult (14) note the four typical chordate features the pharyngeal gill slits (SF), dorsal, hollow nerve cord (starting at NP), notochord (Ch) and post-anal tail (posterior to A).*

1.2.2 Amphioxus a link between past and present

Amphioxus is called "living fossil" due to its resemblance with chordates fossil records lived in the Cambrian (Chen et al., 1995). At the same time the amphioxus adult's anatomy is considered vertebrate-like but simpler, and it occupies a key phylogenetic position for comparative and evolutionary studies in vertebrates (Yu and Holland, 2009).

The origin of chordates has long been debated and still not entirely clear. The idea that ancestral vertebrates were amphioxus-like was reinforced by the discovery in the early XX century of a fossil in the Burgess shale, Yoho national park in Canada, from the middle Cambrian, *Pikaia gracilens*, one of the oldest known chordate (Figure 1.10 A). In 2012 Morris and his collaborators on the basis of 114 available specimens reviewed the *Pikaia* anatomy's, confirming its place in the chordates group. The body of *Pikaia* is fusiform, laterally compressed and possesses about 100 myomeres. The head is small, bilobed and bears two narrow tentacles. There is no evidence for eyes. Apart from a thin dorsal fin (without fin rays) and a series of bilaterally arranged appendages with possible pharyngeal pores at the anterior end, there are no other external features. In addition to the musculature the internal anatomy includes an alimentary canal, the anterior of which forms a prominent lenticular unit that is almost invariably preserved in positive relief. The cavity is interpreted as pharyngeal, implying that the mouth itself was almost terminal. The posterior extension of the gut is unclear although the anus appears to have been terminal. The most prominent internal structure is a reflectively preserved structure, possibly hollow, termed here the dorsal organ. Although formerly interpreted as a notochord its position and size make this less likely. Its original function remains uncertain but it could represent a storage organ. Ventral to the dorsal organ is present a narrow layer of tissue that probably represent the nerve chord and notochord. In addition to these structures, there is also evidence for a vascular system, including a ventral blood vessel (Morris and Caron, 2012).

Subsequently other fossils, belonging to the Cambrian period, were discovered in Chengjiang, Cina; the four main representatives are: *Yunnanozoon*, *Haikouella*, *Haikouichthys* and *Myllokunmingia* (Donoghue and Purnell, 2009; Dzik, 1995;

Holland and Chen, 2001; Janvier, 2003; Mallatt and Chen, 2003; Morris and Caron, 2012). They show a similar body shape, elongate body and laterally compressed, but they had other specific characteristics. *Yunnanozoon* and *Haikouella* show an elongate branchial region with six gill arches and possibly sensory capsules (Holland and Chen, 2001), instead *Haikouichthys* and *Myllokunmingia* had more "vertebrate" characteristics as short branchial region composed of six filamentous gills (Holland and Chen, 2001; Janvier, 2003) and the presence of paired eyes, otic capsules and possible paired olfactory organs (Shu et al., 2003). The first of them *Yunnanozoon lividum* recorded from the early Cambrian, 525-milion-year-old, was a filter feeding animal, 25-40 mm long, with almost all the prototypic characteristics of chordates (Chen et al., 1995). Like the "modern" cephalochordates, it had an anterior pharyngeal region connected through a wide snout, tunnel-shaped, open anteriorly; the notochord runs nearly straight from the snout tip through the suprapharyngeal tissues to the posterior body tip. Segmentally arranged structures above the notochord are in accordance with musculature being divided by *myosepta* into 22-24 myomeres, this organization indicates that *Yunnanozoon lividum* undulated laterally like amphioxus; below the notochord are up to 13 paired of metameric structures, interpreted as gonads, located on the left and right sides of the body (Figure 1.10 B). Two parallel lines running longitudinally through the hypoparyngeal tissue may represent the endostyle and seven evenly spaced biramous structures are identifiable as branchial arches. These morphological characteristics suggested that *Yunnanozoon lividum*is is the ancestor of chordate but some authors described it not as a chordate but as the earliest known hemichordate (Shu et al., 1996). In spite of this wide variety of forms it is not still clear which can be the ancestor of chordate but it is quite sure that ancestor of vertebrates was cephalochordate-like, also because of wide range of common features that cephalochordates and vertebrates share. The adult anatomy of amphioxus is vertebrate-like, but simpler (Figure 1.10 C). Amphioxus possess typical chordate characters, such as a dorsal hollow neural tube and notochord, a ventral gut and a perforated pharynx with gill slits, segmented axial muscles and gonads, a postanal tail, a pronephric kidney, and

homologues of the thyroid gland and adenohypophysis (the endostyle and pre-oral pit, respectively). However, they lack typical vertebrate-specific structures, such as paired sensory organs (image-forming eyes or ears), paired appendages, neural crest cells and placodes (Bertrand and Escriva, 2011b).

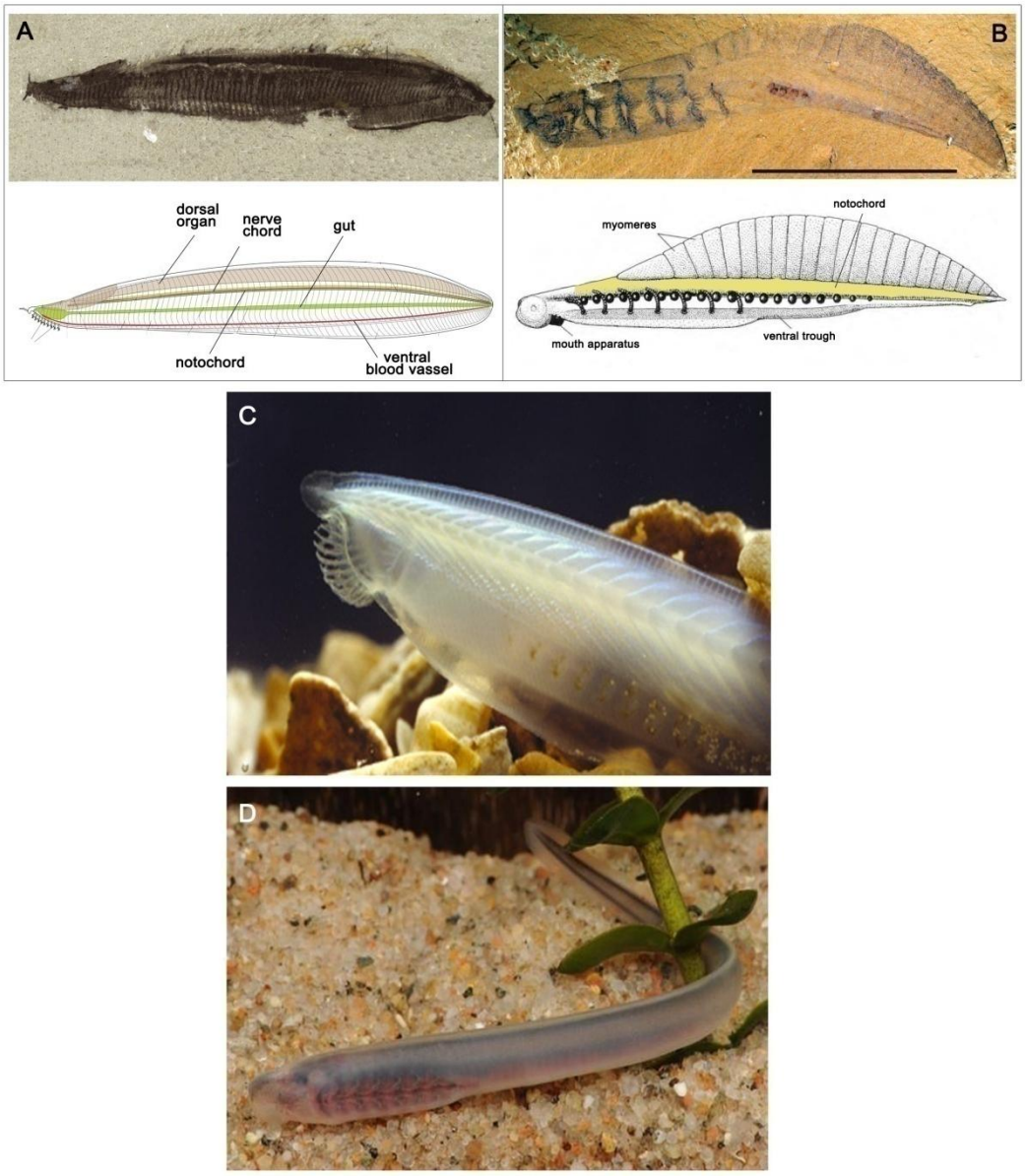

Figure 1.10 -*Cephalochordates of the past and present. (A) Fossil specimens and schematic representation of Pikaia gracilens; (B) Fossil specimens and schematic representation of Yunnanozoon lividum; (C) Rostral part of adult Amphioxus specimen; (D) Ammocoetes larva of lamprey.*

1.2.2 Phylogeny

Cephalochordates together with tunicates (appendicularians, salps and sea squirts) and vertebrates (including ciclostomes: lamprey and hagfish) constitute the three groups of chordate. Adult cephalochordates resemble a small colourless fish, without obvious anterior sense organs and, for this reason, it has been considered for long time the closest living relatives of vertebrates. Morphological similarities and an apparently increased complexity in cephalochordates and vertebrates, relatively to tunicates, improved the theory that tunicates represent the earliest chordate lineage (Hecht et al., 1987). Nevertheless, in 2006 a molecular-based study on large data set established that cephalochordates represent the most basally divergent lineage of chordates, being the sister group of tunicates and vertebrates, named as olfactores (Delsuc et al., 2006). There are only three genera of cephalochordates: *Branchiostoma* comprising about 28 species, *Epigonichthys* 1 species and *Asymmetron* 2 species (Figure 1.11). Probably additional cryptic species exist. All cephalochordates are morphologically very similar and the main difference is visible in *Asymmetrons* and *Epigonichthys* that have gonads only on the right side of the body, whereas *Branchiostomas* has symmetrical gonads (Holland and Onai, 2012; Kon et al., 2007).

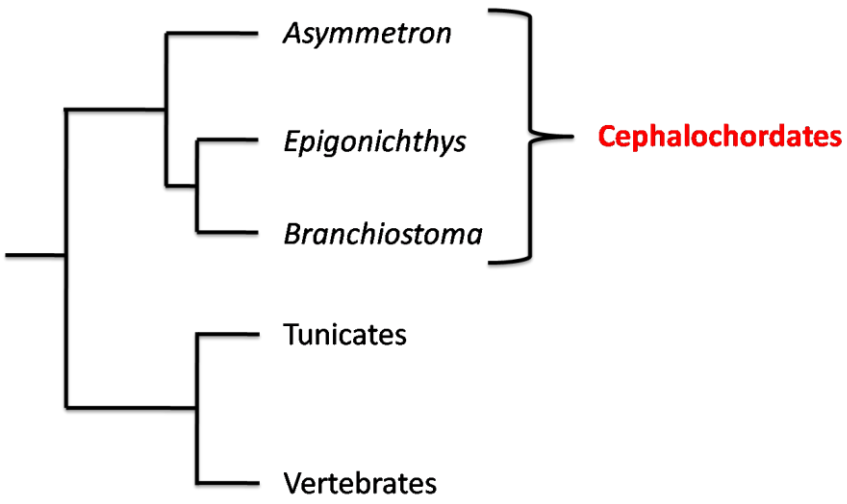

Figure 1.11 -*Phylogenetic relationships within the Chordata (Holland and Onai, 2012).*

Recently, an increasing number of researchers is studying the evolution, development and genome of *Asymmetron* and *Epigonichthys* (Holland and Holland, 2010; Kon et al., 2007; Yue et al., 2014). Nevertheless the majority of the scientific studies have focused their attention on Branchiostoma species, and in particular three of them have been extensively used until now: *Branchiostoma floridae* (Florida, USA), *Branchiostoma belcheri* (East Asia, especially China coast at Xiamen and Qingdao) and *Branchiostoma lanceolatum* (Atlantic and Mediterranean coasts of Europe) (Holland et al., 2004).

The anatomy of adult amphioxus is vertebrate-like and this simplicity can also be expanded to the amphioxus unduplicated genome structure. Two rounds of whole-genome duplication occurred at the stem of the vertebrate lineage, known as the 2R hypothesis (Ohno, 1970). Therefore amphioxus in general posses only a single paralogue (homologous genes that are derived by gene duplication from an ancestral gene) of the two to four paralogues of vertebrate genomes(Brooke et al., 1998; Canestro et al., 2007; Garcia-Fernàndez et al., 2009; Pascual-Anaya et al., 2012; Pascual-Anaya et al., 2008; Pascual-Anaya et al., 2013; Wada et al., 1999). Moreover, the 'pre-duplicative' amphioxus genome possesses one representative of all the gene families that presumably existed in the ancestor of chordates, in contrast to the situation in the two other chordate subphyla, urochordates and vertebrates, which have specifically lost different members of several gene families (e.g. the homeobox-containing genes, tyrosine kinases or nuclear receptors) (Bertrand et al., 2011a; D'Aniello et al., 2008; Takatori et al., 2008). Thus, the morphological and genomic simplicity of amphioxus, together with its key phylogenetic position, make it an invaluable animal model for understanding the invertebrate to vertebrate evolutionary transition.

1.2.3 The model system: Amphioxus

Amphioxus is called "living fossil" due to its resemblance with chordates fossil records lived in the Cambrian and shows all the prototypic characteristics of the chordate group. The dorsal cord or notochord, dorsal hollow nerve tube, a ventral gut, a perforated pharynx with gill slits, post-anal tail, segmented axial muscle and gonads, a pronephric kidney and homologues of the thyroid gland and adenohypophysis (the endostyle and pre-oral pit, respectively) (Bertrand and Escriva, 2011b) (Figure 1.12). However, they lack typical vertebrate-specific structures, such as paired sensory organs, paired appendages, neural crest cells and placodes (Schubert et al., 2006).

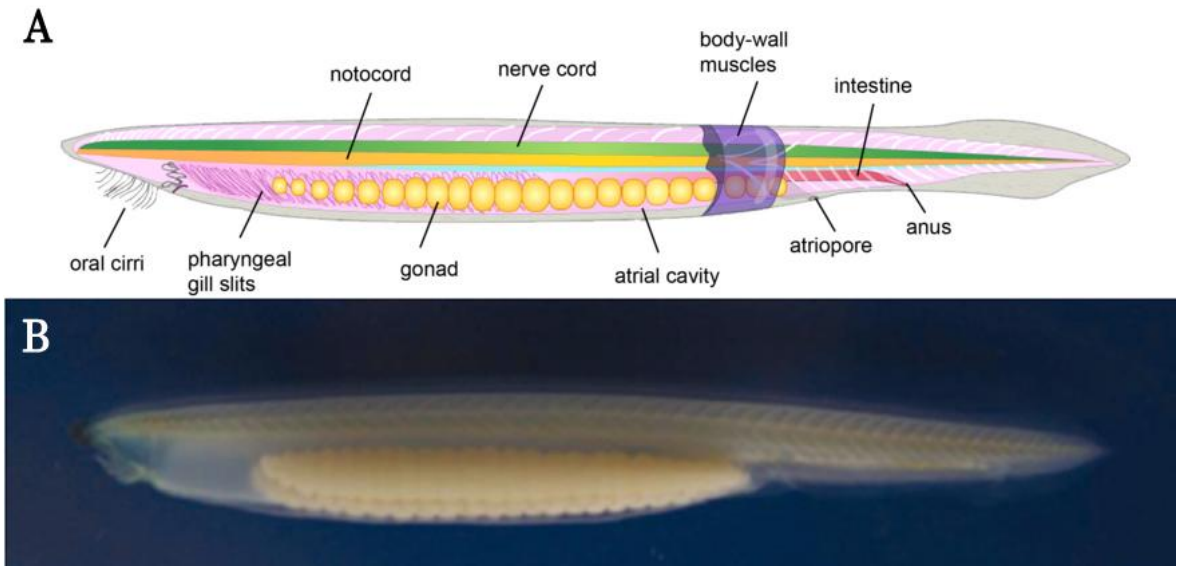

Figure 1.12 -*Mature amphioxus anatomy (A) Schematic representation (B) Adult external morphology.*

The notochord, cylindrical muscularized rod, runs dorsally along the full length of the animal, extending anteriorly beyond the end of the nerve cord (Schubert et al., 2006; Takahashi and Holland, 2004). Immediately above the notochord there is a dorsal tubular nervous system, with only a slight enlarged cerebral vesicle at its most anterior end (Lacalli, 2006). Beneath the notochord is an endodermal-derived digestive tract connected anteriorly to a pharyngeal area with gill slits and ciliated gill bars. The pharynx has a ventrally located ciliated groove or endostyle that

produces mucous needed for the filter feeding mechanisms. Posteriorly to the digestive tract there is the anal opening, beyond which occurs a short post-anal tail. The adult amphioxus posses a laterally-flattened cylindrical shape, usually not more than 6 cm in length and 0.5-1 cm in diameter. Through the transparent skin is possible to see metameric muscle structures along the body length that enable them to swim and burrow into the sand. The sexes of amphioxus are readily separable as they begin to develop their rows of testes or ovaries. Morphologically amphioxus does not show sexual dimorphism, but it is possible to distinguish males and females by observing the gonads to the stereomicroscope (Figure 1.13 and 1.14).

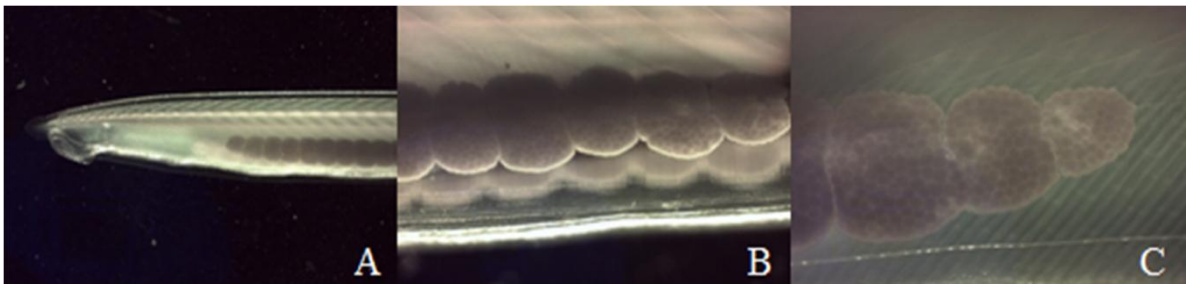

Figure 1.13 -*Female Mature gonads of B. lanceolatum. (A) Anterior part of animal body, (B) Magnification of mature gonads, (C) Higher magnification of gonads where individual eggs are recognizable.*

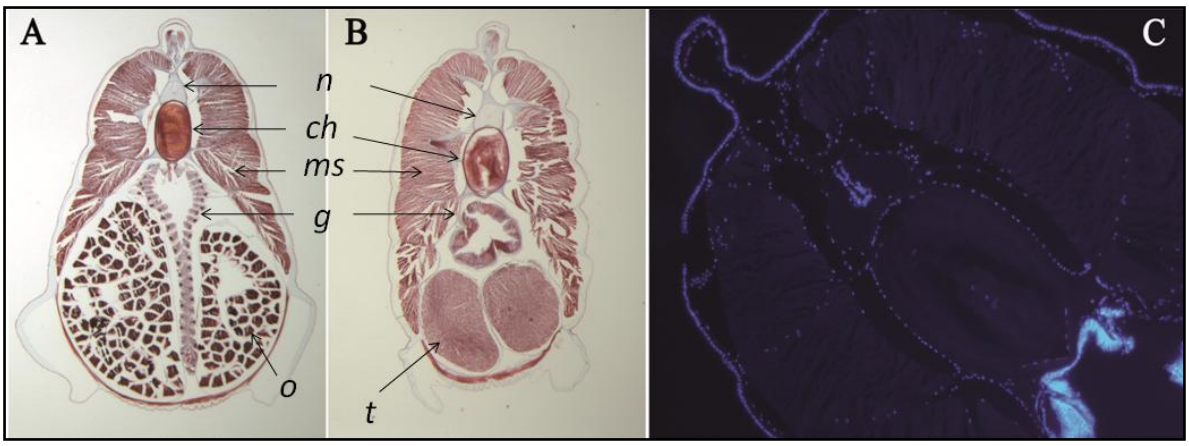

Figure 1.14 - *Adult B. lanceolatum transversal section: (A) Mature female specimen, (B) Mature male specimen. (A+B) Mallory staining, (C) Dapi staining of a transversal section of an adult specimen. Abbreviations: (n) neural tube; (ch) notochord; (ms) muscle; (g) gut; (o) ovary; (t)testis.*

All amphioxus species are filter-feeding marine animals that burrow upright in sand, gravel or shell deposits. With a protruding rostral region it feeds filtering phytoplankton through a complex, ciliated, pharyngeal apparatus. Almost all amphioxus species are found in shallow tropical or temperate waters close to the seashore from 0.5 to 40 mt deep (Adolf et al., 2006; Bertrand and Escriva, 2011b; Desdevises et al., 2011; Gosselck, 1975). Temperature and salinity of the sea water have been shown to be very important in the life cycle of some amphioxus species (Alderton et al., 2001; Webb, 1956a; Webb, 1956b; Webb and Hill, 1958). For example, the migration of amphioxus populations between winter and summer seems to be linked to temperature changes (Webb, 1971) and, a negative correlation between the presence of amphioxus and organic matter content has been noted for some species (da Silva et al., 2008; Webb and Hill, 1958). Several studies have estimated the lifespan of different amphioxus species. Studies conducted in the second half of the 1900 on *B. belcheri* and *B. lanceolatum* populations showed that amphioxus has a life span of three to six years (Chin, 1941; Courtney, 1975). More recent studies, based on different approaches, suggested that different species can have different life span but the average is between three and five years (Chen et al., 2008a; Chin, 1941; Courtney, 1975; Desdevises et al., 2011; Futch and Dwinell, 1977; Gosselck and Spittler, 1979; Nelson, 1969; Wells, 1926), and interestingly they suggest that amphioxus appear to grow continuously during their entire life span (Stokes, 1996).

Concerning the spawning behavior, all known amphioxus species spawn after the sunset during the reproductive breeding season, normally in late spring and summer. The duration of the spawning season, however, may vary between different species, but for all amphioxus it happens only once per year. The reproductive season in *B. lanceolatum*, for example, occurs for 3-4 months in spring and summer (Fuentes et al., 2007; Fuentes et al., 2004; Wu et al., 1994). Adult animals swim up to the water surface, lay their gametes in the water column and then sink gently back to the sand bottom. For all amphioxus species thousands of embryos remain planktonic until mouth metamorphosis occurs, maybe 1-3 months

after fertilization; subsequently juveniles change their habitat and migrate to the sand where they become benthic animals (Figure 1.15).

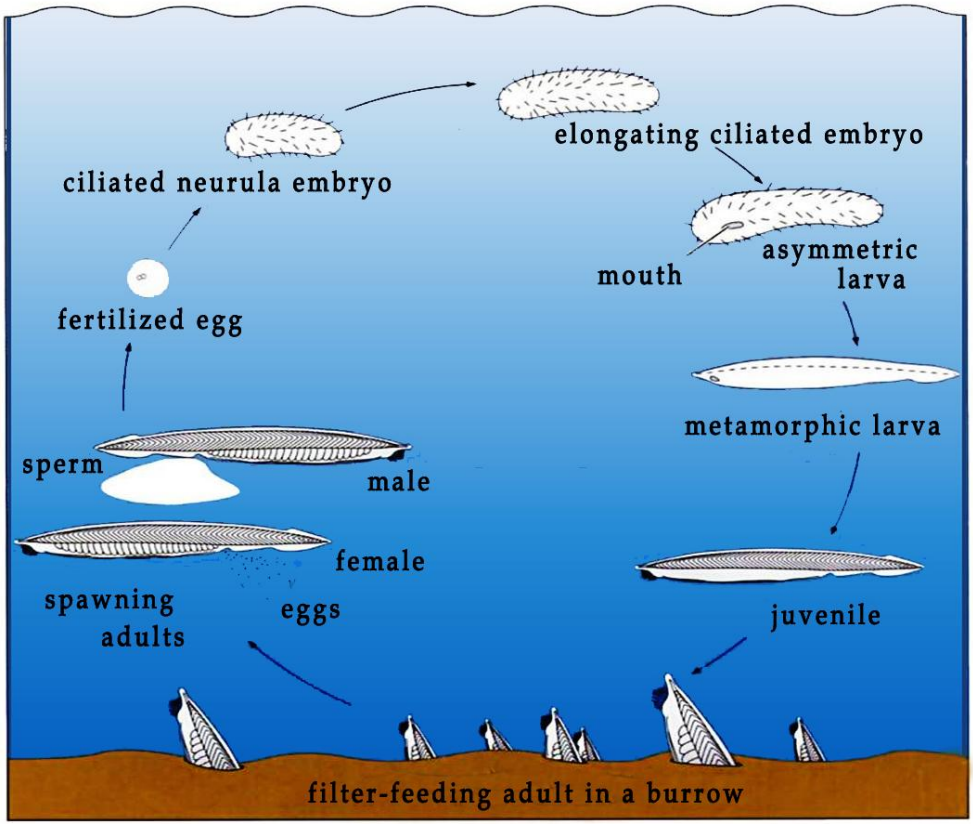

Figure 1.15- *Amphioxus life cycle.*

1.2.4 Development and larval anatomy

Early development in amphioxus resembles that of echinoderms, while later development is close to that of vertebrates (Holland et al., 2004). After Kovalevsky (Kovalevsky, 1867) other investigators, particularly Berthold Hatschek (Hatschek, 1893), William Erskine Kellicott (Kellicott, 1913) and Edwin Grant Conklin (Conklin, 1932), examined the embryology of amphioxus with ever more precision, focusing their attention on the European species *B. lanceolatum*.

Amphioxus unfertilized eggs, roundish and about 100–140 µm in diameter (Bertrand and Escriva, 2011b; Conklin, 1932), have a low yolk content (oligolecithal) and are arrested at second meiotic metaphase with the first polar body closely apposed to the vitelline layer (Holland and Onai, 2012). The eggs maturation occurs under the stimuli induced by sperm entry.

The egg segmentation is holoblastic (whole zygote) and cleavages are roughly synchronous in time through seventh cleavage (up to 128-cell stage).

The resulting hollow spherical blastula is commonly deuterostomic: consisting of a single layer of cells, cleavage is arguably radial, and the embryology is at least superficially indistinguishable from echinoderm's.

Gastrulation and neurulation first begin to demonstrate their chordate affinities (Conklin, 1932; Whittaker, 1997).

During gastrulation, after flattening of the vegetal zone cells of the blastula, an ingression (epiboly) occurs and the blastocoelic space is slowly eliminated. So the embryo becomes cap-shaped with formation of double layer of cells, an outer ectoderm and inner mesoderm, and deepened archenteron, the primitive gut cavity. During this process the embryo becomes bilaterally symmetrical quite elongated antero-posteriorly, flattened dorsally and rounded ventrally as well as anteriorly; at the postero-dorsal aspect the archenteron opens directly to the outside by a narrow blastoporal aperture.

From a fairly uniform layer of superficial cells, the non-neural ectoderm and neuroectoderm will form. Instead a layer of endodermal cells lining the archenteron, and a portion of them will give rise to the notochord (Holland and Holland, 2007; Holland and Onai, 2012) (Figure 1.16).

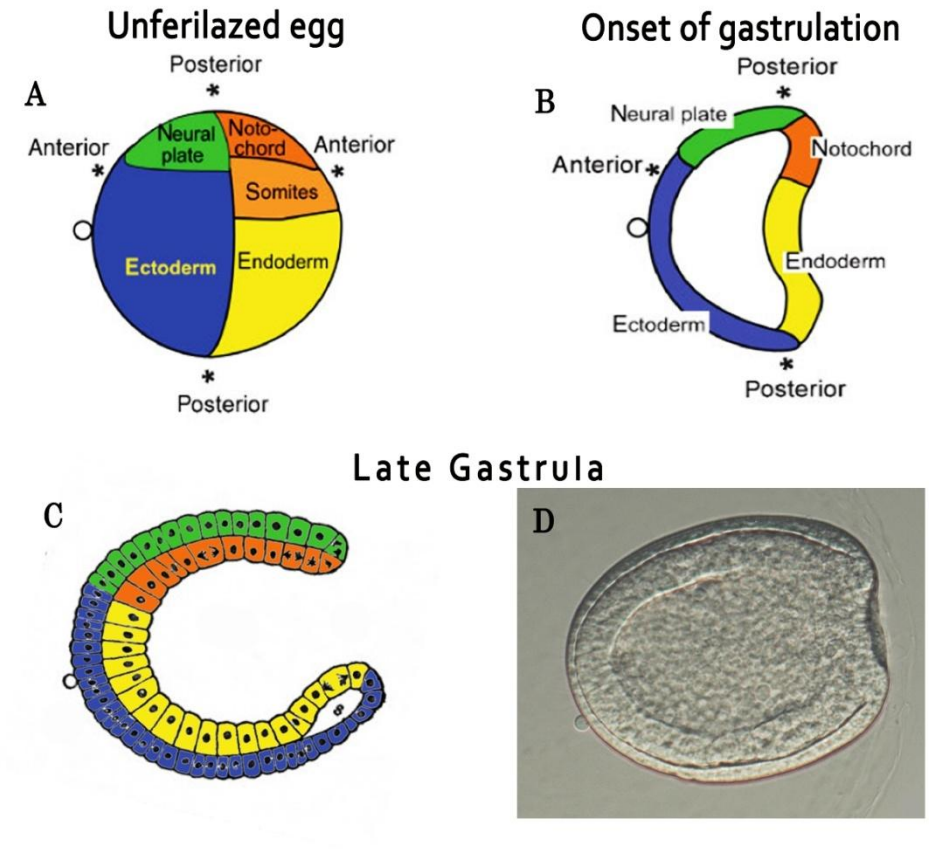

Figure 1.16 -*B. lanceolatum early developmental stages. (A) Fate map of amphioxus embryo, (B) Schematic position of tissue in early gastrulation, (C) Schematic representation of late gastrula (D) Embryo at late gastrula stage (Conklin, 1932; Holland and Onai, 2012; Kellicott, 1913).*

During neurulation the formation of the most important organ-systems takes place: the mesoblastic somites, the nervous system and the notochord.

Amphioxus' neurula is ciliated and, when it reaches 8 somites stage, it hatch and commences a planktonic existence. The neuroectoderm dissociates from the surrounding tissues and sinks to form pronounced V-shape furrow developing into postero-antero direction creating a closed neural tube that opens anteriorly at the neuropore and posteriorly by the neurenteric canal connecting (temporarily) with the gut cavity. The basal layer of the nervous groove will be the ventral side of the nervous tube, like in vertebrates.

During the time of the neural plate enclosure and neural tube formation, the notochord and mesoderm are developing from the adjacent chordamesodermal plate that constitute the roof of the archenteron just below.

Due to the invagination of midline cells of chordamesodermal plate three interdigitations forms: the first one in the middle of the embryo will yield the notochord primordial and by the seconds one laterally will yield primordium of the first couple of somite. Later the ventral epithelium of the archenteron bends round on itself to form the digestive tract, pharynx and other endodermal derivates.

At the end of neurulation and the beginning of larval formation the animals become a nearly the perfect representative of the common, generalized, primitive embryonic body form of all chordate embryos. It is characterized by an elongated structure, cylindrical in shape and somewhat compressed laterally; four basic organ-forming epithelial tubes, epidermal, neural, endodermal, and mesodermal, orientated around a primitive axis, the notochord; and distinct body regions: head, pharyngeal area, trunk and tail (Nelson, 1969) (Figure 1.17).

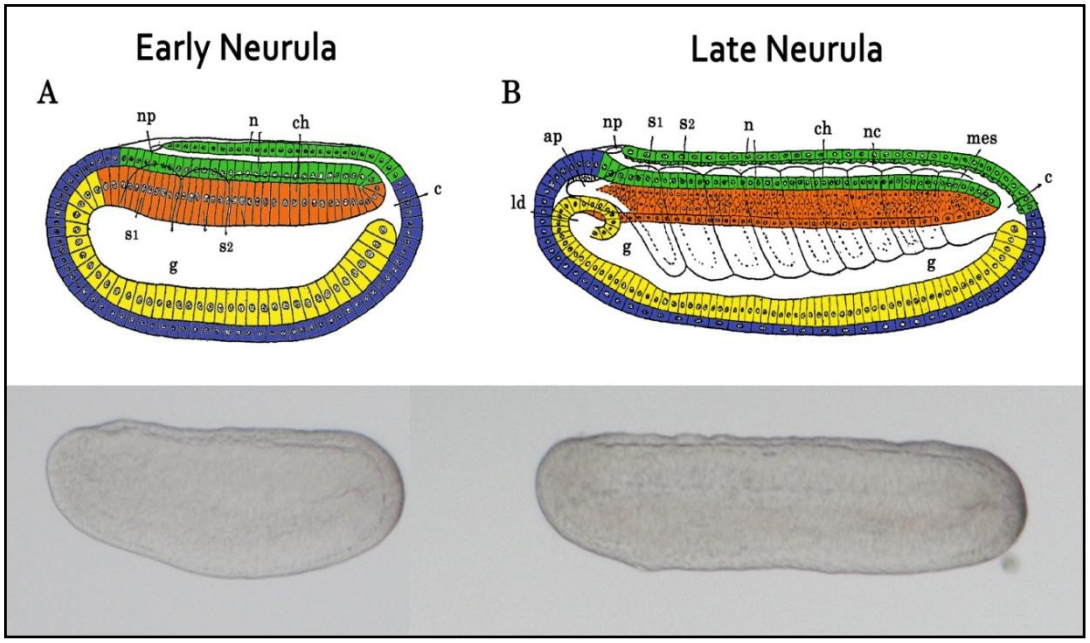

Figure 1.17 -*B. lanceolatum neurula stages. (A)Schematic representation and morphology of an early neurula. (B) Schematic representation and morphology of a late neurula. Abbreviations: ap, anterior process of first somite; c, neurenteric canal; ch, notochord; g, gut cavity; ld, left anterior gut diverticulum; mes, unsegmented mesoderm; n, nerve chord (its rudiment in A); nc, neurocoel; np, neuropore; s1 and s2, first and second mesodermal somites (Kellicott, 1913).*

Following the formation of 13-15 pairs of somites (Hirakow and Kajita, 1994; Kellicott, 1913; Whittaker, 1997), the embryo continues elongating and in this phase is commonly called *pre-mouth larvae* (Figure 1.18).

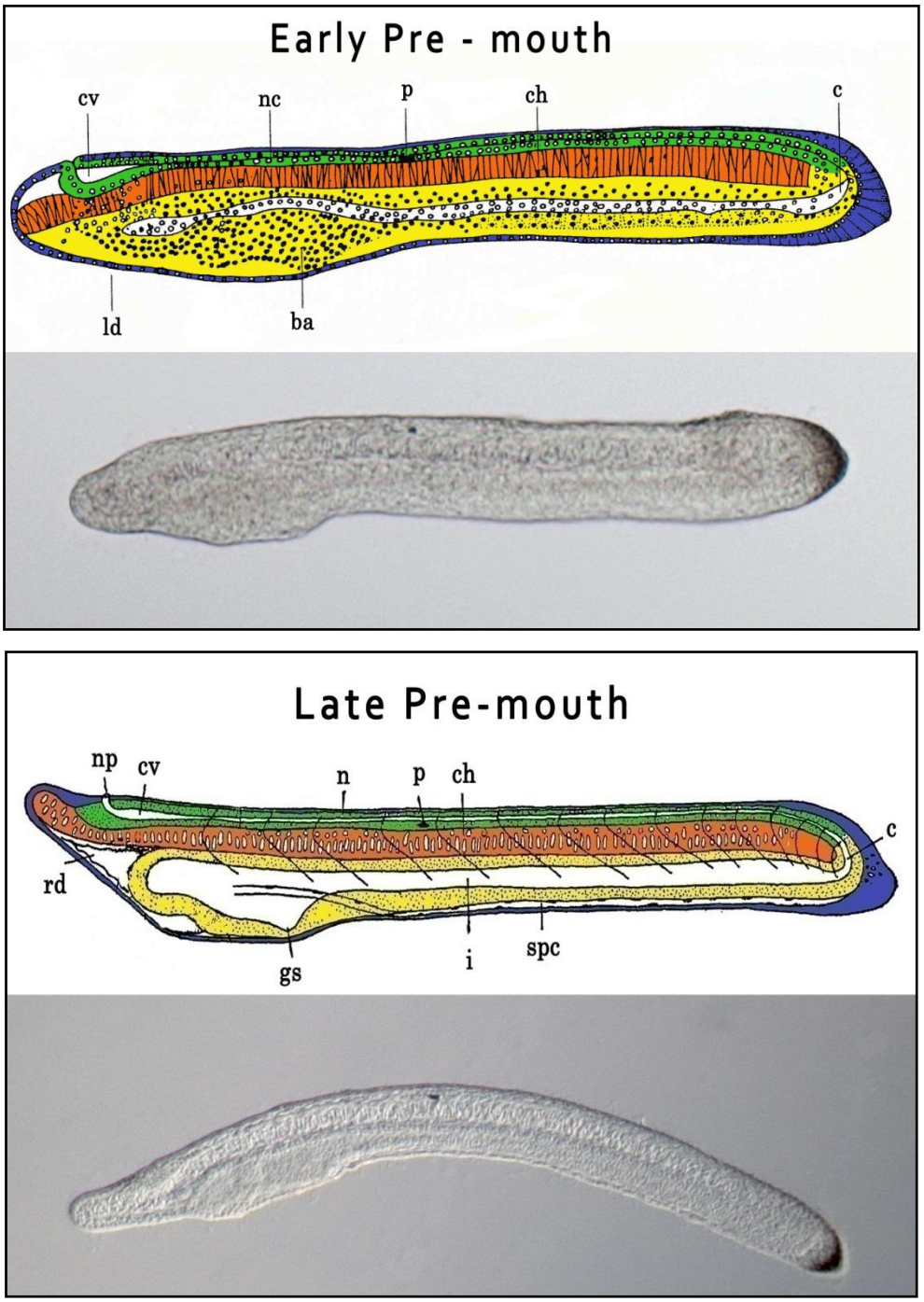

Figure 1.18 -*Schematic representation and external morphology of pre-mouth larvae at different developmental stages. ba, branchial anlage c, neurenteric canal; ch, notochord; cv, celebral vesicle g, gut cavity; gs, rudiment of first gill slit; i, intestine ld, left anterior gut diverticulum; n, nerve chord; nc, neurocoel np, neuropore; p, pigment spot in nerve cord; rd, right anterior gut diverticulum; spc, splanchnocoel (body cavity) (Conklin, 1932; Kellicott, 1913; Whittaker, 1997).*

Amphioxus' larvae undergo morphological changes particularly in the anterior region (Garcia-Fernandez and Benito-Gutierrez, 2009). The dorsal organs such as the neural tube, the notochord and the muscular lamella do not much change morphologically but become structurally more complex (Hirakow and Kajita, 1994). The embryo has continued to elongate and showing marked asymmetry. Along the right anterior side of the body, the first gill slit begins to appear as a partial dissociation of cells in the epidermis. On the left-hand side of the embryo a similar dissociation of epidermal cell, indicates the future position of the mouth. Anterior to the mouth region, the preoral pit has already formed and it is opened to exterior portion over there an elongating rostrum is forming. Few hours later the initiation of gill slit and mouth formation will be completed (Figure 1.19).

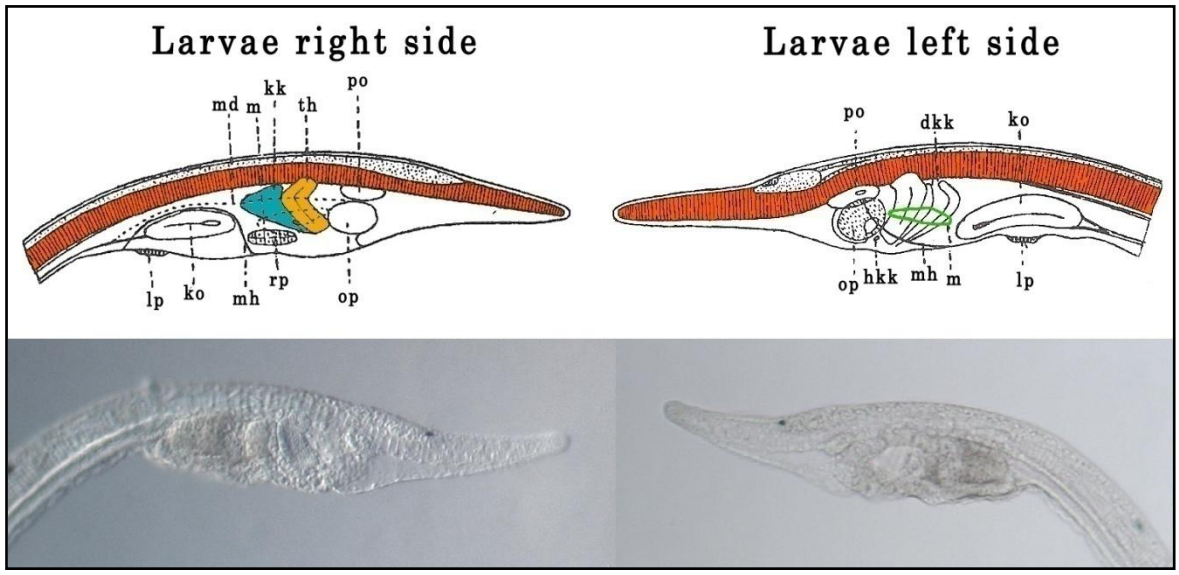

Figure 1.19 -*Schematic representation and morphology of larva with one gill-slit, seen from right side and left side. Abbreviations: dkk,intestinal opening of the club-shaped gland; hkk, cutaneous opening of the club-shaped gland; kk, the club-shaped gland; ko, first gill pouch; lp, left postoral papilla; m, mouth; md, midventral line of intestine; mh, ventral median line of epidermis; op, unpaired papilla; po, preoral pit; rp, right papilla; th, endostyle (Barrington, 1965).*

The posterior portion of the embryo has begun to flatten and take on the appearance of a caudal fin; however, there is not yet an anal opening. At second gill slit opening stage, posteriorly to the first on the right-hand side of the embryo,

near the posterior end of the embryo, the anus open on the right-hand side of the body; after that the animals start the feeding phase (Stokes and Holland, 1995).At this developmental stage is possible to recognize two structures that, for a long time, has aroused great interest in researchers: the endostyle and the club-shape gland (Figure 1.18).

The endostyle, or hypopharyngeal groove is a flagellate gutter located in the ventral midline of the pharynx consisting of a complex mucus-secreting epithelium that joins the epithelium on the frontal surface of the gill and pharyngeal bars. Initially it was thought involving in mucous production which traps food particles in the buccal water which pass the pharynx (Olsson, 1963); subsequent studies have also compared this organ to the thyroid of vertebrate for its capacity to selectively binds iodine, and synthesize and release thyroid hormones (Fredriksson et al., 1984).

The second organ characteristic of the larval stage is the club-shaped gland (csg). In 1892, Hatschek showed that this structure arises as an evagination from the pharyngeal endoderm in late embryos and soon develops into a tube connecting the pharyngeal lumen with the external environment; the external opening is a pore in the epidermis, near the anteroventral edge of the mouth (Hatschek, 1893). The functions of the gland and its fate during the larva-to-juvenile metamorphosis have long been controversial. Several homologies have been proposed between the amphioxus csg and structures in other animals on the basis of morphology, but according to the last theories the club-shaped gland of amphioxus is present throughout the larval stage and appears to supply a component of the mucus that traps food particles in the pharynx. So the endostyle and the club-shaped gland cooperate to produce a thin vertical curtain of mucus to capture ingested particles and then transport them toward the most posterior gut regions (Holland et al., 2009). During metamorphosis the club-shaped gland disappear, probably through a process of apoptosis, and the endostyle of juvenile and adult amphioxus presumably becomes the major (or even exclusive) source of mucus for capturing food particles in the pharyngeal lumen. In addition, the post-larval endostyle continues to be the major site for iodination (Ericson et al., 1985), possibly because

of the continued synthesis of thyroid hormones influencing tissue growth and maintenance in the juvenile and adult amphioxus.

The metamorphosis takes place after pelagic larval life, the duration of which depends on the environmental conditions and species, and animals after metamorphosis settle into sand substratum. The most remarkable feature of the amphioxus metamorphosis is the transformation from a left-right asymmetry to a symmetric appearance due to some modifications in pharyngeal region and digestive system. During metamorphosis, the larval mouth is shrunken forward and moves from its original position on the left body surface ventrally to anterior region. Modifications occur in digestive system as well. In larva there is a single row of gill pores in the mid-ventral cephalic area that, during metamorphosis, expands to the right side getting its counterparts. The two novel series of slits are properly adjusted on their respective sides and then the slits on each side commence to elongate in a direction at right angles to the long axis of the body. So, both rows of gill pores are destined to the left-right pair wise positioning. Also the endostyle moves from the right side of the pharynx to the ventral floor and expand longitudinally (Kaji et al., 2013; Paris et al., 2008; Paris et al., 2010; Wlllcy, 1891).

1.2.5 Larval nervous system

The "simple" Amphioxus nervous system basically consists of a dorsal nerve cord and a diffuse net of peripheral neurons, which contrasts greatly with the complexity of vertebrate nervous system. Nonetheless, increasing data on gene expression has faced up this simplicity by revealing a mounting level of cryptic complexity, with unexpected levels of neuronal diversity, organization and regionalization of the central and peripheral nervous systems (Benito-Gutierrez, 2006). The neuroanatomical differences in the nervous system between species appear minimal, and during the development the nerve cord increase not only in size, from 15 to 100 μm at metamorphosis but also in complexity (Wicht and Lacalli, 2005).

The amphioxus nervous system specification begins, as said in the previous paragraph, at gastrula stage. The presumptive ectoderm is conditioned in its final fate, by contact interaction with cells in the roof of the archenteron. Particularly the interaction appears to come only from presumptive notochordal tissue in archenteron roof (Whittaker, 1997); experimental data have shown that only the notochord, but neither mesodermal nor endodermal cells from an already invaginated plate, will induce secondary neural structures when transplanted into a young gastrula (Tung et al., 1961).Very soon after hatching the walls of the spinal cord thicken constricting the neurocoel, and becoming differentiated into three regions: (1) a thin epithelial layer, the ependyma, lining the neurocoel; (2) a dorso-lateral and lateral columns of nerve-cell bodies (grey substance) connecting respectively with the dorsal and ventral spinal nerves; and (3) ventral columns composed of nerve fibers (white substance). In the cephalic region the walls of the spinal cord become comparatively thin and the cavity dilates considerably. At first the brain vesicle lies beneath the epidermis, and around the neuropore its walls is continuous with the superficial ectoderm. When the dorsal fin appears in the mid-line the neuropore is pushed to one side, usually the left. Gradually the brain sinks away from the epidermis, the neuropore become into a tunnel-shaped depression and gradually the anatomic larval structure forms (Kellicott, 1913).

Amphioxus' Central Nervous System (CNS), like in all chordates, consists of a hollow nerve cord that enlarges in the antero-dorsal part, undergoes specification during development. Is it possible to recognize different regions, that many authors often associate with those of vertebrates: a diencephalic forebrain (the telencephalon is lacking), a small midbrain, a hindbrain and spinal cord (Candiani et al., 2011; Candiani et al., 2012; Lacalli, 1996; Lacalli, 2006; Wicht and Lacalli, 2005).

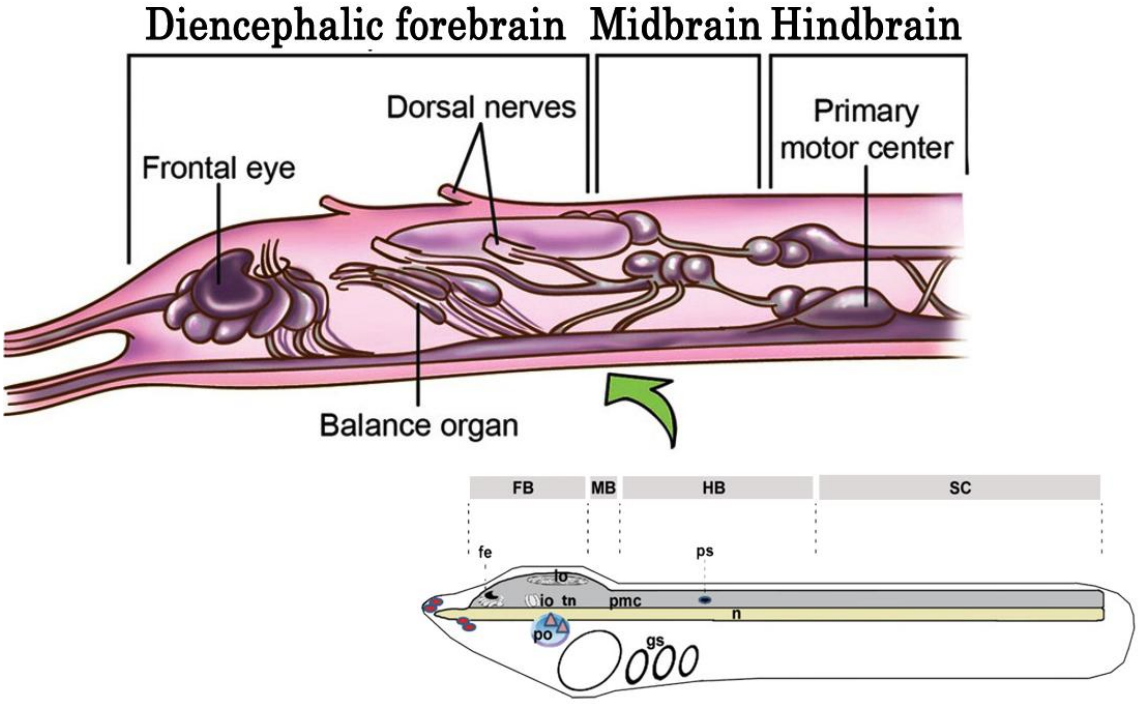

Figure 1.20 -*Schematic representation of the larval nervous system with magnification of central nervous system and its structures (Candiani et al., 2011; Feinberg and Mallatt, 2013).*

The forebrain and the small midbrain are together termed as Cerebral Vesicle (CV) (Candiani et al., 2011; Holland and Holland, 1999), and it is easily distinguishable from the rest of the cord. It is placed at level of somite 1 and up to the anterior part of somite 2, thanks to slightly bulbous anterior zone. In this area it is possible to distinguish different areas, characterized by several landmarks. One of the most evident is the frontal eye, located at the anterior tip of the nerve cord. It consists of a pigment cup, oriented so it opens dorsally, and four rows of neurons; the first

two rows consist of sensory neurons, probably photoreceptor cells, with cilia that project out the neuropore and basal axons, and behind the putative photoreceptor cells are the other two rows of neurons, that communicate synaptically with the dendrites of neurons involved in the locomotory control center (Wicht and Lacalli, 2005). Another area of the CV notable is the infundibular region. The cells that compound this area are secretory, rather than neurons, but they lie within areas with a high neuron density; it is thought to represent primary sensory cells. The most distinctive is the club-shaped cilia, which suggests they may function to detect displacement, i.e., therefore a balance organ (Lacalli and Kelly, 2000). The lamellar body is the second major contributor to the infundibular area. The lamellar body is generally accepted as a homolog of the vertebrate pineal organ, which suggests that either the cells themselves or their downstream targets in the neuropile are responsible of the circadian rhythm. There is no direct experimental evidence for such rhythm in either adults or larvae, but the larvae have diurnal patterns of vertical migration in the plankton (Wickstead and Bone, 1959), which implies the presence of a circadian clock. The third component of the CV is the primary motor center (PMC) that contains the anterior most motoneurons in the nerve cord and a number of large premotor interneurons. The important cells, from an organizational standpoint, are three pairs of large paired neurons (LPNs), extensively innervated by sensory inputs. The fundamental component is the third pair, the LPN3s, cross-innervated in a bilaterally symmetrical fashion; these neurons exerting a direct controlling influence over both fast and slow swimming (Bone, 1989). Their fiber output makes synapses with the ventral compartment motoneurons (VC, fast) and an unusual intercellular junctions with the dorsal compartment motoneurons (DC, slow) (Lacalli, 2002).

More posteriorly, there are ventrolateral nerve cells of the hindbrain, most of which consist of paired neural cells located ventrolaterally in the neural tube and may correspond to differentiating DC motoneurons that innervate the dorsal compartment of the myomeres. The hindbrain-like region (HB), that starts from the posterior part of the PMC and extends caudally over the first pigment spot (ps), has an uncertain posterior limit (Candiani et al., 2007). Caudally, the nerve

cord reaches to the tip of the caudal fin where, just above the caudal end of the notochord, almost complete metamorphosis, it forms a terminal enlargement of variable form, the caudal ampulla (Urata et al., 2007; Wicht and Lacalli, 2005). The Peripheral Nervous System (PNS) of amphioxus is composed of several types of neurons, and at least two types of epidermal sensory cells, widely distributed along the epithelium surface. The Type I receptors are primary sensory neurons having axons projecting to CNS, whereas the Type II receptors are axonless secondary sensory neurons with synaptic terminals arising at short distances from the cell body (Candiani et al., 2010). The first evident functional response of the larva is to mechanical stimulation, and this correlates with the early appearance of primary Type I sensory neurons in the rostrum and tail. Other neuronal cell types identified in the epidermal tissues are Type II sensory neurons, putative chemioreceptors with a collar of branched microvilli and basal synapses to peripheral nerves, which develop as the larva matures (Lacalli and Hou, 1999; Stokes, 1996; Wicht and Lacalli, 2005).

During neurulation, the gene expression patterns are highly dynamic within the central nervous system and reveal discrete molecular boundaries, most of them hidden at a morphological level. Many scientific studies have shown that gene expression is similar in the CNS of both amphioxus and vertebrates. Examples are the expression of highly conserved genes involved in rostro-caudal patterning such as *Otx*, *Hox* and *Gbx* (Benito-Gutierrez, 2006; Candiani et al., 2011; Castro et al., 2006; Holland and Holland, 1996; Williams and Holland, 1996), but also the expression of genes involved in the neuronal specification. For example, the *ERR*, *islet*, *Shox*, *Krox*, *Mnx* genes are expressed in developing motor neurons in both amphioxus and vertebrates (Bardet et al., 2005; Benito-Gutierrez, 2006; Candiani et al., 2011; Ferrier et al., 2001; Jackman and Kimmel, 2002; Jackman et al., 2000).

1.3 NO/NOS Amphioxus

Nitric Oxide is probably one of the oldest bioregulatory systems controlling metazoan physiology (Feelisch and Martin, 1995), nevertheless very few information are available in literature on NOS genes in cephalochordates.

In preliminary studies, published in 2006, Godoy and collaborators investigated the putative involvement of the alcohol dehydrogenase class III (ADH3) in NO homeostasis. They performed an immunostaining on *B. floridae* larvae using an universal anti-NOS antibody directed against the C-terminal epitope (DQKRYHEDIFG) that is highly conserved among the different NOS proteins in vertebrates, insects and crustaceans (Pollock et al., 2004). The larvae showed a strong signal confined to the midgut and hindgut of the developing intestine and the dorsal region of the club-shaped gland (csg), the enigmatic secretory organ located on the right side of the larval pharynx between the endostyle and the anterior-most pharyngeal gill slit (Godoy et al., 2006) (Figure 1.21).

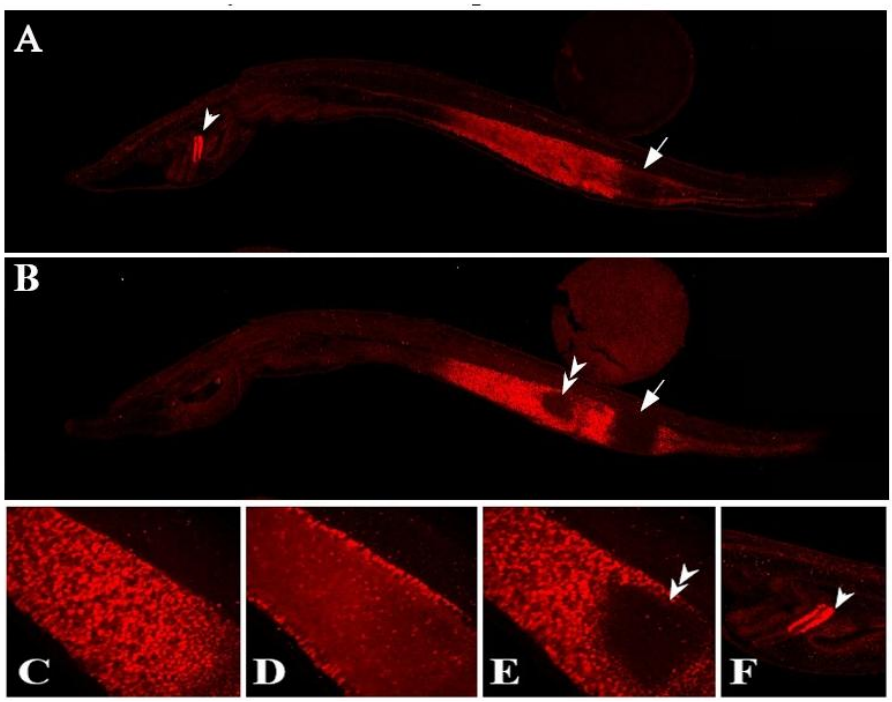

Figure 1.21 -*Whole-mount immunostaining of 48hpf B. floridae larvae with an universal anti-NOS antibody. (A) Right-sided view; (B) Left-sided view; (C-E)Magnified view of the right side, right and left side of the gut NOS localization; (F) Detail of the NOS staining in the dorsal region of the club-shaped gland (Godoy et al., 2006).*

In 2008, Chen and collaborators studied the putative role of the dimethylarginine-dimethylaminohydrolase (DDAH), endogenous NOS inhibitor, that may be involved in the regulation of endogenous NO synthesis. They characterized the NOS expression pattern in several adult tissues with *in situ* hybridization experiments on *Branchiostoma belcheri* sections: for example they found NOS expression in the central canal of the nerve cord, wheel organ, epithelial cells of gut and midgut diverticulum (Figure 1.22 A-D). The NOS was expressed in the ciliary epithelial cells on the inner side of branchial lamellas, the wall of gill blood vessels, septal coelom, and in endostyle (Figure 1.22 E). Moreover NOS was found in ovary, in the cortical region cytoplasm of oocyte and in epidermis cells of metapleural fold and the macrophages in the lymphoid cavities of metapleural fold (Chen et al., 2008b) (Figure 1.22F-H).

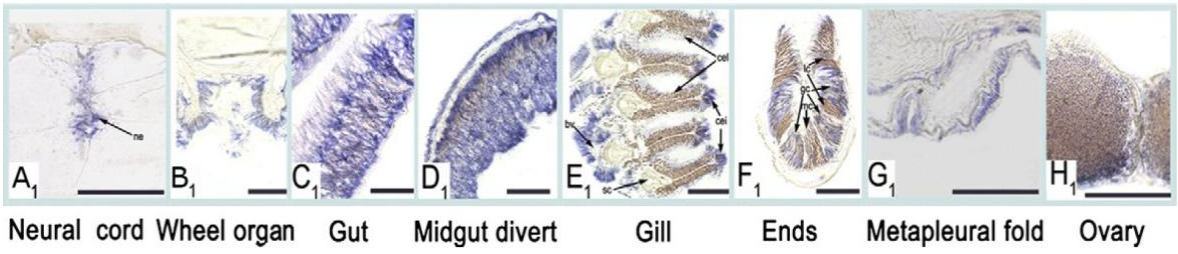

Figure 1.22 -*NOS expression pattern in different tissues of adult amphioxus (Chen et al., 2008b)*

In the 2011, Yu Shuang and collaborators investigated the amphioxus immune system studying expression patterns of immune defence-related genes in epidermis, gill epithelium, intestinal epithelium, and macrophages in adult *B. belcheri,* and they suggested that in the alimentary canal the NOS play an important role in immune defence (Lin et al., 2011) (Figure 1.23).

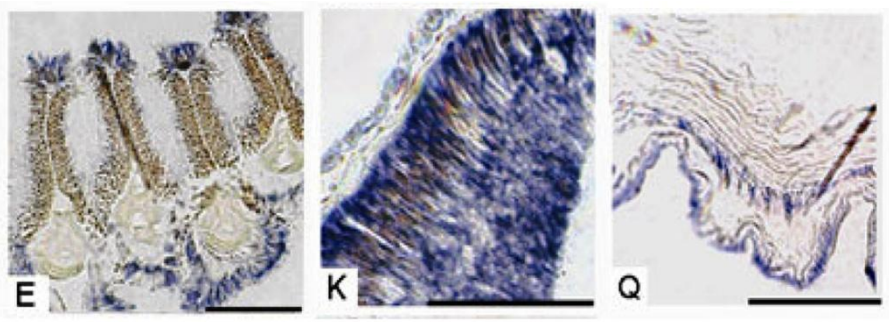

Figure 1.23 -A*mphioxus NOS expression pattern by in situ hybridization. (E) gill epithelium and branchial coelom macrophages, (K) intestinal epithelium and perienteric coelom macrophages, (Q) metapleural fold epidermis and metapleure coelom macrophages (Lin et al., 2011).*

In the same years Andreakis and collaborators analyzed the genome of *B. floridae* (Putnam et al., 2008) and discovered the existence of three district NOS genes, two constitutive (NOS-A and NOS-C) and one inducible NOS (NOS-B) (Figure1.7). The authors concluded that recurrent lineage-specific duplications of an ancestral metazoan NOS (indicated as D in Figure 1.7) led to multiple NOS genes in different animal species, as it is the case of amphioxus genes resulted to be the product of a lineage-specific duplication event (Figure1.24) (Andreakis et al., 2011).

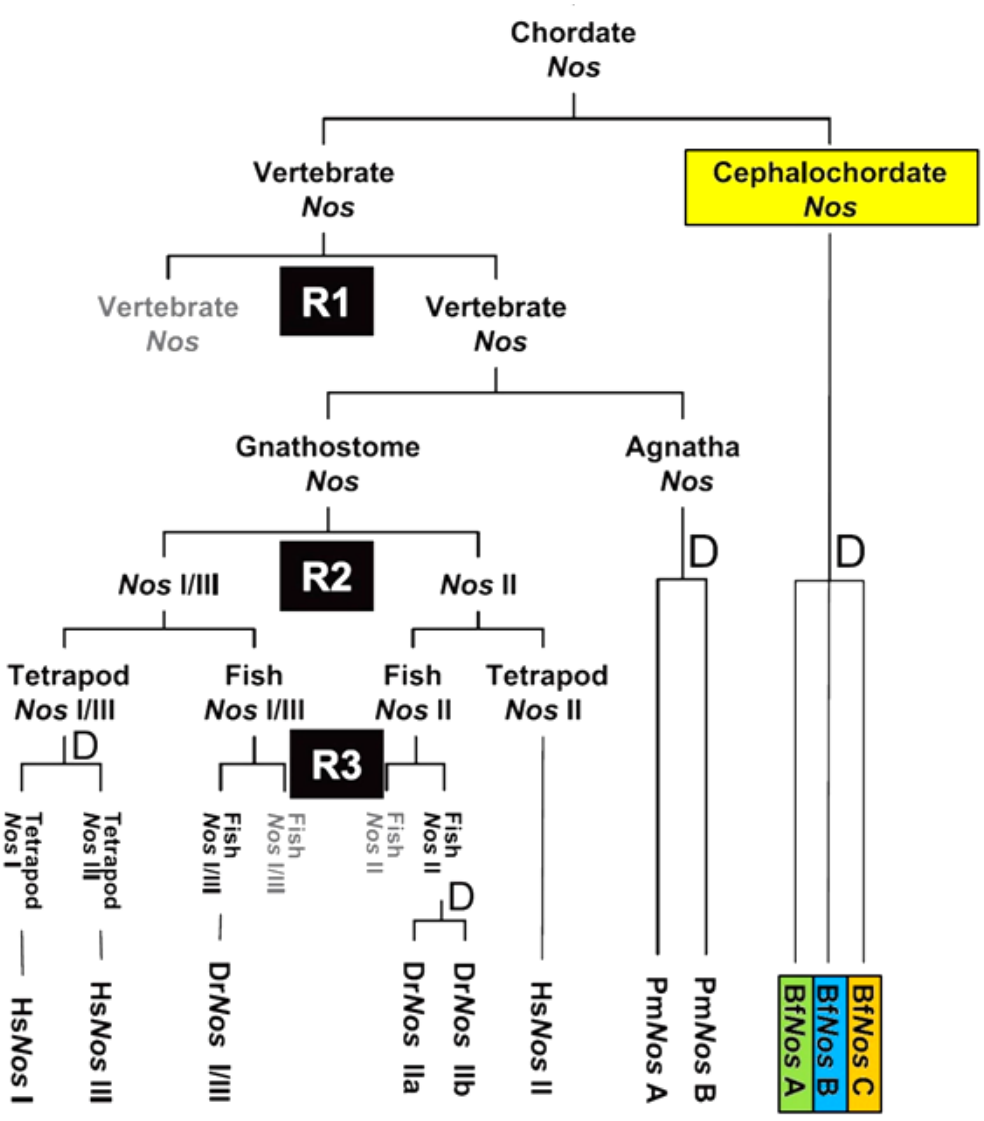

Figure 1.24 -*Evolutionary events regarding NOS genes in chordates are whole-genome duplications (R) and lineage-specific duplications (D). Inferred gene losses during vertebrate evolution are depicted in gray (Andreakis et al., 2011).*

Chapter 2 - Material and Methods

Annona Giovanni, PhD

2.1 Animal's culture and embryos collection

The amphioxus used in the present work belong to the Mediterranean species *Branchiostoma lanceolatum*, an endemic species of the Gulf of Napoli with a broad distribution along the Italian and Mediterranean coasts, with populations becoming increasingly rare probably due to the increment of pollution substances due to human activity.

2.1.1 Adult *B. lanceolatum* sampling

The adult amphioxus has been sampled in the Golf of Naples from 2011 to 2015 at Capo Posillipo (Table 2.1), an historical site rediscovered thanks to an old manuscript describing the precise coordinates of the most numerous colony (Bone, 1958). The animals were caught using a drudge, with the support of the SZN vessel "Vettoria", dragged on the soft bottom and collecting 5-10 cm of sand. After the sand collection between 5 and 12 meters deep, it was sifted directly on boat using a net with a 1.25mm mesh (Figure 2.1).

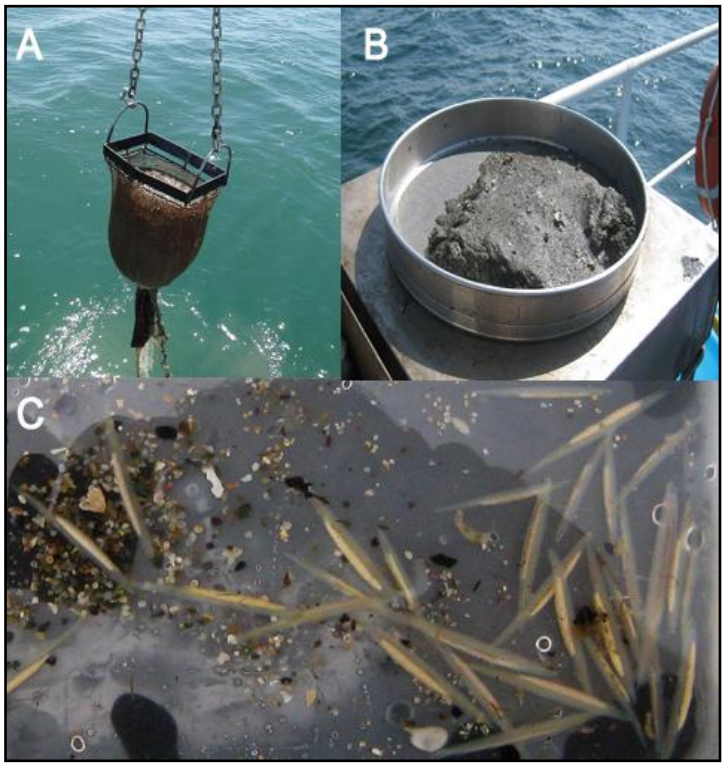

Figure 2.1 - *Adult B. lanceolatum sampling. (A) Drudge; (B) Sorting of the sand; (C) Adult amphioxus samples.*

Since the number of animals was never high, due to the sharp decline that the amphioxus population has suffered in the Gulf of Napoli, we imported animals from the same species also from Banyuls-sur-Mer (France), where there is the most abundant amphioxus population of the Mediterranean sea. Thanks to the support of a grant from the Association of European Marine Biological Laboratories (ASSEMBLE http://www.assemblemarine.org/) I was hosted in Dr. Hector Escriva laboratory at the Observatoire Océanologique de Banyuls-sur-Mer, where a remarkable quantity of fixed embryo and adult animals was obtained.

Table 2.1- *Branchiostoma lanceolatum* sampling in the Gulf of Napoli (Italy)

Data	Place	Depth	number	Average size	Gonads	T (°C)
19/01/2011	CO		3	AD 2,7 cm	1 (-), 2 (+)	
09/11/2011	COPO	9 mt 8 mt	1 14	JUV 1 cm AD 3-4 cm	4 (+)	
30/11/2011	PO	7mt	5	AD 3-4 cm	1 (+)	
18/01/2012	PO	8 mt	1	JUV	1 (-)	
15/02/2012	PO	7 mt	10	JUV 2 cm AD 4 cm	4 (++)	
27/03/2012	PO	6 - 7 mt	9	JUV 2,5 cm AD 3,5 cm	5 (+), 2 (++)	16
02/05/2012	PO	7 - 10 mt	8	JUV 2,2 cm AD 3 cm	2 (+++) 1 (++)	17
14/05/2012	NS		0			20
15/07/2012	PO		0			25
12/09/2012	PO		0			27
19/10/2012	PO	7 - 11 mt	3	JUV 1,2 cm AD 4,5 cm	(-)	25
15/11/2012	PO	6 - 10 mt	4	JUV 1,8 cm AD 3,2 cm	(+)	20
13/12/2012	PO	6 - 7 mt	4	JUV 1,8 cm	(-)	17
31/01/2013	PO	6 - 9 mt	22	JUV 2 cm AD 3,2 cm	21 (-), 1 (+)	14,5
	CO	5 - 6 mt	0			
14/02/2013	PO	7 - 10 mt	22	JUV 1,8 cm AD 3,3 cm	(-)	14
05/04/2013	PO	8 - 10 mt	12	JUV 2 cm AD 2,9 cm	(++)	15
03/05/2013	FV	7 - 8 mt 14 - 15 mt	0			19
10/05/2013	ISP	7 - 9 mt	5	JUV 2,3 cm	(+)	20
13/05/2013	IS	5 - 7 mt	4	JUV 1 AD3	(-)	23
11/06/2013	IS	6 - 9 mt	13	JUV 9 AD 4	(-)	23
01/07/2013	IS		0			
08/01/2014	PO	9 - 11 mt	18	JUV 1,7 cm	(-)	16
23/10/2014	PO	10 - 15 mt	25	JUV 1,7 cm	(-)	22
18/03/2015	PO	6 - 10 mt	45	AD 2 cm	14 (-) 30 (+) 1 (++)	14

Symbols reported in the table	
CO	Castel dell'Ovo (NA) - 40°44'17'' N - 14°14'17'' E
PO	Capo Posillipo - Villa Gallotti (NA) - 40°48'33'' N - 14°12'55'' E
FV	Foce Fiume Volturno River (CE) - 1°00'92'' N - 13°55'367'' E
ISP	Ischia Porto (NA) - 40°45'025'' N - 13°55'940'' E
(-)	no gonads
(+)	Begin of gametogenesis
(++)	midgametogenesis
(+++)	complete gametogenesis

2.1.2 *B. lanceolatum* facility

From 2011 collected amphioxus where brought to the "Aquaculture of Marine Organisms" facility at Zoological Station Anthon Dohrn of Naples (Figure 2.2). The "Neapolitan" and "French" animals were kept in different breading tanks, about 50–100 animals for 20 litres of sea water. The sand came from the original capture sites and the animals were kept in open circulating system with continuous aeration and filtrated sea water. The temperature of the sea water in the tank was the same that in the Gulf of Napoli during the autumn and winter seasons, while in spring and summer, the period of gonadic maturation for these animals, it was kept in controlled temperature condition (17°C), lower than the natural one, to avoid the natural emission of sperm and eggs in the tank. The light cycle of 12 hours of light and 12 hours of dark was provided. Animals were fed daily with a 1:1 mix of microalgae of *Isochrysis galbana* and *Tetraselmis sp.* strains (Fuentes et al., 2007).

Figure 2.2 -*Amphioxus facility.*

2.1.3 *B. lanceolatum* spawning

Between end of spring and beginning of the summer the *B. lanceolatum* gonads development, started in winter, arrive to maturation. As mentioned above, to avoid the natural emission of sperm and eggs, the animals were kept at low temperature (17°C). The induction of artificial spawning was performed applying an heat shock to ripe animals. Selected animals, with visible mature gonads, were placed in a water bath settled at 5-6 degree of temperature higher than temperature of the culturing system; the day after the animals were separated singularly in glass beakers containing 100 ml filtered sea water to avoid the uncontrolled fertilization. After 36 hours of exposure to the temperature stress, at the sunset the animals start to spontaneously release the gonads (resembling the natural spawning). The experiment is resumed in Figure 2.3.

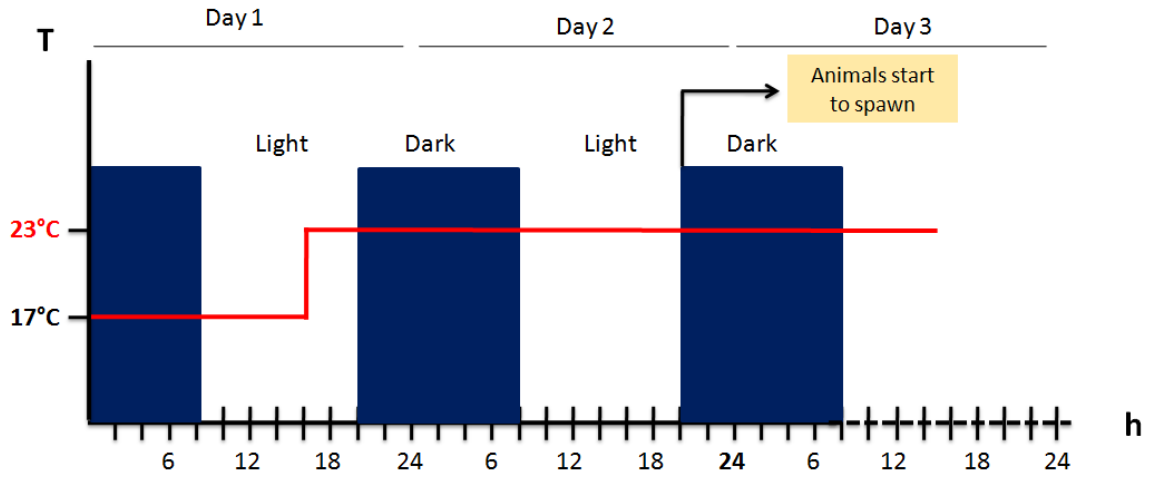

Figure 2.3 - *Schematic timing representation of induced spawning in B. lanceolatum.*

In the afternoon of the spawning days, the oocytes undergo the first meiotic division with formation of the first polar body and then arrest at second meiotic metaphase (Holland and Onai, 2012). The mature gonads, at this point, are released through the atriopore, in the number of several thousand (Figure 2.4 A). Upon release of the gametes, adult animals are removed from beakers, the sperm forms several males is mixed to increase the fecundation percentage and kept on

ice. 200-300 eggs were distributed into petri dishes with scratched bottom to avoid that they attach to it, then they were fertilized with some drops of sperm mix. After approximately 10 minutes the percentage of fertilized eggs was checked by the elevation of the fertilization membrane (Figure 2.4 B). In case that less than 65% of eggs were fertilized, another drop of sperm was added. Subsequently, embryos were washed twice with fresh sea water FSW and left to grow up to desired developmental stage in petri dishes at 18°C (Figure 2.4C and Figure 2.5).

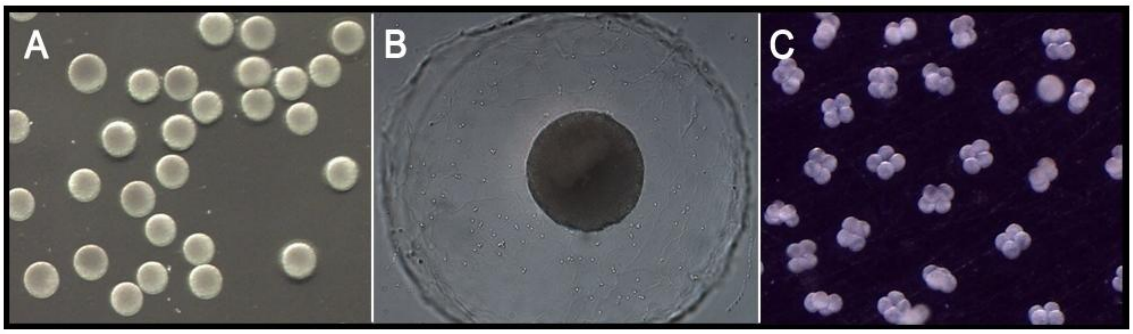

Figure 2.4 - *B. lanceolatum fecundation and first cleavages. (A) Unfertilized eggs; (B) fertilized egg with elevation of the fertilization membrane; (C) Zygotes at early second cleavage stages.*

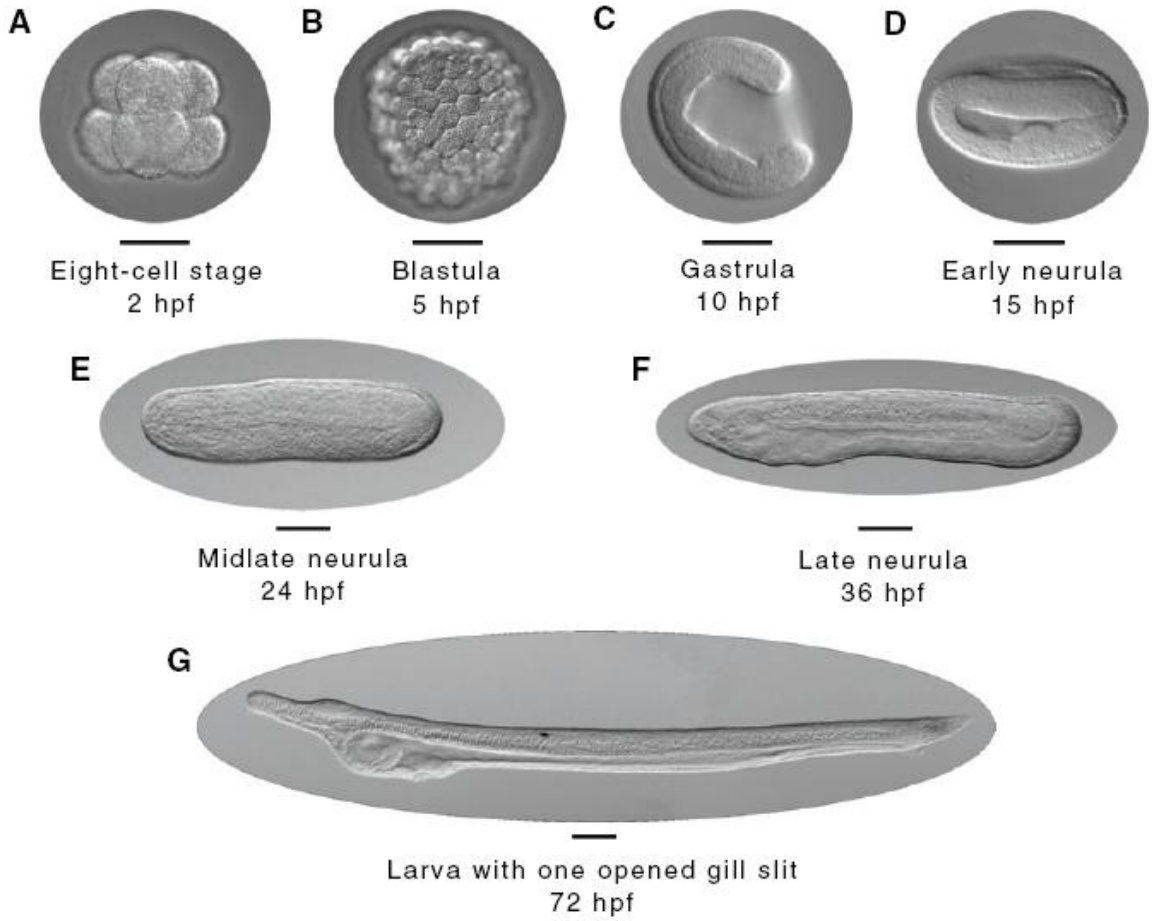

Figure 2.5 -*The most representative embryonic and larval stages of the B. lanceolatum life cycle are presented; the developmental timing for each stage at 18°C is also indicated. (A-C)The early stages of development, before neurulation, are similar to those observed in other invertebrate deuterostomes such as the sea urchin. (D-G)By contrast, the later stages of development, after neurulation, are similar to those of vertebrates (Bertrand and Escriva, 2011b).*

2.1.4 Embryo collection

Amphioxus embryos were kept into the petri dishes with scratched bottom in fresh sea water (FSW) at 18°C.

2.1.4.1 Collecting embryos for quantitative PCR (qPCR)

Embryos for total RNA extraction were collected and fixedin Eurozol (EuroClone, UK), with a proportion of about 500 embryos/larvae per ml, and stored at -80ºC until use.

2.1.4.2 Fixation for in situ hybridization experiment

When reached the desired stage of development, embryos were concentrated in the middle of the plate with circular movements, collected in the minimum volume of sea water, about 75-100 µl, and transferred into 1 ml of fresh prepared and filtered (0.22 µm) 4% PFAin MOPS/EGTA solution (0.1M MOPS pH 7,5; 2 mM $MgSO_4$, 1 mM EGTA; 0.5 M NaCl in DEPC H_2O).

After the embryos were fully deposited on the bottom of the eppendorf tube, the 50% of fixative solution was renewed and then the embryos were incubated ON at 4°C. The next day, embryos were washed at least three times in ice-cold 70% EtOH (dilute in DEPC water) and kept at -20°C until use.

2.1.4.3 Collecting for NO quantization assay

Embryos, at the desirable developmental stage, were concentrates using a mesh and subsequently were pelleted with a light centrifugation (1500-3000 rpm for 2-4 minutes) to remove as much as possible the water and frozen at -80°C in eppendorf tubes.

2.1.4.4 Embryos collection for in vivo experiments

For *in vivo* experiments such as NO localization or drug treatments, the embryos were kept into the petri dishes in FSW at 18°C until they reached the desired stage of development.

2.2 Biomolecular techniques

2.2.1 RNA Extraction and purification

To eliminate RNAase contaminations all the procedures were carried out in sterile condition, using gloves and RNAase free plastic disposable. Total RNA was extracted from embryos and larvae at several developmental stages: gastrula, neurula, pre-mouth larvae, larvae 3dpf, larvae 5dpf (in proportion of about 500 embryos or larvae), and small adult (about 1.2 cm) in 1 ml Eurozole solution (Euro Clone, UK). The reagents contain phenol and lysis buffer. According to the protocol, Eurozole was added to the sample in a proportion of 9:1. Samples were homogenized using a pestle. Then 0.1 volume of chloroform was added, mixed gently and centrifuged at 14.000 rpm at 4°C. The aqueous phase was collected and mixed with equal amount of pure chloroform. After the centrifugation, the aqueous phase was precipitated with two volumes of 100% Et-OH, ON at -20°C. Then the sample was centrifuged for 30 minutes at 14.000 rpm at 4°C. The obtained pellet was washed with 70% Et-OH, centrifuged as before, air-dried and resuspended in DEPC H_2O. The sample's concentration was measured with a "NanoDrop 1000" spectrophotometer (Thermo, USA) and RNA integrity was checked on a 1% agarose gel. The total RNA was kept at -80°C until use.

2.2.2 Reverse transcription

The first strand of cDNA was obtained by *in vitro* reverse transcription using 0.5-1 μg of total RNA. This enzymatic reaction drive the synthesis of DNA strand complementary to the RNA template using an RNA polymerase. The reaction was carried out with the SuperScript VILO cDNA Synthesis kit (Invitrogen, India). 20 μl of reaction was performed in the PCR machine according to the following setting program: 25°C for 10 minutes, 42°C for 60 minutes, 85°C for 5 minutes. Then the cDNA obtained was kept at -20°C until use.

2.2.3 Polymerase Chain Reaction(PCR)

Polymerase chain reaction (PCR) is a method that allows exponential amplification of short DNA sequences within a longer double stranded DNA molecule. Each amplification reaction was conducted in a volume of 12,5 to 100 µl of reaction mix depending for the purpose of the experiment and it was composed by sterile H_2O, 1X reaction buffer, 1.75 mM $MgCl_2$, 0.2 mM dNTP, 50 pM of each primer, 1 U/µl of GoTaq DNA polymerase and 1 ng of DNA template for each µl of final reaction. The amplification cycles were conducted by means of Thermal Cycler Perkin-Elmer-Cetus. After denaturation at 95 ^oC for five minutes, 30 amplification cycles were performed as follows: denaturation at 94 ^oC for 30 seconds, annealing at 55-65 °C for 30 seconds (depending on the primers), extension at 72 °C for 0.5-1.5 minutes (considered 1 minute to synthesize 1 kb). An extra extension cycle was carried out at 72 ^oC of 10 minutes to complete all DNA strands.

To purify the amplified DNA from the excess of buffer and dNTPs, the Invitrogen PCR Purification kit was used according to the protocol's instructions. The concentration of the obtained DNA was measured using the "NanoDrop 1000" spectrophotometer (Thermo, USA) and checked on a 1-1.5% agarose gel with the appropriate molecular marker.

2.2.4 DNA/RNA gel electrophoresis

The DNA concentration or the length of a linearized plasmid was evaluated with a DNA gel electrophoresis. The concentration of the agarose was chosen according to the length of the expected fragment. For short fragments 1.5% agarose gel is more suitable and for fragments longer than 250 bp is better to use a 1% agarose gel. The gel were prepared with 1XTBE buffer (1.1 M Tris; 900 mM Borate; 25 mM EDTA; pH 8.3) and Ethidium Bromide 0.5 µg/ml. DNA samples were mixed with Loading Buffer (Gel Loading Buffer (6X); 0.25% Bromphenol Blue; 15% Ficoll 400, 120 mM EDTA, 0.25% Xylene Cyanol) and the appropriate molecular marker. Electrophoresis was normally settled at the voltage of 90-100 V.

In order to evaluate the quality and relative quantity of RNA the procedure was similar to the DNA electrophoresis with slight modifications to avoid RNA degradation (not in denaturation conditions): the electrophoresis camera was RNAse-free, the running buffer was fresh prepared.

2.2.5 Molecular Cloning

This techniques allow to obtaining multiple copies of a given nucleotide sequence of interest. It consists of three phases: ligase, transformation and hosting bacterial growth.

2.2.5.1 DNA ligation

T4 DNA Ligase catalyzes the formation of a phosphodiester bond between juxtaposed 5'-phosphoryl and 3'-hydroxyl termini in duplex DNA. The PCR fragments were ligated with the commercial plasmids p-GEM-T Easy vector (Promega, USA). Each ligation reaction was carried out in a final volume of 20µl in distilled H_2O and containing 50-100 ng of vector DNA linearized. The moles of insert DNA were added in 3-5 fold vector moles and 2 µl of ligation buffer (10X T4 DNA Ligase Buffer: 500 mM Tris-HCl pH 7.5, 100 mM $MgCl_2$, 100 mM dithiothreitol, 10 mM ATP, 250 µg/ml bovine serum albumin) and 1 µl of T4 DNA Ligase (1 unit/µl) (Promega). The reaction mix was incubated at 4°C overnight or two hours at room temperature, and used to transform competent bacteria.

2.2.5.2 Bacterial transformation

The transformation of vectors containing DNA of interest was performed by electroporation in bacterial cells *Escherichia coli* provided by the Molecular Biology Service of SZN and stored at -80°C. When needed the cells were gently defrosted on ice for 10 minutes, and 40 µl were mixed with 4 µl of dialyzed vector, then the mix was transferred quickly into electro-cuvette. The electric shock was performed in a "Bio-Rad Gene Pulser" applying a constant voltage of 1.7 V.

2.2.5.3 Bacterial growth in liquid and solid culture medium

The cells transformed were placed in 800 ml of Luria Bertani (LB) medium shaking at 270 rpm at 37 °C for 1 hour, after that the cells were plated on LB solid medium (NaCl 10g/l, tryptone 10 g/l, yeast extract 5 g/l, agar 15 g/l) (in volume of 200 and 600µl) in the presence of ampicillin (50 µg/ml) to which the plasmids were resistant. IPTG and X-gal (40 µl + 40µl respectively) were added for the blue-white screening technique and grown overnight at 37°C.

2.2.6 PCR colony screening

To detect positive colonies after the cloning experiments, white colonies were individually picked using a sterile plastic tip and sink it into 12.5 µl of PCR reaction mix in PCR tube for 5 minutes and mixed well. After PCR amplification using forward and reverse primers corresponding to the specific plasmid sequence, by electrophoresis analysis the samples presenting a band of the expected size were identified and the plasmidic DNA was purified from the corresponding bacterial colonies.

E. coli colonies were grown ON in 3 ml of LB and 0.1 mg/ml of antibiotic, at 37°C, shaking at 270 rpm. After 16 hours, the colony in LB was separated on two parts: 500 µl aliquot was mixed with 500 µl of 100% Glycerol and freeze at -80°C as stock, all the rest (2.5 ml) was used to purify plasmidic DNA, according to the protocol supplied of GenElute™ Plasmid Miniprep Kit (Sigma, USA). The obtained DNA was measured with a NanoDrop1000 spectrophotometer (Thermo, USA).

2.2.7 DNA sequencing

The DNA sequencing was carried out at the Molecular Biology Service of SZN using Automated Capillary Electrophoresis Sequencer 3730 DNA Analyzer (Applied Biosystems, USA) using a BigDye® Terminator v3.1 Cycle Sequencing Kit (Life Technologies).

2.2.8 Riboprobe synthesis

Particular attention was paid to design primers to amplify the three NOS genes (Table 2.2) and avoid overlapping DNA regions since these genes are very similar between them, and so to avoid false positive results. Gene amplification was carried out using cDNA of mix larval stages for NOS-B and NOS-C, while for NOS-A was amplified from adult animal cDNA.

The RNA polimerization reactions were done using a PCR template using the M13F and M13R primer. The PCR product was purified using "MinElute PCR Purification Kit" (Qiagene) and then used for the synthesis of the riboprobe. If the PCR band was not unique, the DNA band of interest was cutted from the gel and purified by using "GenElute Gel Extraction Kit" (Sigma). The RNA transcription reaction was carried out using RNA-polymerase Sp6, T7 or T3. Two riboprobes for each gene were synthesized. The "sense-riboprobe" served as a negative control, while the "antisense-riboprobe"revealed the gene expression pattern due to its sequence complementary features with the endogenous mRNA. Riboprobes were labelled by Digoxigenin (DIG, Roche). Labelling and RNA transcription were performed in one step according to Roche standard protocol with 1µg of PCR template for a final volume of the reaction of 20 µl at the temperature of 37°C. Then, 1 U/µl of DNaseI-RNAse free (Roche) was added to the reaction, mixed and incubated for 20 minutes (to remove the DNA template). Then, the mix was placed on ice for 5 minutes and the riboprobe was precipitated adding 80 µl of TE buffer (Tris-Cl, EDTA), 300 µl of 100% Et-OH and 10 µl of 4M LiCl. The solutions were mixed gently and left ON at -20°C. The next day, the tubes were centrifuged for 30 minutes at 4°C at the maximum speed (14.000 rpm). The supernatant was discarded and the RNA pellet on the bottom of the tube was washed with 1 ml of the ice cold 100% Et-OH, then, centrifuged at 4°C at the maximum speed for 15 minutes. All traces of the Et-OH were discarded, the RNA pellet was air-dried and then eluted in 50 µl of DEPC H_2O.

The riboprobe concentration was measured with a "NanoDrop 1000" spectrophotometer (Thermo, USA) and with a "dot-blot" immunostaining (section

2.15). Usually the riboprobes synthesized *in vitro* have concentration of about 100 ng/µl. The riboprobes were kept at -80°C until use.

2.2.9 Riboprobe quantification

Riboprobes concentrations were evaluated by "dot-blot" immunostaining, using anti-DIG Alkaline Phosphatase (AP) conjugated antibodies against the RNA control (Roche). RNA sample at standard dilutions were prepared with dilution buffer according to these proportions: DEPC H_2O: 20X SSC: formaldehyde (5:3:2). 1µl of each RNA sample dilution were spotted on a Hybond N membrane (Amersham) in parallel to the DIG-labelled RNA standard dilutions (Roche). Samples were UV-cross-linked to the membrane by Stratalinker for 30 seconds. The membrane was incubated in the blocking solution (BS) containing 5% BSA in 0.1M maleic acid pH 7.5, at RT for 30 minutes and then in BS with anti-DIG AP antibody, at a final concentration 0.15 U/ml at RT for 1 hour. Then, the membrane was washed from not conjugated antibodies by three washed in 0.1M maleic acid pH 7.5 and 0.15 M NaCl, in detection solution (100 mM Tris-HCl pH 9.5; 100 mM NaCl; 50 mM $MgCl_2$) and then incubated in the dark in detection solution containing 50 mg/ml of 5-bromo-4-chloro-3-indolyl-phosphate (BCIP) and 50 mg/ml nitroblue tetrazolium (NBT). Due to the AP enzymatic reaction in presence of NBT and BCIP substrates, the insoluble blue-purple precipitate appears. After 10 minutes the reaction was stopped by tab H_2O washing. The intensity of the coloration of the samples spot was compared with reference one of known concentration. Thus, the approximate concentrations of riboprobes for the *in situ* hybridization experiments was established.

2.3 Primers for WISH and qPCR design

Because of the high similarity between the three NOS genes a deep analyses was performed to find specific sequences in order to design specific riboprobes synthesis and qPCR (Table 2.2) for each gene. Each primer was design manually identifying specific sequences for each gene. The primers melting temperature (Tm) were checked using Sigma-Aldrich software "OligoEvaluator" (http://www.sigmaaldrich.com/).

Table 2.2 -*Table of primers for WISH and qPCR*

Primer name	Sequence (5′→3′)		PCR product
Cloning/WISH primers			
Bl NOS-A	FORWARD	GCCCCGTGAGTTTCCAACTG	1076 bp
	REVERSE	GGAGCTGGTTTGGTCAAATC	
Bl NOS-B	FORWARD	CGGTACAATCCAGAGAAACG	830 bp
	REVERSE	CGTACCCCTGGAACTGGAAC	
Bl NOS-C	FORWARD	TCGGCCGAACGTAATTGCCG	787 bp
	REVERSE	GCCCGCATGAAGAACTGGCTG	
Bl SoxB1c	FORWARD	GTCTGCCAGGTGGTCTGATC	578 bp
	REVERSE	GACTGAGGGGAACTGTACCG	
qPCR primers			
Bl NOS-A	FORWARD	AGTACAGTCATCTCCAGAAC	F-R1 = 221 bp F-R2 =258 bp
	REVERSE-1	CAGATAGAAGCGCTGCAAGA	
	REVERSE-2	GTTTGGTCAAATCATGGACG	
Bl NOS-B	REVERSE	AGTTTACTCCCGGCGATCA	191 bp
	FORWARD	GCGTTTGCCGCCATGTTCT	
Bl NOS-C	REVERSE	CAGGATTCTGCGCGTTTGC	197 bp
	FORWARD	CATGAGCGAGGCTAGCTCC	
Bl L-32	REVERSE	GGCTTCAAGAAATTCCTCGTC	117 bp
	FORWARD	TCACGCAAGAGGAAACTCATT	
cDNA sequencing primers			
T3	ATTAACCCTCACTAAAGGG		
T7	AATACGACTCACTATAGGG		
SP6	GATTTAGGTGACACTATAG		
M13F	CGTTGTAAAACGACGGCCAGT		
M13R	TTTCACACAGGAAACAGCTATGAC		

2.4 Whole mount *in situ* hybridization (WISH)

Embryos and larvae at the desired developmental stage were rehydrated with three 1X PBT (1XPBS; 0.1% Tween20) washes at RT. To facilitate the riboprobe penetration into the tissues at late developmental stages the embryos were incubated for 5 minutes in PBT 1X with Proteinase K (5µg/ml) that digests membrane proteins. The reaction was stopped by adding 4 µl of 10% glycine and then changing the solution for 2 mg/ml glycine in 1XPBT. The embryos were fixed again in 4%PFA in PBT for 1 hour at RT and then washed in 0.1 M tri-ethanol-amine with acetic anhydride at two different concentrations, 1:400 and 1:200. This treatment is important for decreasing the background but it also appears to inactivate RNases and may help in producing a strong signal. Embryos were washed in PBT and pre-hybridized in hybridization buffer HB (50% deionized Formamide; 100 µg/ml Heparin; 5X SSC; 0.1% Tween20; 5 mM EDTA; 1X Denhardt's; 1mg/ml; total Yeast RNA; DEPC H_2O). Then embryos were hybridized ON at 65°C in HB with 0.1 ng/µl of riboprobe.

The day after, the excess of riboprobe was washed out by wash solution I (WS-I) (50% dionized Formamide; 5X SSC; 1% SDS in DEPC H_2O) and WS-II (50% deionized Formamide; 2X SSC; 1% SDS in DEPC H_2O) at 60°C, then by WS-II, WS-III (2X SSC in DEPC H_2O). After this last step it is possible to treat embryo with RNAse A (2 µl of 10mg/ml) and RNAse T1 (1 µl of 10000 U/ml to add to 1 ml of WS-III) to remove RNA single strand and remove the background. Subsequently the very last washes were done in WS-IV (0.2X SSC) at RT. Then the blocking step was performed by washing embryos in WS IV with 100 µl of sheep serum in 1 ml (final volume) and changing this solution for Blocking Reagent (BR) (PerkinElmer) for one hour and replaced BR with the AB mix ON at 4°C. To prepare 6 ml of antibodies solution 6 mg of BR in 800 µl of PBS with 0.1% Triton X-100 were preheated 30 minutes at 70°C, then was added 200 µl of 20 mg/ml BSA, 200 µl of sheep serum and 1:2.000 anti-DIG AP antibody. The mix was incubated one hour on a rotator at 4°C, and then the total volume of the mixture was filled up to 6 ml with 400 µl of 2 mg/ml BSA and 200 µl of sheep serum in PBT.

Then, the AB was recovered and the embryos were washed 4-5 times in PBT for 20 minutes on a rotator. To detect the signal the AP reaction was performed: the embryos were incubated in 0.22 μm filtered AP buffer in the dark (0.1 M Tris pH 9.6; 0.05 M $MgCl_2$; 0.25 M NaCl; 0.1% Tween 20; 0.5 μg/μl of Levamisole) and after the AP buffer was substituted to BM-purple AP substrate (Roche), until the colour appeared. Then, the reaction was stopped by PBS washing. Embryos were fixed in 4% PFA in PBS for one hour, washed in PBS and kept for imaging in 80% glycerol in PBS with 0.1% NaN_3 to prevent the bacterial contamination.

2.5 Quantitative PCR(qPCR)

Temporal accumulation of RNA messages for developmental stages gastrula, middle neurula, pre-mouth larvae, larvae 3dpf, larvae 5 dpf and small adult (1,2 cm) was monitored using real-time quantitative polymerase chain reaction (qPCR). Specific primer sets (Table 2.2) for each gene were manually designed. Primer pairs were chosen to amplify products of 100–300 bp in length. Blast searches were used to ensure that primers were specific for each individual gene. The qPCR was carried out in a ViiA™ 7 Real- Time PCR System (Applied Biosystems) using the SYBR™ Green reagent (Life technologies). Empirically, the optimal work concentration of cDNA have been found, through serial dilutions. Then, the reaction carried out in multi well plate. 10 μl of reaction contained 1 pM/μl of each primer, 5 μl of SYBR Green reagent and 1 μl of diluted 1:20 cDNA. The reaction was performed in tree steps: i) hold stage was performed by incubation at 95°C for 20 seconds; then ii) PCR amplification was carried out by 40 cycles of repeating conditions: 95°C for 1 seconds and 60°C for 20 seconds; iii) melting curve stage: 95°C for 15 seconds, 60°C for one minute and 95°C for 15 seconds. The data were handled by software supported with PCR equipment (look the section 2.21 Software). The relative ratio was controlled by manual calculations, using "Users bulletin", ABI PRISM 7700 Sequence Detection System 1997 and the theory of data normalization by Rebrikov and Trofimov (Rebrikov and Trofimov, 2006). For the expression level in the developmental stages, data for

each gene were normalized against ribosomal protein L32 mRNA, which is known to be expressed at constant levels during develompent (Kozmikova et al., 2013).

2.6 NO quantization: Griess assay and DAN assay

2.6.1 Bradford protein assay

Bradford protein assay is a simple and accurate method to determinate the concentration of solubilised proteins. This assay is based on the binding of coomassie brilliant blue with proteins. This dye binds protein give rise to a colored product with an absorption peak at 595 nm. The measurement is made by spectrometer and the color intensity is related with the protein amount using a calibration curve. In order to obtain a calibration curve, three known quantity of bovine serum albumin (BSA) were used: 3µg, 6µg and 9µg. For each samples 200µl of Biorad reagent solution was added and up to 1 ml with PBS 1X.

The several samples for each developmental stage were concentrated (such explained in the section 2.1.4.3**)** and homogenized in 500µl of 1X PBS using a plastic sterile pestel, subsequently several cycle of sonication was performed to obtain the membranes fractionation. The sonication was performed on ice with 3 cycles of 1 minute, with amplitude of 30%. After the homogenization, a centrifugation of 10 minutes at 13.000 rpm allowed to obtain a supernatant which contains the proteins. The protein extract concentration was determined by Bradford assay. The samples for the assay contain 5µl and 10µl of protein extract, 200µl of Bradford reagent and PBT1X up to 1 ml. The final protein concentration is given by the average of the value obtained from the two dilutions.

2.6.3 DAN assay

Studies of NO quantification were hampered by the physiological short half-life of this gaseous free radical, so alternatively, integrated nitric oxide production can be estimated from determining the concentrations of nitrite and nitrate final

products. The measurement of nitrate/nitrite concentration is routinely used as an index of NO production (Moshage et al., 1995).

Before to measure the concentration of nitrites all the nitrates were converted to nitrites using the nitrate reductase (NaR).

In the attempt to measure NO-derived NO_2 generated under physiological conditions, different fluorometric methods have been developed. One method has employed the use of the aromatic diamino compound 2,3-diaminonaphthalene (DAN) as an indicator of NO formation (Miles et al., 1996). The relatively non fluorescent DAN reacts rapidly with N_2O_3 generated from acidified nitrite (nitrous acid) or from the interaction of NO with oxygen to yield the highly fluorescent product 2,3-naphthotriazole. This assay offer additional advantages of specificity, sensitivity, and versatility (Bryan and Grisham, 2007) but because of the fast decay of fluorescence this assay has a restricted time limit (Hu et al., 2014).

To obtain a standard curve useful to quantify nitrite concentration in our samples, was measured the absorbance of sodium nitrite solution at different molarity: 0µM (blank); 2,5 µM; 5 µM; and 10 µM in 1XPBS , adding NaR and its cofactors.

We used 50µg of total protein in a final volume of 80µl in each samples in order to normalize the values. For the conversion of nitrates in nitrites we added a mix of 20µl of NaR (final concentration 0.8 U/ml) and its cofactors FAD and NADPH (final concentration 15µMand 0.06 mM, respectively) both in the samples used for analyses and calibration curve. After two hours of reaction, needed for nitrates conversion, 10µl of reactive DAN (0,05 mg/ml dissolved in HCl 0.62 M) were added to the samples, then after ten minutes of incubation in the dark 15 µl of NaOH 2.8M were added to stop the reaction. Then the samples were quickly measured using the spectrofluorometer. The concentration of NO was reported as nmol of NO per mg of protein.

2.6.4 Griess assay

The Griess reaction first reported by Johann Peter Griess in 1879 as a method of analysis to quantify nitrite, index of NO concentration. Nitrite is first treated with

a diazotizing reagent, e.g., sulfanilamide (SA), in acidic media to form a transient diazonium salt. This intermediate is then allowed to react with a coupling reagent, N-naphthyl-ethylenediamine (NED), to form a stable azo-compound. The intense purple color of the product allows nitrite assay with high sensitivity. The absorbance of this adduct at 540 nm is linearly proportional to the nitrite concentration accordingly NO concentration in the sample (Sun et al., 2003).

The calibration curve used to quantify nitrite concentration in our samples, was obtained using sodium nitrite solutions at several Molarity as reported in the in the previous paragraph.

We used 50µg of total protein in a final volume of 150µl in each samples in order to normalized the assay. For the conversion of nitrates in nitrites we added 150µl of a mix contain NaR, in final concentration 0.24 U/ml, and its cofactors FAD and NADPH (final concentration 5µM and 0.2 mM, respectively) both in the samples used for analyses and calibration curve. After 2 hours of reaction, needed for nitrates conversion, samples and standard curve solution were incubated for ten minutes in the dark with equal volume of 1% (wt/v) sulphanilamide in 5% H_3PO_4 and then for ten minutes with equal volume of 0,1% (wt/v) N-(1-naphthy)-ethylenediaminedihydrochloride. The samples were measured at the spectrophotometer and the result were expressed as nmol of NO per mg of protein.

2.7 NO detection: DAF-FA DA assay

The cell-permeant diaminofluorophore 4-amino-5-methylamino-2'-7'-difluorofluorescein diacetate (DAF-FM-DA, Molecular Probes) was used to detect NO production sites in living amphioxus (Bryan and Grisham, 2007; Kojima et al., 1999). This reagent, not fluorescent, is permeable and passively diffuses through biological membranes. Inside the cell the compound is rapidly de-esterified by intracellular esterase and quickly reacts with NO to form a fluorescent compound: benzotriazole (λ_{ex}=495nm, λ_{em}= 515nm).

3dpf larvae were incubated in presence of a concentration of 5µM DAF-FM-DA in the dark, at room temperature, for 20 minutes in filtered sea

water; after the reaction time, 6 washes of 5 minutes each has been done (Comes et al., 2007).

In order to slow down larval movement during the treatment the anesthetic MS222 (Sigma) were applied. The treated larvae were analyzed using a Zeiss confocal laser scanning microscope LSM 510 with fluorescent filter (λex= 470±40 nm, λem= 525±50 nm).

2.8 Variation of NO endogenous levels during development

To investigate the role of NO in larval development of *B. lanceolatum* an inhibitor of NO production was used. The L-Nω-Nitroarginine (L-NA or L-NNA), a competitor of L-Arginine is one of the first synthetic NOS inhibitors studied (Vìtecek et al., 2012), in fact its capability to block NO synthesis was recognized in the early nineties (Moore et al., 1990; Rees et al., 1990a). In the NO formation reaction, it substitutes L-Arginine leading to a decrease of endogenous NO levels. Due to a poor solubility at neutral pH, L-NA is often substitute from its analogue L-Nω-Nitroarginine Methyl Ester (L-NAME) that is preferred for the better lipophilicity characteristics and therefore useful for *in vivo* experiments (Rees et al., 1990b). L-NAME may act as a weak NOS inhibitor, but it is readily hydrolyzed by ubiquitously present esterases to L-NA in biological systems (Griffith and Kilbourn, 1996). Embryo at gastrula, neurula, and larvae at pre-mouth and 3dpf stages were treated with three L-NAME concentrations: 100µM, 500µM, 1mM - dissolved in FSW. The samples were left to develop in petri dishes at 18°C and were fixed in PFA 4% in MOPS/EGTA when they reached the required stage embryo. Samples developed in FSW and in the same developmental conditions in absence of the drugs were used as control. The larvae morphology was analyzed using a microscope Zeiss Axio Imager M1, equipped with an Axiocam digital camera.

2.9 NOS phylogenetic analysis

2.9.1 Cephalochordate evolutionary study

To better understand the evolutionary relationships among NOS genes in cephalochordates a phylogenetic study was performed.

NOS sequences cloned from *Branchiostoma lanceolatum* and all NOS genes gathered from published genomes and transcriptomes and genomic databases for other basal animals are listed in Table 2.3.

2.9.2 Bony fishes and chondrichthyes evolutionary study

In order to study in deep the scenario of fish NOS evolution, teleosts fishes, chondrichthyes fishes and cyclostomes sequences were analyzed. Sequences of man, frog, lizard and tunicate were used as outgroups (Table 2.2). The protein sequences were obtained by blast analysis of NOS sequences in principal genome/transcriptome browser:

NCBI	www.blast.ncbi.nlm.nih.gov/Blast.cgi
Ensemble	www.ensembl.org/index.html
UCSC	www.genome-euro.ucsc.edu
Elephant shark genome	www.esharkgenome.imcb.a-star.edu.sg
SkateBase	www.skatebase.org
SalmonDB	www.salmondb.cmm.uchile.cl
NFIN	www.nothobranchius.info
Japanese Lamprey Genome	www.jlampreygenome.imcb.a-star.edu.sg

Table2.3 -*NOSs gene sequences accession number used in the phylogenetic study. The symbol (-) indicates that the gene is not present in the organism or that it is not found in genome/transcriptome..*

Species	nNOS Acc. Numb.	eNOS Acc. Numb.	iNOS Acc. Numb.
Homo sapiens	AAB49040	AAA36365	AAB60366
Anolis carolinensis	ACAT00000016633	ACAT00000008211	ACAT00000015866
Xenopus tropicalis	XETT00000048371	XETT00000025059	XETT00000027328
Branchiostoma lanceolatum	Data not published	–	Data not published
Branchiostoma floridae	**A** - XM_002260801 **C** - XM_002605780	–	XM_002608682
Branchiostoma belcheri	**A** - 081950_PFF0 **C** - 226820_PRF0	–	117620_PFF0
Ciona intestinalis	XP002120267	–	–
Ciona Savinyi	CSAVG00000009725	–	–
Strongylocentrotus purpuratus	NW_001469593	–	–
Petromyzon marinus	Data not published	–	–
Eptatretus burgeri	Data not published	–	–
Lethenteron japonicum	A- JL5361 B- JL15861	–	–
Scyliorhinus canicula	ctg17724	–	AAX85385
Squalus acanthias	Q9I9M2_2	–	–
Leucoraja erinacea	–	ctg94789	ctg31742
Callorhinchus milii	XP007900533	–	XP007898890
Poecilia reticolata	XP008416108	–	–
Maylandia zebra	XP004566752	–	–
Stegastes partitus	XP008290591	–	–
Cynoglossus semilaevis	XP008334475	–	–
Pundamilianyererei	XP005743120	–	–
Neolamprologus brichardi	XP006803925	–	–
Oreochromis niloticus	XP003454198_2	–	–
Xiphophorus maculatus	XP005803890	–	–
Astyanax mexicanus	AMXP00000001199	–	**(a)** XP_00000010494 **(b)** X_P00000012193

Gadus morua	GMOP00000016303	–	–
Takifugu rubripes	TRUP00000041970	–	–
Oryzias latipes	ORLP00000001296	–	–
Lepisosteus oculatus	LOCP00000004106	LOCP00000005356	LOCP00000006811
Gasterosteus aculeatus	GACP00000018746	–	–
Tetraodon nigroviridis	TNIP00000003370	–	–
Danio rerio	DARP00000099822	–	2a_DARP00000019431 2b_DARP00000048847
Latimeria chalumnae	LACP00000008032	–	LACP00000020283
Ictalurus punctatus	AHA57575	–	–
Nothobranchius furzeri	0000737	–	–
Funduls heteroclitus	AAS21300.2	–	–
Sciaenops ocellatus	ACU98970	–	–
Anguilla anguilla	g15096_t1	–	–
Carassius auratus	–	–	(a) AAX85387 (b) AAX85386
Ctenopharyngodon idella	–	–	ADT78701
Megalobrama amblycephala	–	–	AIE77026
Cyprinus carpio	–	–	CAB60197
Carassius carassius	AEV43393	–	(a) AEV43390 (b) AEV43391
Hippocampus kuda	ACL35630	–	–
Claris batrachus	BAO79759	–	–
Platichthys flesus	CAJ29300	–	–
Oncorhynchus mykiss	CDQ73326	–	NP001117831
Salmo salar	SS2U026776	–	–

Note - *The sequence for Anguilla anguilla (in red) was obtained from transcriptome analyses*

2.9.3 Sequences analysis

Each protein was classified studying its functional domains characteristic of each NOS class gene. The sequences, for both phylogenetic studies, were aligned using the ClustalW algorithm (Thompson et al., 1994) and MEGA5 (Tamura et al., 2011) with default parameters. Then, the human nNOS sequence was taken as a reference to take the length of the data sets. When the extremities of the proteins were not comparable they were trimmed to avoid regions of unreliable alignment. Sequences that spanned less than 50% of the human NOSI and had more than 10% of missing characters over the total number of aa per sequence were excluded from the final calculation to avoid erroneous arrangements and increase the power of the nodal support.

Phylogenetic tree has been computed using the Maximum likelihood (ML) and the Bayesian (MrBayes 3.1.2) methods(Huelsenbeck and Ronquist, 2001; Ronquist and Huelsenbeck, 2003). The conventional convergence has been reached when standard deviation value of split frequencies stayed <0.01, while the robustness of the obtained trees has been analysed with 2.000.000 bootstrap replicates.

Chapter 3 - Results

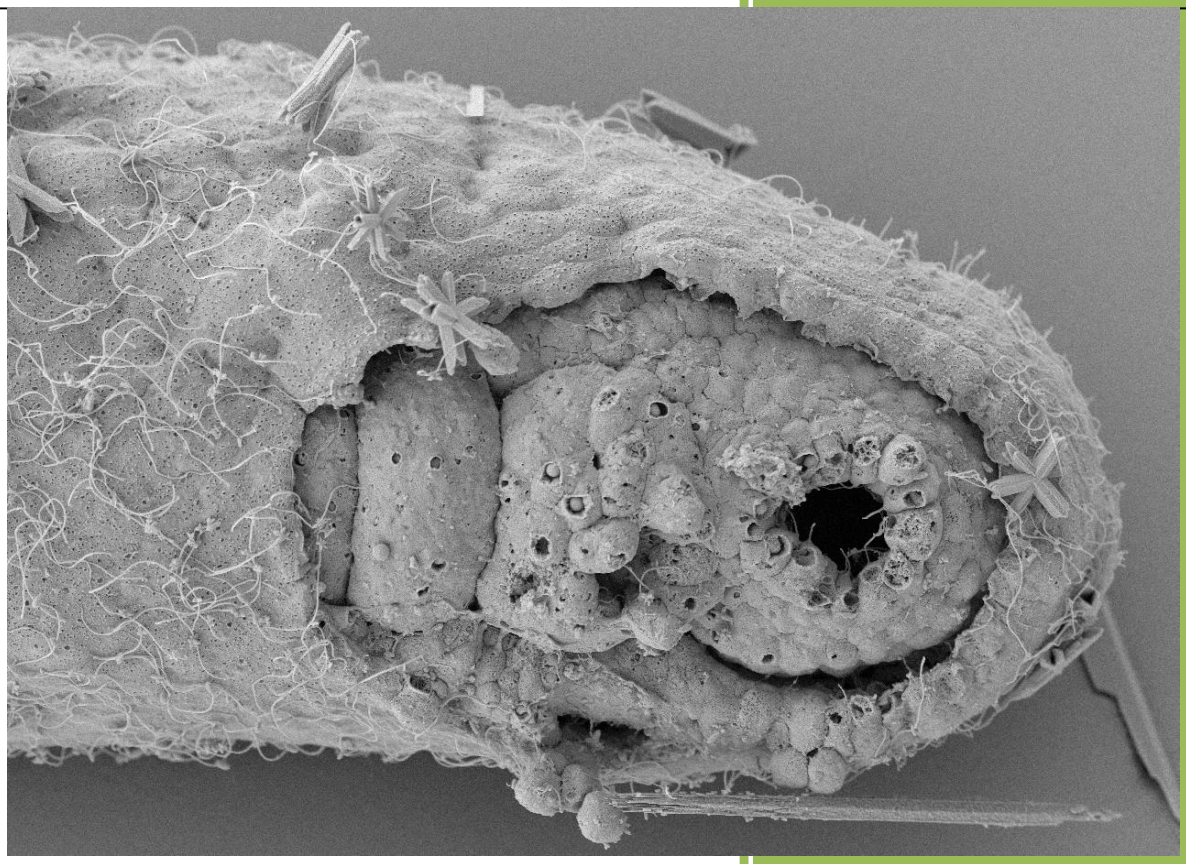

Annona Giovanni, PhD

3.1 NOS phylogeny

To gain insights in the evolutionary history of NOS genes in amphioxus was decided to perform a phylogenetic study adding new NOS sequences from key chordate species to the set of sequences used from Andreakis and collaborators (Andreakis et al., 2011). Was included NOSs sequences from three Branchiostoma species and from the recently available transcriptome of a basal cephalochordate: *Asymmetron lucayanum* (Yue et al., 2014). Moreover, with a second phylogenetic analyses we explored the issue of the presence of canonical NOS genes in chondrichthyes and in the lineage of the bony fishes, since it was missing in the current literature.

3.1.1 Cephalochordates NOS phylogeny

Branchiostoma sp, as described before, have three different NOS genes resulted from lineage-specific duplications. In order to establish a possible evolutive scenario we performed an evolutionary study considering the NOS proteins from three amphioxus species, the basal cephalochordate *Asymmetron lucayanum*, tunicates such as *Ciona intestinalis* and *Ciona savinyi,* and basal vertebrates as lampreys *Lethenteron japonicum* and *Petromizon marinus,* and hagfish *Eptatretus burgeri.* The sea urchin *Strongylocentrotus purpuratus* NOS was chose as outgroup. The phylogenetic tree highlighted that in Asymmetron two NOS genes are presents, orthologs of the amphioxus NOS-A and NOS-B. A duplication event was found in the two lamprey as well, even if these sequences, at the moment, are partial and therefore the orthology inside the group is still not really clear. Interestingly the unique sequence isolated from the hagfish *E.burgeri* branched at the base of cyclostome group.

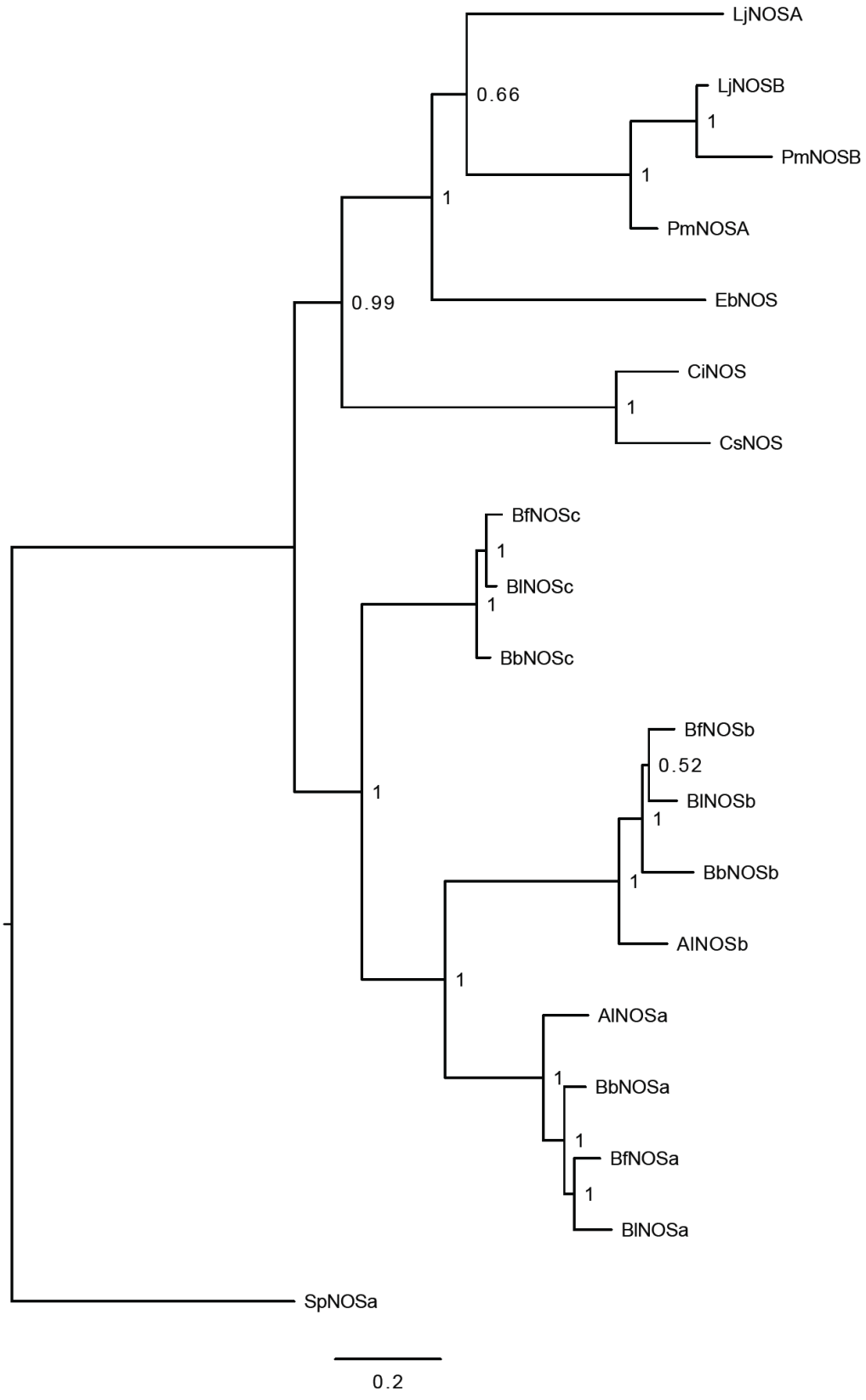

Figure 3.1 -*Cephalochordates NOS phylogenetic tree.*

3.1.2 Bony fishes and chondrichthyes NOS phylogeny

For the study of NOS phylogeny in fishes was analyzed all available NOS protein sequences of 29 teleost fishes, 4 chondrichthyes fishes, 3 cyclostoms and sequences of human, frog and lizard. The unique *Ciona* NOS protein was used as outgroup. The analysis of the sequences indicates that all the fishes, both bony fishes and chondrichthyes, have a neuronal NOS containing the typical PDZ domain (Figure 3.2). Regarding the inducible NOS, the phylogenetic tree indicated that all sharks have one copy of this gene, while in teleost lineageseveral different scenarios can be observed. The iNOS is lost in some species, i.e. *Nothobranchius furzeri* and *Oryzias latipes*, while it is present in one copy in other species, i.e. *Oncorhynchus mykiss* orthe basal fish *Latimeria chalumnae*, or it was found duplicated in some other fish species, as for example in *Danio rerio* or *Astyanax mexicanus*.

The endothelial NOS seems to have a completely different evolutionary history, infact it was absent in all the available fishes genomes except in the spotted gar, *Lepisosteus oculatus,* opening to new interpretations about the NOS evolution (see Discussion).

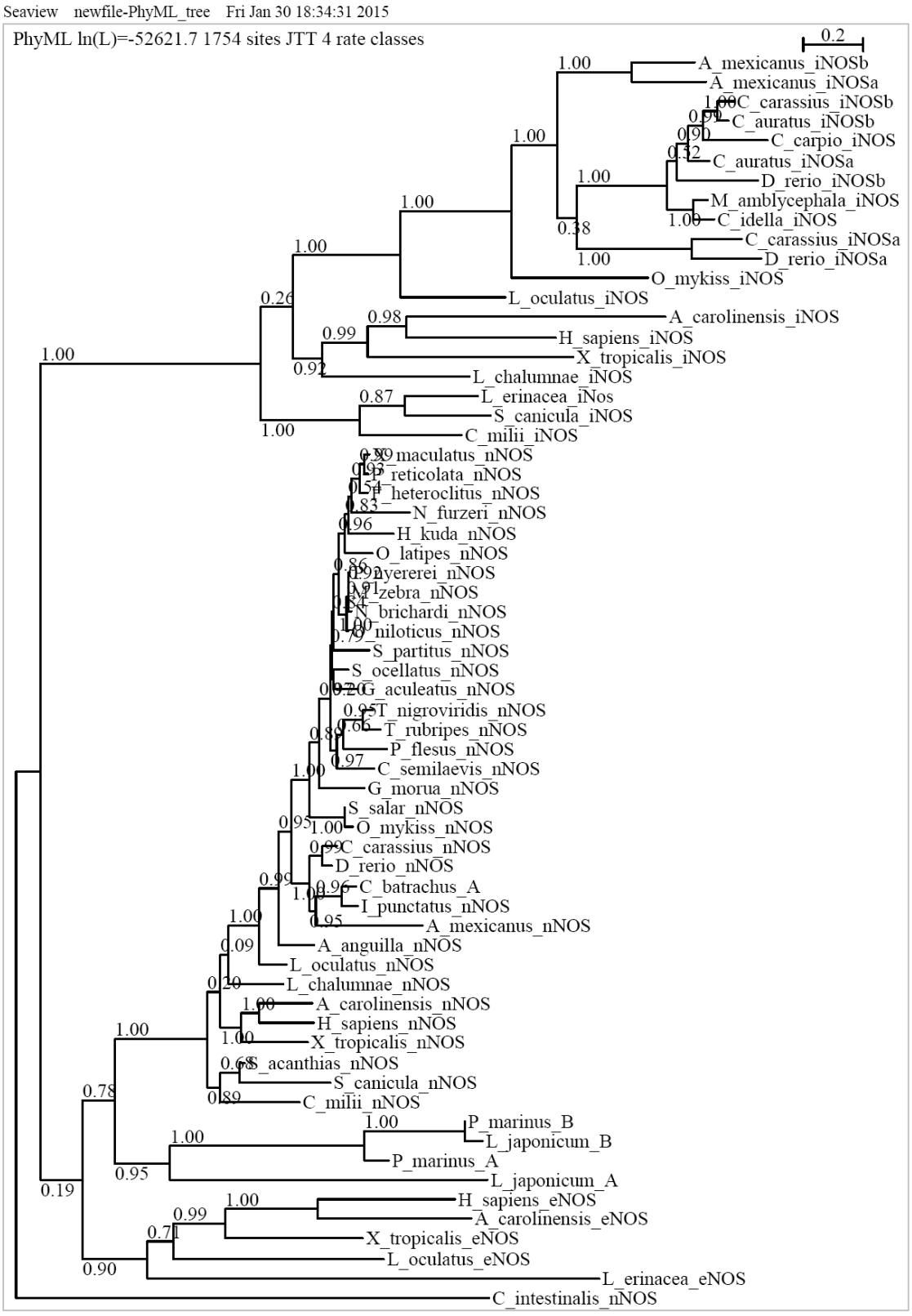

Figure 3. 2 - *Bony fishes and chondrichthyes NOS phylogenetic tree.*

3.2 Characterization of the expression levels of NOS genes in development

In order to characterize the expression levels of the three NOS genes during *B. lanceolatum* development, a quantitative PCR (qPCR) was carried out using total RNA extracted from embryos and larvae at different developmental stages: gastrula (10 hpf), middle neurula (24 hpf),pre-mouth larvae (48 hpf), 3 dpf larvae (72 hpf), 5 dpf larvae (96 hpf), and small adult (1.2cm long). The data obtained from the qPCR were normalized using the housekeeping gene encoding the ribosomal protein L32, AmphiRPL32, which expression is constant during embryogenesis (Kozmikova et al., 2013). To quantify and to represent the NOS expression levels in a graph all the data were reported in function of the developmental stage in which the expression level was the lowest.

3.2.1 *B. lanceolatum* NOS-A gene expression levels

The q-PCR experiments for the NOS-A gene in *B. lanceolatum* did not showed significant results (data not shown). In particular during the developmental the expression level was very low and a moderate increase was found in adult. Nevertheless the results were significantly relevant because the values were under the minimum threshold value of the technique.

3.2.2 *B. lanceolatum* NOS-B gene expression level

The q-PCR experiments for NOS-B showed high expression levels in early embryonic stages. In particular at gastrula the highest level of expression for this gene was detected, followed by a slight decrease at neurula. Later in development the gene seems to completely turn off, as well as in adult (Figure 3.3).

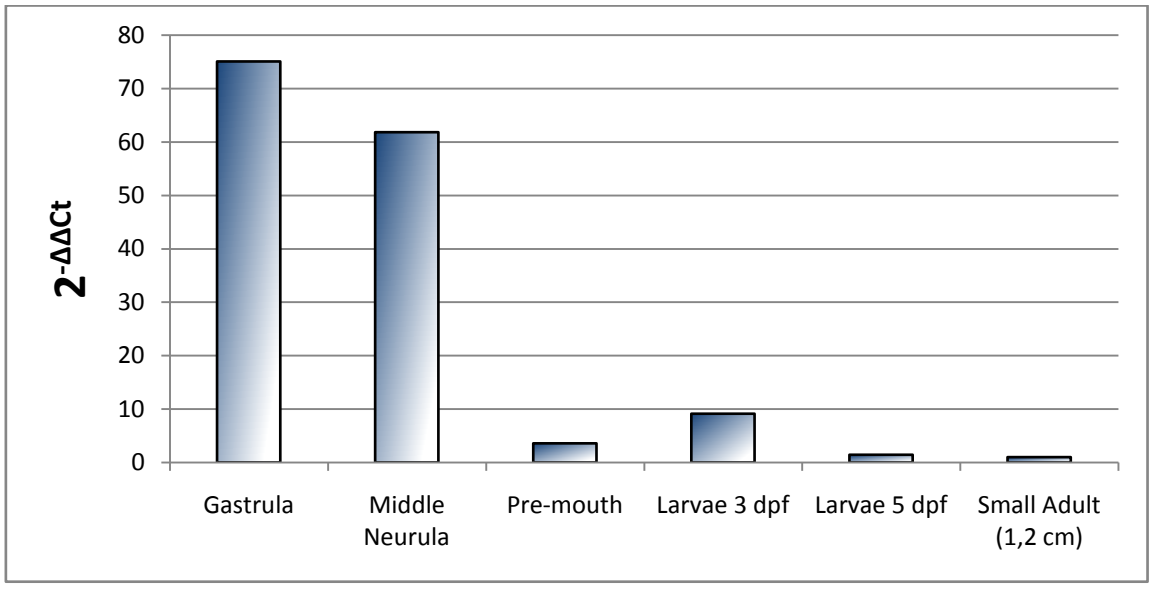

Figure 3.3 - *B. lanceolatum NOS-B expression profile during development.*

3.2.3 *B. lanceolatum* NOS-C gene expression levels

The activation of the NOS-C gene in *B. lanceolatum* seems to be subsequent that of the NOS-B. This gene begins to be express at pre-mouth larvae stage, but only at 3 dpf larvae is possible to observe a peak of its expression, the higher level of the several developmental phases. After a decrease at five days of development was observed, becoming very low in small adult amphioxus (Figure 3.4).

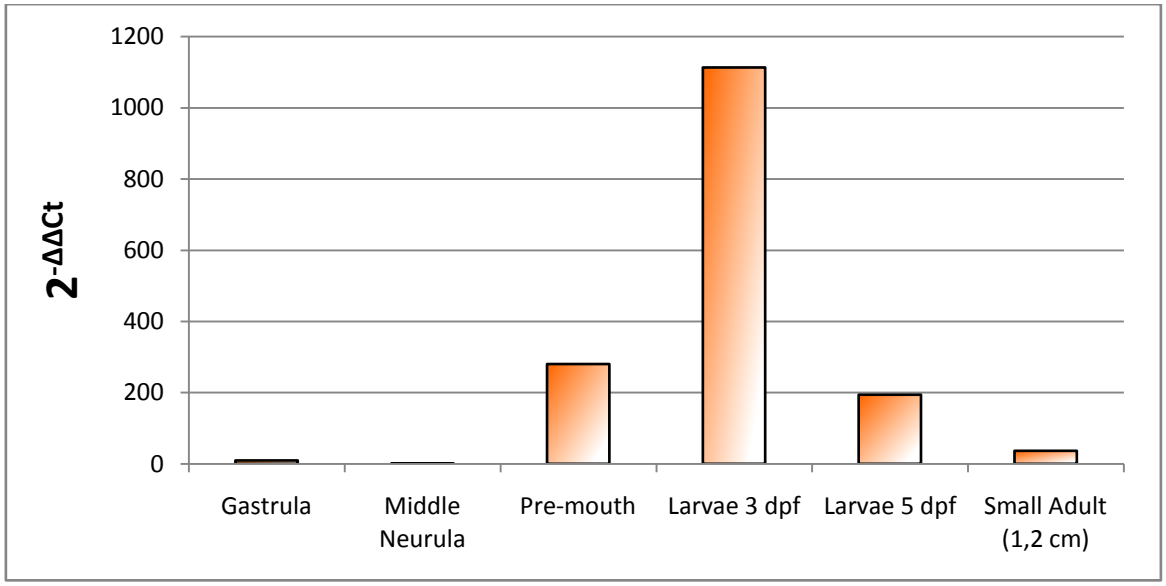

Figure 3. 4 -*B. lanceolatum NOS-C expression profile during development.*

3.3 Characterization of the expression profile of NOS genes in development

In order to reveal the expression pattern of the three paralogs NOS-A, NOS-B and NOS-C, whole mount *in situ* hybridization experiments (WISH) were performed. NOS-B and NOS-C were amplified by a mix of developmental stages cDNA and NOS-A were amplified by cDNA from adult animals. The three genes were cloned and sequenced. The probes, indicated in Table 2.2 were designed in order to avoid cross-hybridization. Antisense riboprobes has been used to detect the three NOS transcripts localization in several developmental stages of amphioxus.

3.3.*1 B. lanceolatum* NOS-A gene expression

As highlighted in the quantitative PCR experiments the NOS-A expression is too low to be detected by *in situ* hybridization experiment in any developmental stage. Several attempts were performed and no specific signal was detected for this gene (data not shown).

3.3.2 *B. lanceolatum* NOS-B gene expression

The NOS-B gene expression in *Branchiostoma lanceolatum* is limited to few developmental stages. The expression starts at early gastrula on the lateral portion of the roof of the invaginated endoderm, in the contact side between endoderm and ectoderm (Figure 3.5 A). Afterwards the signal increase in the middle gastrula stages, along the contact point between the two embryonic layer but not uniformly (Figure 3.5 B); in the diblastic embryo, in one portion of the area surrounding the blastopore the gene NOS-B is not expressed (Figure 3.5 C). The results of q-PCR experiment show a pick of expression also at gastrula stages but the *in situ* hybridization experiments did not show any specific pattern of expression at this developmental stage.

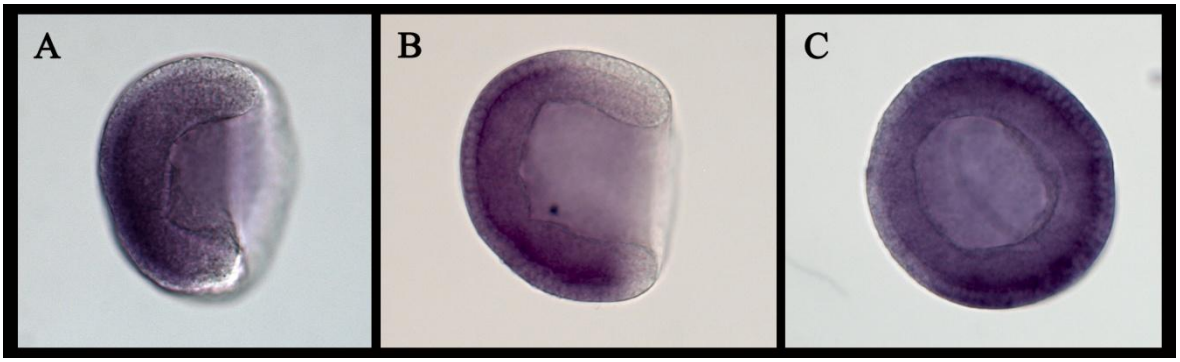

Figure 3.5 -*NOS-B gene expression at gastrula stage. (A) early gastrula stage; (B) middle gastrula stages, lateral view; (C) middle gastrula stages, blastopore view.*

3.3.3 *B. lanceolatum* NOS-C gene expression

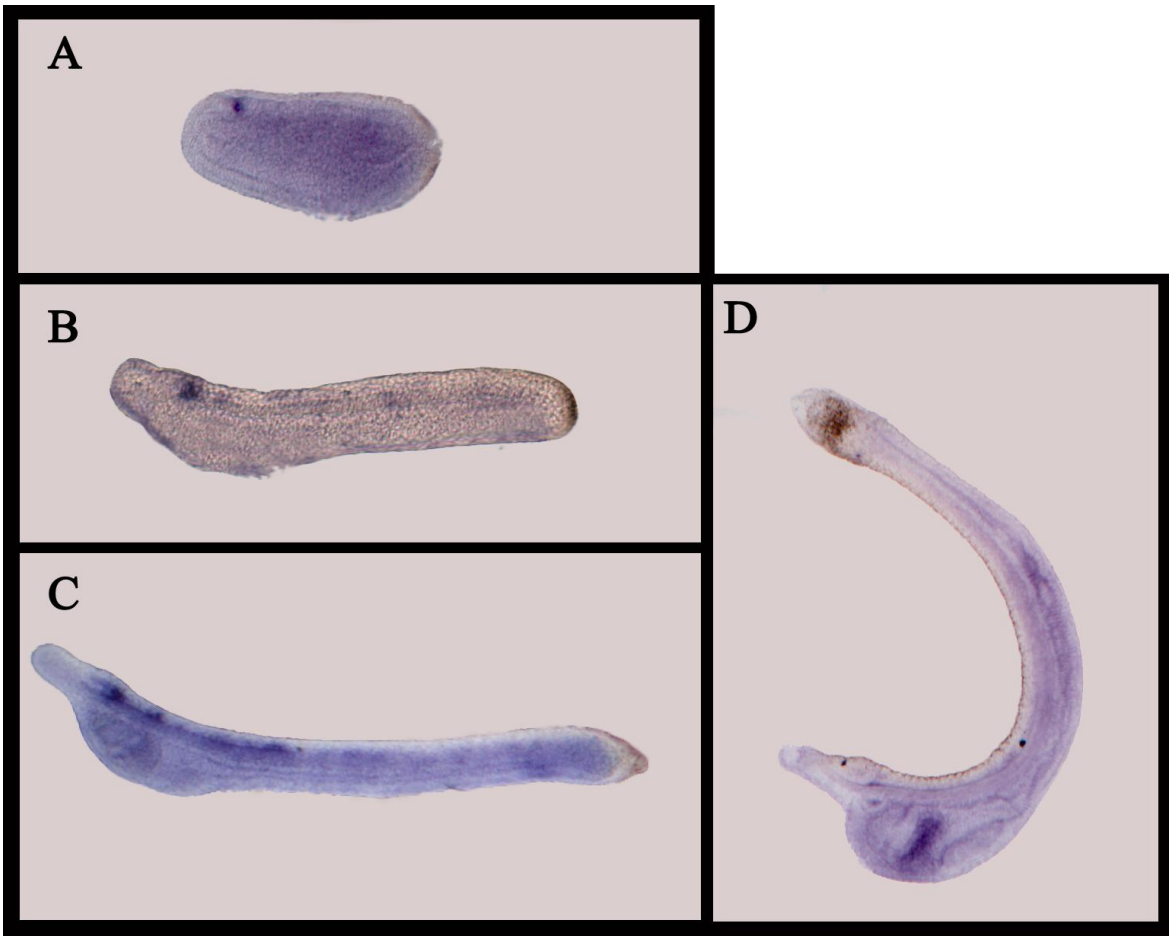

Figure 3.6 -*NOS-C gene expression during the embryonic development. (A) middle neurula stage; (B) late neurula/early pre-mouth larvae; (C) pre-mouth larvae; (D) larvae 3 dpf.*

The gene start to be expressed at middle neurula stage of development (Figure 3.6 A), later than the NOS-B. The expression is localized at few cells in the anterior part of the rudiment of the nerve chord, near the neural pore, stage (middle neurula) in which not yet had the fusion between the two edges of the dorsal portion of the future nervous tube. After few hours of development, there is a light increase of the number of positive cells in the same area (Figure 3.6 B), where at this stage begin to form the cerebral vesicle. At pre-mouth larvae stage (Figure 3.6 C), when the neural tube is completely formed, there is the highest embryonic gene expression level for NOS-C. Moreover at this stage the expression start to be evident in the rostral part of the neural tube until the pigment spot. At 3 days post fertilization (3 dpf) the expression in the neural tube disappear quite completely, but another organ appear to be positive at this stage: the club-shaped gland (Figure 3.6 D), that is closely connected with the endostyle (Holland et al., 2009).

3.3.4 *B. lanceolatum* SoxB1 gene expression

In the *in situ* hybridization experiments were used the SoxB1 gene as control for the experimental procedures. This gene is expressed in the central nervous system (CNS) contributing to neural induction and differentiation (Kan et al., 2004; Kishi et al., 2000). In amphioxus three SoxB genes are present (SoxB a, b and c), and for my experiments we used the paralogue SoxB1c that at middle neurula is expressed in the entire neural tube and marks the foregut; at late neurula stage the expression in the neural tube and foregut persists, SoxB1c positive cells also appear in the hindgut (Meulemans and Bronner-Fraser, 2007)(Figure 3.7).

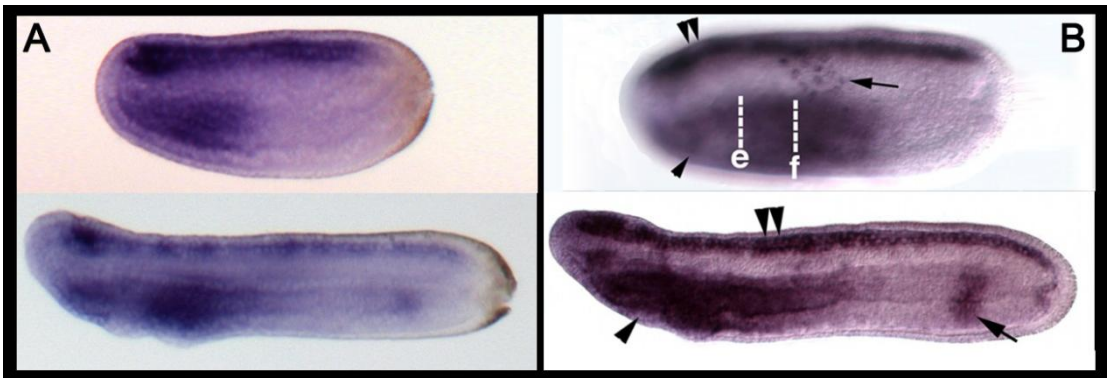

Figure 3.7-*B. lanceolatum SoxB1c expression profile. (A) in situ hybridization used as control for our experiments, (B) in situ hybridization published (Meulemans and Bronner-Fraser, 2007).*

3.4 Endogenous NO level duringdevelopment

3.4.1 Griess assay

The endogenous levels of Nitric Oxide (NO), were measured by monitoring nitrite formation by the Griess reaction (Green et al., 1982). For these series of experiments was used a pellet of embryo consisting of about 1.000 embryo or larvae and one small adult animal of 1.2 cm long. The Griess assay showed a variable amount of NO in the different developmental stages (Figure 3.1). The NO levels, of the same order of magnitude, indicated a average gas production at gastrula stages with a gradual decline until the pre-mouth larvae stage where was detected the lowest level of gas, 4 nmol nitrite/mg protein, and later an higher peak of NO level at 3 dpf larvae, 29.2nmol nitrite/mg protein. In later embryonic stages was found, again, a gradual decrease of NO level

.

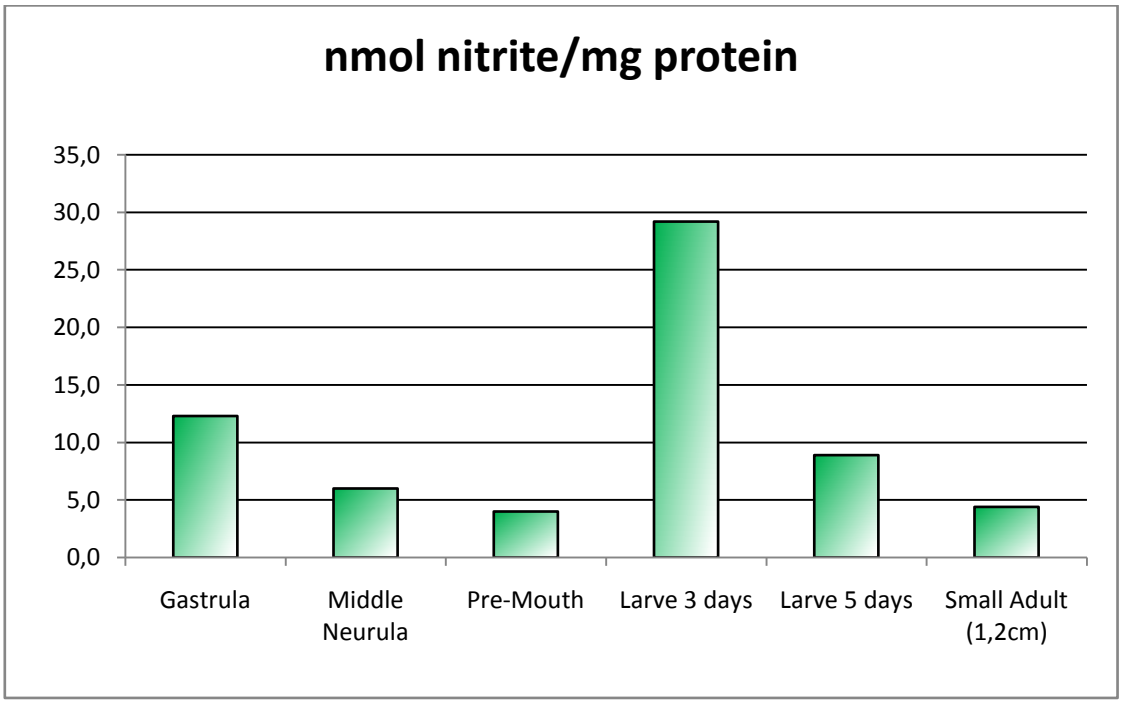

Graph 3.1 -*NO level during the development of Branchiostoma lanceolatum measured by monitoring the nitrite formation by the Griess reaction.*

3.4.2 DAN assay

To confirm the endogenous levels of NO, obtained with Griess assay, we performed a second NO detection analysis using the 2,3-diaminonaphthalene (DAN) that react with nitrite form the fluorescent product 1-(H)-naphthotriazole. The detection of the fluorescence produced was measured using a spectrofluorometer.

As in the previous experiment the NO levels show the same order of magnitude. Contrarily to the previous experiment, the NO value at gastrula is lower than other developmental stages, 3.54 nmol of nitrite per mg of protein, and increase lightly until reaching the pre-mouth larvae, where the NO value is of 11.06 nmol nitrite/mg protein. As in the Griess assay I found that the highest level of endogenous NO is present at 3 dpf larvae, with 64.20 nmol of nitrite per mg of protein, followed by a decrease of NO concentration at the following embryonic stages.

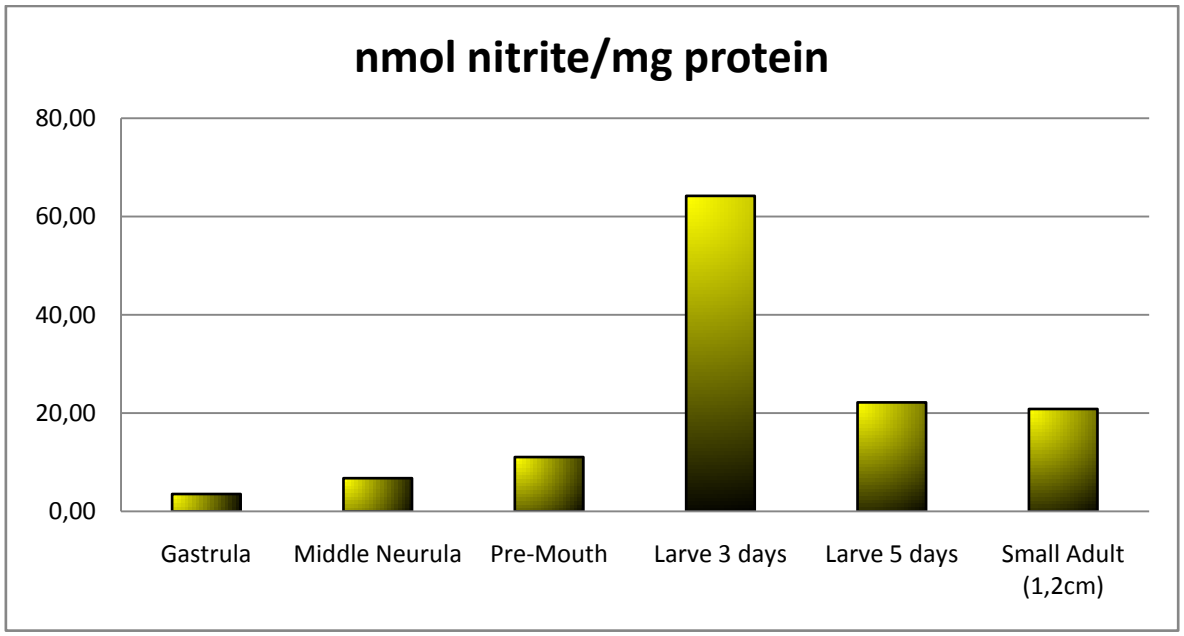

Graph 3.2 -*NO level during Branchiostoma lanceolatum development measured by monitoring nitrite formation.*

3.5 NO localization

To analyze the embryonic territories in which the gaseous NO is involved was used the cell-permeant diaminofluorophore 4-amino-5-methylamino-2′-7′-difluorofluorescein diacetate (DAF-FM DA). Treatments with this drug were performed at the neurula stage with the aim to interfere with the highest endogenous level NO at the 3 dpf larvae. Our results showed that at larval stage NO is mainly present the central portion of the body, particularly in the lateral and ventral area; probably the cells in which NO is detected are two class of neurons: epidermal neurons (red arrows) and ventral epidermis neurons (blue arrows).

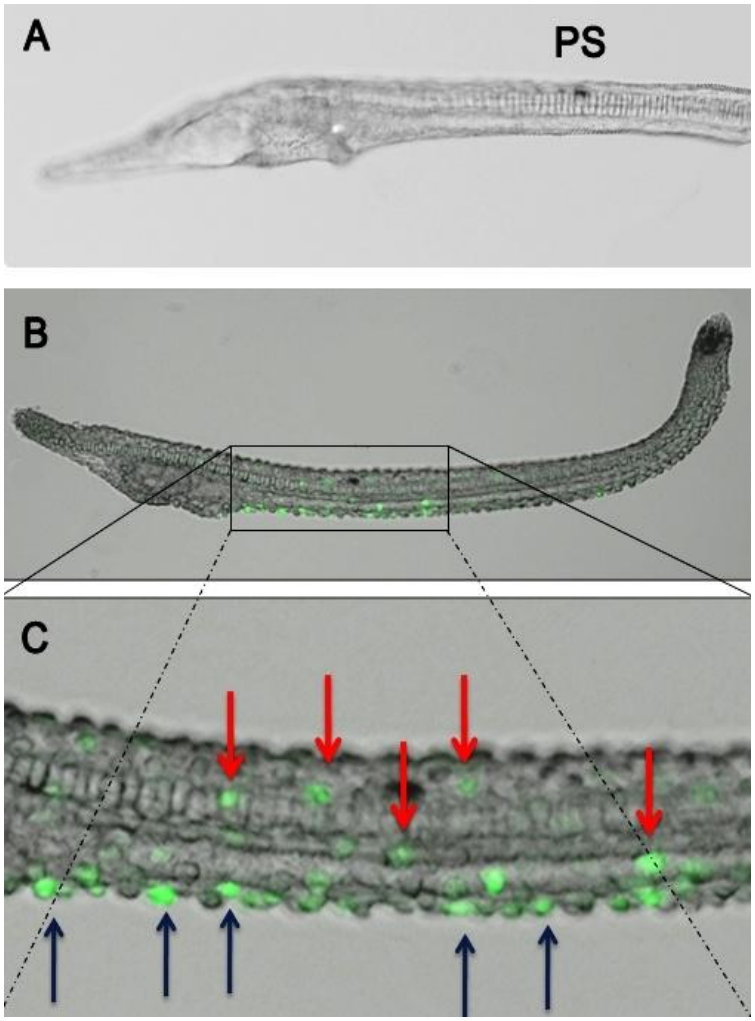

Figure 3.8 -*DAF-FA DA experimental assay in 3dpf larvae: (A) control; (B) 3dpf larvae after treatment; (C) magnification of central part of the body of a treated animal. Red arrows indicate putative epidermal neurons and blue arrows ventral epidermis neurons.*

3.6 Role of NO during the development

In order to understand the involvement of NO during amphioxus development a pharmacological treatments was performed on order to decrease the endogenous level of NO. For this purpose live embryos was treated at several developmental stages with several concentrations of L-NAME (N_{ω}-Nitro-L-arginine methyl ester hydrochloride) that is a competitor of the substrate of the NOS enzyme, the L-Arginine: gastrula, neurula and pre-mouth larvae. The treatment starting from gastrula and pre-mouth stage with different drug concentration did not give any phenotype (green symbols, data not show). Conversely, treatments done starting at neurula stage showed alterated phenotypes in a concentration dependent manner (Figure 3.3, yellow and red symbols).

The colorful symbols in the graph indicate the drug concentration at which the treatment was performed. Green symbols indicate that no one abnormal phenotype was found, while yellow and red symbols indicate the severity of phenotype obtained after treatment, showed in the Figure 3.9.

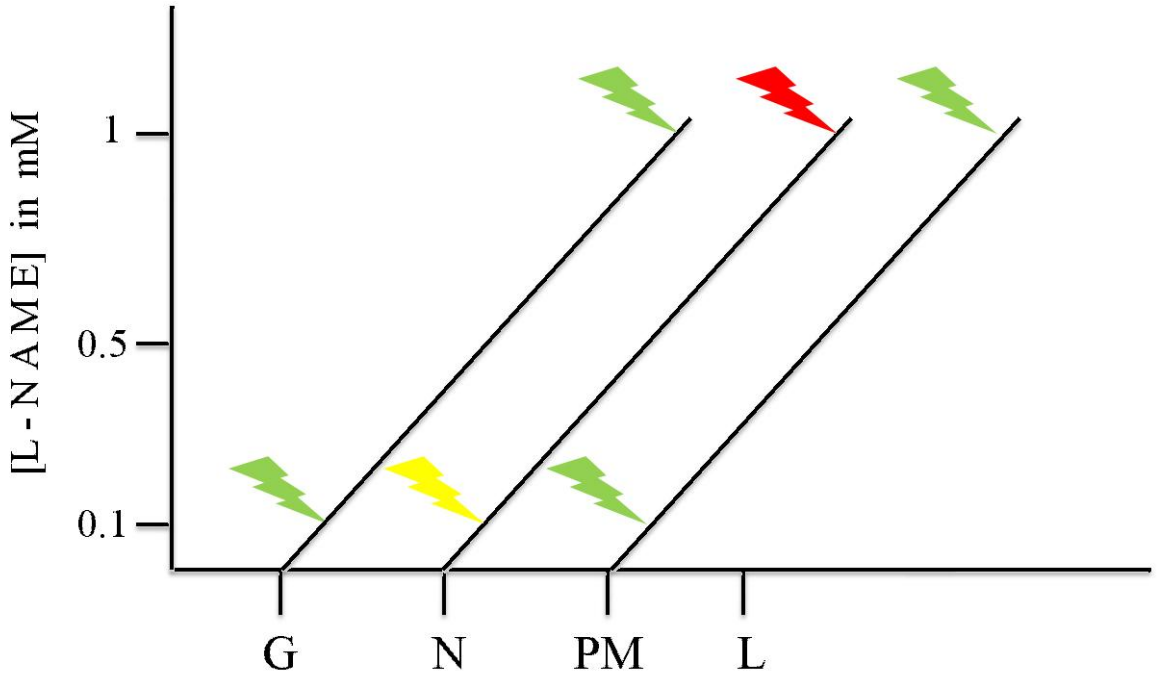

Figure 3.3 -*Schematic representation of L-NAME pharmacological treatment in different developmental stages. Colorful symbols indicate the severity of the phenotype.*

At low L-NAME concentration (0.1 mM, yellow symbols) larvae have abnormal development of mouth and gills area. Nevertheless, increasing the drug concentration to 1 mM it was observed that the mouth region was severely compromised. While the general morphology remained quite normal, in fact, the mouth and gill slits were impaired within 60% of the larvae showing the completely absence of the mouth opening (Figure 3.9 D, red symbols).

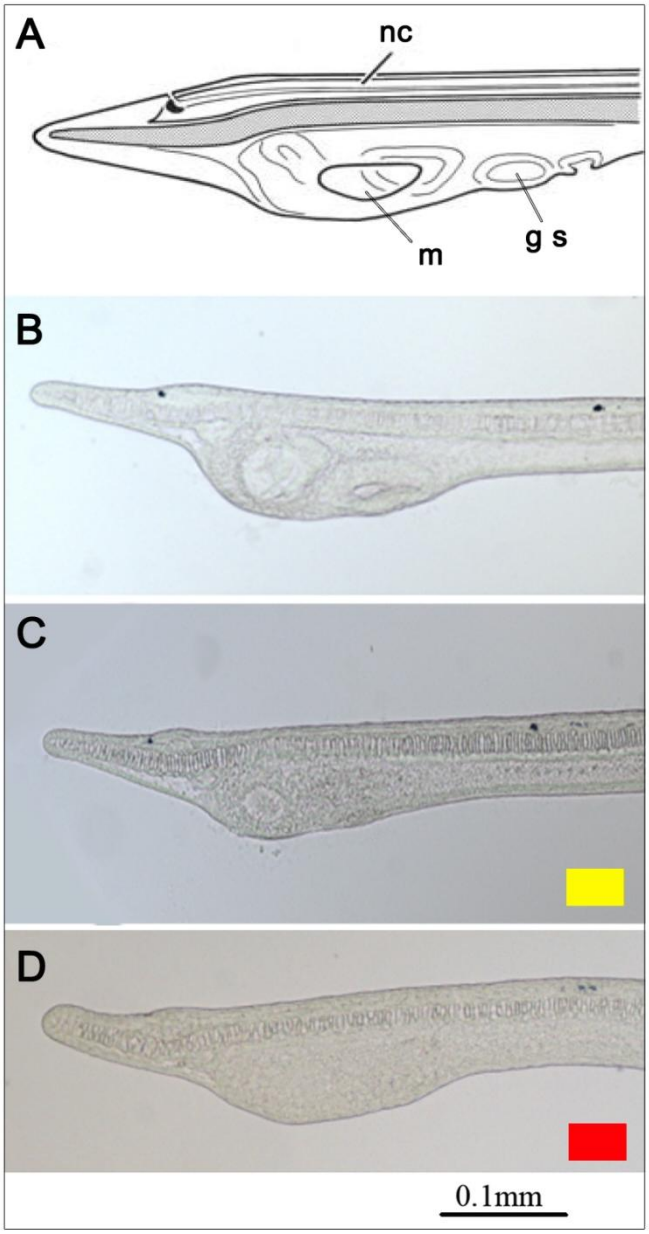

Figure 3.9 -*Scheme of wild type and treated larvae. (A) schematic representation of a normal larva; (B) wild type phenotype; (C) larvae whit abnormal development of mouth and gills area; (D) more severe phenotype with absences of the mouth opening.*

Chapter 4 - Discussion

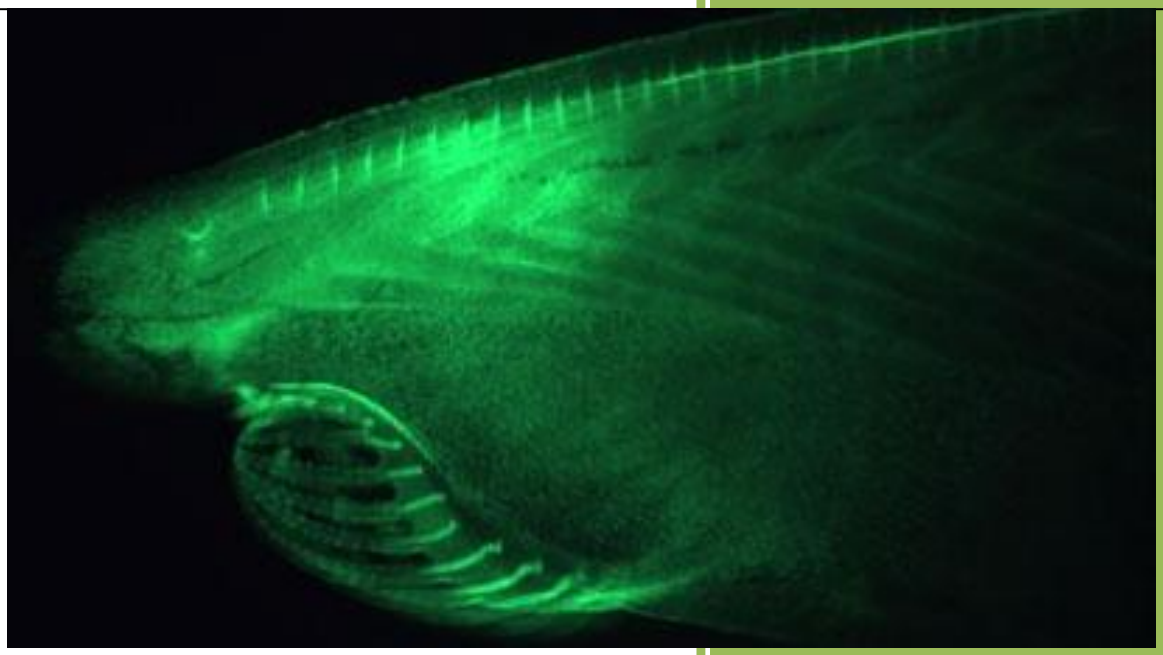

Annona Giovanni, PhD

The Nitric Oxide (NO) pathway is one of the oldest bioregulatory systems controlling human and animal physiology. NO have probably played a crucial role in the early stages of the evolution of life providing protection to primitive microorganisms, neutralizing the aggressive oxidative effect of ozone levels (O_3) rising in the earth atmosphere. NO does not require the help of carrier molecules in order to cross cell membranes and can easily reach intracellular target molecules by free diffusion. Therefore it is quite obvious that NO acquired novel functions beyond the mere enhancement of survival (Feelisch and Martin, 1995). To gain insights in the evolutionary history of NOS genes in cephalochordate and in the group of the fish a phylogenetic study was performed. Andreakis and collaborators already clarify the number, classification and homology of the amphioxus NOSs (Andreakis et al., 2011) but the evolution of these gene in the cephalochordate group was still an open question. Our analyses show that in the basal *Aymmetron leucanum* only two paralogues are present, the NOS-A and NOS-B, while three NOS genes are present in the branchiostoma's group. We propose different hypothesis to try to explain the possible evolutionary scenario. A possible explanation could be the loss of NOS-C gene in Asymmetron or that a possible gene duplication of the neuronal NOS occurred specifically in the branchiostoma's group leading to the current situation of a duplicate neuronal NOS gene and an unique inducible NOS-B. The Asymmetron sequences were obtained by an embryonic transcriptome data collection, therefore another possibility is that the neuronal gene NOS-C is present in the genome but it is never expressed during embryogenesis, like occurs for the NOS-A in *B. lanceolatum*. Deeper studies will give us the answer, probably when the genome of *Aymmetron leucanum* will be available.

Moreover data analysis, collected sequences and the evolutionary tree give us the possibility to study the NOS evolutionary history of other basal animals. During our study we found that in cyclostomes, the most basal group of vertebrates, show a different NOS content. Lampreys, *Petromyzon marinus* and *Lethenteron japonicum,* possess two NOS genes, while in hagfish *Eptatretus burger*, only one NOS gene is present. Like in the case of asymmetron the data obtained for hagfish belong to a

transcriptome, so we cannot assert with certainty that in the *Eptatretus burger* is not present another NOS gene.

To go deeper in the evolution study of NOS gene we looked for the NOS sequences fish available in online databases. All the fishes, either bony and cartilaginous ones, has a neuronal form, while none of them has an endothelial NOS gene, except the spotted gar *Lepisosteus oculatus (Donald et al., 2015).* This is interesting from an evolutionary and physiological point of view because it is still a mystery how the majority of fishes substituted the endothelial NOS activity in heart and vessels.

Major differences was been found in the fast evolving inducible NOS for which is always present in one copy in chondrichthyes while in teleosts a different scenario is present. The iNOS is lost in some species, i.e. *Nothobranchius furzeri* and *Oryzias latipes*, while it is present in one copy in other species, i.e. *Oncorhynchus mykiss* or the basal fish *Latimeria chalumnae*, or it was found duplicated in some other fish species, as for example in *Danio rerio* or *Astyanax mexicanus*. This result confirm that the neuronal gene, involved in the neurotransmission, is always present and in some species, where the inducible NOS in absent, the neuronal gene could compensate the activity in the immune defense system (Jiang et al., 2013). During amphioxus development, the NOS-C starts to be expressed at neurula stage, when the neural tube is forming. A signal is present in few cells in the most anterior part of the neural tube, like for other genes involved in neurotransmission pathway. Interestingly, in 2012 Candiani and collaborators studied genes encoding biosynthetic enzymes as glutamic acid decarboxylase (GAD) and transporters as Vesicular Glutamate Transporter (VGLUT) and vesicular GABA/Glycine transporter (VGAT) of the most common animal neurotransmitters and assayed their expression pattern during embryo and early larvae developmental (Candiani et al., 2012). The expression territories of VGLUT, GAD and VGAT were very similar to that of NOS-C gene, and they start to be expressed at the same developmental stages at 14-16 hpf, neurula. Moreover later in development, at pre-mouth larvae stage the genes involved in neurotransmission are present mainly in the anterior half of the larvae body, from the rostral sensory vesicle to

the mid-caudal pigmented spot. Apparently this is exactly the same for NOS-C expression at same developmental stages. During the development, the number of NOS-C positive cells increases until the pre-mouth larvae stages, when the neural tube is forming. Taking all this into consideration, double *in situ* hybridization experiments, with some of these neurotransmitter markers, should be performed in future to test this hypothesis. In the teleost fish *Danio rerio* the nNOS expression in the brain initially is restricted to the ventrorostral cell cluster (vrc), subsequently the expression occurs in ventrocaudal cell cluster (vcc), dorsorostral cell cluster (drc) and hindbrain cell clusters (hc), followed by an increase in expression from 40 hpf and the presence of different nNOS mRNA-expressing cell populations in all many regions ofthe brain at 55 hpf (hatching larvae) (Holmqvist et al., 2004). Probably a comparison between vertebrates and cephalocordates neuronal NOS gene expression pattern seems to be too risky, however considering recent studies (Wicht and Lacalli, 2005) which compared different areas of nervous system between amphioxus and vertebrate, is possible to compare gradual increasing of NOS-C expression from the cerebral vesicle to the half neural tube with the spatial and temporal distribution of nNOS mRNA-expressing cell populations in embryonic zebrafish development.

In conclusion, it seems that the NOS-C is the only NOS gene involved in neurotransmission and it is somehow involved in developing CNS in amphioxus.

My experiments showed an high NOS-C enzymatic activity and an increase of Nitric Oxide concentration mainly in the larvae of 3 days post fertilization (3dpf). This larvae stage is considered pre-metamorphic with a peculiar morphology with a formed neural tube and the mouth opening on the left of the body, and the presence of transitory larval organs: the endostyle, pre-oral pit and the club-shape gland. The function of these organs has long been debated and still the question is not completely resolved. Recent studies seem to agree that the club-shaped gland, the tube connecting the pharyngeal lumen with the external environment, cooperates with the endostyle to produce mucopolysaccharides in the capture of ingested particles and then to transport them to caudal gut regions (Holland et al., 2009). Interestingly, Kaji and collaborators characterized the oral innervations in

pre- and post- metamorphic larvae demonstrating a highly innervation of the pharynx area (Figure 4.1), indicating that the club-shaped gland, the pre-oral pit and the endostyleare probably are promoters of important processes as mouth opening, metamorphosis and immunity (Kaji et al., 2009)

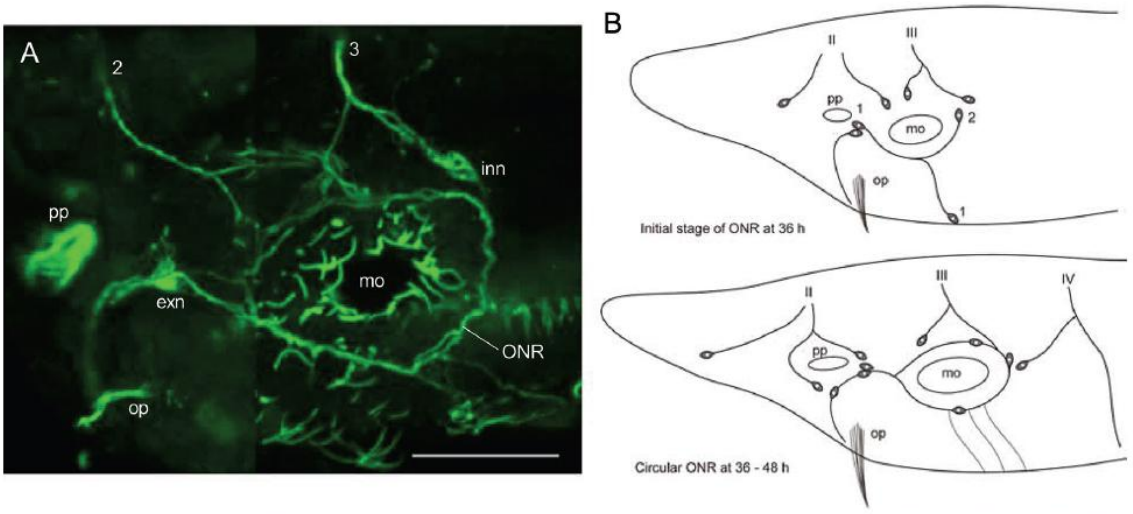

Figure 4.1 -*Neuron organization in the mouth and pharynx area. (A) Mouth neural innervation visualized by anti-acetylated alpha tubulin monoclonal antibody. (B)Schematic representation of neuron organization in 36 hpf and 48 hpflarvae. Arabic numerals and Roman numerals in B denote centrally derived left nerves. Abbreviation: exn, extrinsic neuron; mo, mouth; inn, intrinsic neuron; ONR, oral nerve ring; op, oral papilla; pp, preoral pit* (Kaji et al., 2013)

Between the many regulatory roles of NO it is known that it is able to regulate the apoptosis process (Kim et al., 2001). Comes and collaborators have proven that NO is a critical endogenous regulator of metamorphosis in *C. intestinalis*, controlling the initiation of the caudal regression through repression of the caspase-3 activation (Comes et al., 2007). In amphioxus several caspase are present that play important roles in adult amphioxus immunity (Xu et al., 2011). In an attempt to understand the caspase functions during amphioxus development, Xu and collaborators treated embryos soon after fertilization with four specific caspase inhibitors. Anti-caspase2 treated embryos at 30 hpf were shorter compared to controls, and interestingly showed the delayed opening of mouth (Xu et al., 2011).

Analyzing our results, we hypothesized that the high level of expression of NOS-C gene and of NO concentration at larvae stages can be linked with the reorganization processes that occur in this developmental phase. In particular the NOS-C positive cells found in the club-shape gland could be responsible of the high NO production, which in turn is involved in the morphogenic process and possibly in the induction by apoptosis needed for the mouth opening.

To confirm this hypothesis, an NOS inhibitor was used during amphioxus development. The L-NA/L-NAME treatment is commonly used to decrease the endogenous level of NO. *Ciona intestinalis* treated larvae, for example, show that NOS inhibition accelerates metamorphosis but does not affect the subsequent juvenile development (Comes et al., 2007). Interestingly, our experiments showed that treatments with medium concentration of NOS inhibitors interfered with the normal development of the mouth, while high concentrations produced a phenotype in which the mouth appear to be completely absent. These functional experiments seem to confirm, therefore, the involvement of the gaseous neurotransmitter NO in the mouth specification and in particular that the NOS-C gene is the major contributor of NO synthesis. To better understand the role of NO in mouth formation we used the Scanning Electron Microscopy (SEM) technique to visualize morphologically the absence of mouth opening (Figure 4.2).

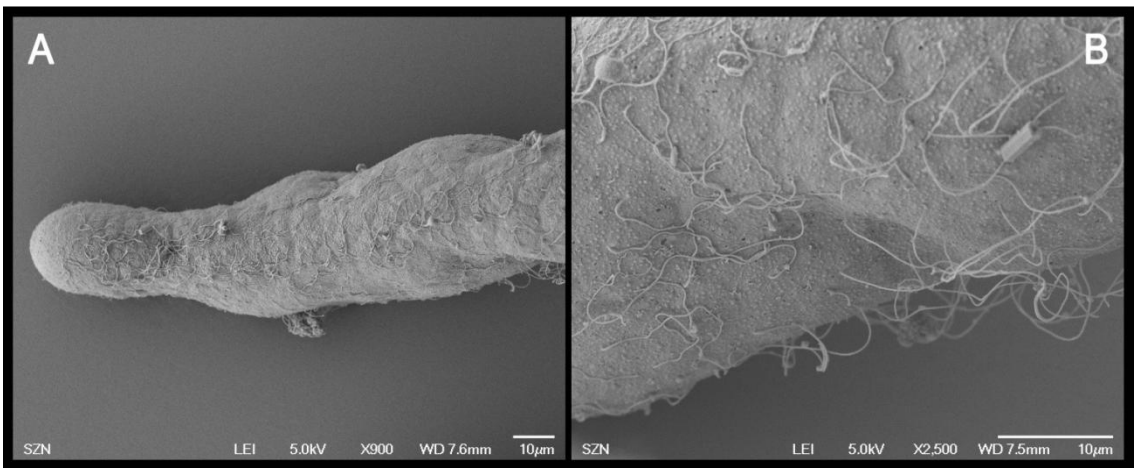

Figure 4.2 -*Amphioxus pre-mouth larvae at Scanning Electron Microscopy (SEM). (A)Rostral portion of Amphioxus larvae.(B) Magnification of the invagination spot where the future opening of the mouth.*

On the other hand, as reported by Andreakis and collaborators, the NOS-A derive from a specific gene duplication event but no implication in embryo development was found neither by gene expression analyses and by q-PCR nor by several *in situ* hybridization experiments. One possibility is that the NOS-A enzyme is involved in adult animal physiology, like it occurs in other model systems, as rat (Rodrigo et al., 1994) and fish (Holmqvist et al., 2000) for example. Another possible explanation is that the NOS_A gene could be a pseudogene with no apparent functions (Gerstein and Zheng, 2006) To confirm these theories further studies are needed.

During the early steps of development, two main morphogenetic processes, cell proliferation and morphogenetic cell movements, are tightly integrated. Active cell duplication is required to generate a sufficient number of cells and specific coordination is necessary during morphogenetic cell movements in gastrulation to organize the body plan during embryogenesis. It has been discovered that NO is involved in cell division and cell motility at gastrulation (Kuzin et al., 1996; Peunova et al., 2007). Kuzin and collaboratores discovered that in the fly *Drosophila melanogaster* (protostome) NO can play a broader role as a general regulator of cell proliferation and differentiation during organism development and morphogenesis (Kuzin et al., 1996). Peunova and collaborators established, studying *Xenopus leavis* ,that also in this animal model system (deuterostome) NOS regulates both the cell division and cell motility machineries during development (Peunova et al., 2007). Changes in NO availability affect these two processes in a reciprocal manner: NO suppresses cell division and facilitates cell movement, whereas a deficit of NO increases cell proliferation and hinders cell movement. Our quantitative-PCR experiments showed high NOS-B expression level in the first developmental phases, in particular at gastrula stages, then confirmed also by *in situ* hybridization experiments. These results and the similarity with Drosophila and Xenopus studies, lead us to hypothesize that also in amphioxius the NOS-B gene may provide the input to stop the cell proliferation at gastrula and on the other hand to start all the process involved in tissue reorganization, typical of the neurula stages. Our experiments indicated that an

expression level start at gastula stage but further studies needed to understand if this gene is expressed also in earlier stages and even if it is of maternal origin.

The amphioxus nervous system is composed of about 20.000 neurons. In addition to the dorsal central nervous system (CNS), amphioxus also have a peripheral nervous system (PNS) comprising several types of sensory neurons (Wicht and Lacalli, 2005) Among these amphioxus sensory neurons, the solitary type I receptor cells are the most abundant population of the epidermal sensory neurons (ESNs) and are scattered along the body of developing amphioxus larvae and adults. The cell body of the receptor is located within the epidermis, and a long axon from the base of the cell body extends into the CNS.

In order to detect endogenous NO by the sensitive and NO specific DAF-FM-DA fluorescence assay was performed. In *Ciona intestinalis* revealed that NO at late larva stage, present as a diffuse signal mainly localized in the posterior part of the sensory vesicle and in the tail (Comes et al., 2007) where is present an high concentration of neurons, of several types (Imai and Meinertzhagen, 2007a; Imai and Meinertzhagen, 2007b). In the same way NO detection assay was used by Lepiller and collaborators to study the endogenous level of NO in 5-day-old zebrafish larvae (Lepiller et al., 2007) The staining pattern obtained mainly consisted in theheart region, forming bones with pharyngeal jaw bones, the notochord and the caudal fin.

Our NO localization experiments showed that NO-positive cells were present along epidermis and in the ventral part of the body. This can indicate that NO can be synthesized in the CNS and it migrate along the axon versus the peripheral neurons where it can act in the several pathway in which it is involved.

Conclusion

The use of model organisms to study structures, organs and complex biological processes, has enabled countless scientific discoveries and still occupy an important role in biological fields.

To better understand the evolution and function of the NOS genes in chordates, we choose a "living fossil" model organism as the cephalochordate Amphioxus considered as *vertebrate-like* animal but simpler from a genetic and morphological point of view.

The amphioxus is the best available stand-in for the ancestor of the vertebrates. Amphioxus has a body plan, central nervous system, circulatory system and that are, but simpler, and this "simplicity" is also reflected at the genomic level.

Our experiment showed that two of three NOS genes are expressed during amphioxus embryological development. The two genes was consequential, one expressed in the early developmental stages during morphogenic processes that drives the body formation and the second one expressed later during the neural tube specification. it has been hypothesized that the NOS-B, with earlier expression was involved in the block of cell proliferation and tissue reorganization and that NOS-C was the gene involved in the neurotransmission pathway.

Quantitative experiments indicated that the gaseous neurotransmitter NO was present, in higher concentration at 3 days post fertilization stage when the m-RNA NOS-C positive cells was present in the clup-shape gland (csg). It is known that NO is involved in apoptotic process as regulator of caspase action and analyzing our results we hypothesized that the NO produced in the csg area was involved in the apoptotic process inducing the mouth opening. To confirm these theories a treatment with a NOS inhibitor, L-NAME was performed. The treatment on NOS inhibition seems to confirm our theories, in fact the treated larvae showed an interesting phenotype, with the complete absences of the mouth opening.

To gain insights in the evolutionary history of NOS genes in cephalochordates a phylogenetic analyses was performed between basal members of the chordate phylum. With the available data we cannot state the exact evolutionary scenario of

the NOSs in cephalochordates, but we could only hypothesizethat the third NOS is not present in the basal cephalochordate Asymmetron, therefore an invention of Branchiostomidae, or that it has been lost in Asymmetron.

Thanks to this research we discovered that also in amphioxus NO is involved in tissue specification at early stages of development and moreover a new processes in which NO is involved in the control of the apoptosis that is invoved in mouth specification, the but still many questions remain open regarding the roles of this molecule in amphioxus.

Acknowledgment

I would like to thank all the people that helped me during this intense and passionate period of PhD thesis.

First of all I own my deepest gratitude to Salvatore D'Aniello, the person who gave me the possibility to do this formative experience and that trusted in my capabilities, always in a friendly and patient way.

I thank Professor Paolo De Girolamo , for his support and precious advises. I acknowledge Dr. Maria Ina Arnone for her hospitality, the stimulating scientific discussions and to make me feel a component of the group.

I am grateful to all the people that contributed to the accomplishment of my PhD: Dr Anna Palumbo and Dr. Immacolata Castellano for their scientific support and the precious collaboration; Dr. Héctor Escrivà and Dr. Stèphanie Bertrand for samples providing and for making lighter the long nights during the season spawning season in France; Dr. Jr-Kai Yu and Dr. Yi-Hsien Su for the possibility to increase my knowledge in their laboratory in Taipei; Dr. Jia-Xing Yue for the precious support with the Asymmetron NOS sequences; Dr Juan Pascual-Anaya and Dr Shigeru Kuratani for the help with the phylogenic analyses and for the precious sequences of the basal vertebrates (Lamprey and Hagfish); Dr Ron Dirks for having made available transcriptomic data of *Anguilla anguilla;* Dr. Demian Burguera for his scientific support.

I would like to thank not my colleagues but my Friends of the past and the present that in these years "supported" me in anyway.

I should to thank the department of Department of Biology and Evolution of Marine Organisms of the Stazione Zoologica Anton Dohrn that has provided the support and equipment I needed to produce and complete my thesis as well as and all the Zoological Station services: the Molecular Biology Service, the Fishery Service, the Marine Models for Research Service and the Electron and Confocal Microscopy Service.

I have to thank Marie Curie grant (Carrer Integration Grant to Salvatore D'Aniello n. FP7-PEOPLE-2011-CIG) that has so generously founded my studied during last three years.

Finally but most importantly I have to thank my family and
you that never stopped believing in me.

Collaborative project

In the framework of my PhD project I had the possibility to collaborate with Filomena Ristoratore research group at the Stazione Zoologica Dohrn. They were interested in clarifying the orthology, chromosomal synteny organization and developmental expression pattern of Rab32/38 subfamily genes within chordates. In the next page I report the synthesis of background, results and conclusions of the manuscript that at the moment of my thesis submission was under revision in BMC Evolutionary Biology.

My contribution to this collaborative project was to perform whole-mount *in situ* hybridization experiments for the amphioxus Rab32 expression during development, as shown in the Figure used embryos of the local amphioxus species, *Branchiostoma lanceolatum*, from the Gulf of Napoli. Moreover, I participated in the figure preparation, critical discussion of the results and finally in the manuscript writing.

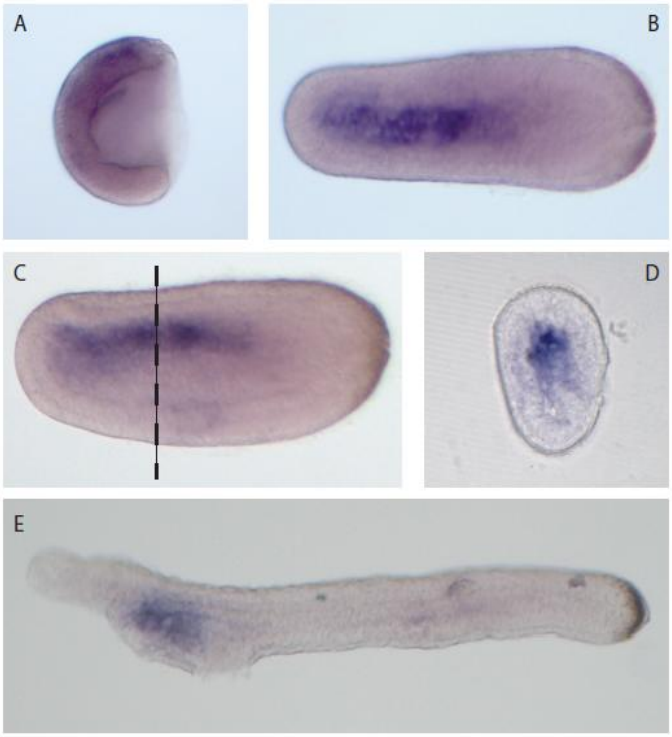

Figure 1 -*Amphioxus Rab32 expression pattern during development. (A) Gastrula, (B) Middle Neurula dorsal view, (C) Middle neurula Dorsal view, (D) Middle neurula section , (E) Pre-mouth larva.*

Manuscript under revision in BMC Evolutionary Biology.

Rab32/38 duplicated genes in chordate pigmentation: an evolutionary perspective

Ugo Coppola, Giovanni Annona, Salvatore D'Aniello* and FilomenaRistoratore*

Department of Biology and Evolution of Marine Organisms

StazioneZoologica Anton Dorhn, Villa Comunale, 80121 Napoli, Italy.

*Corresponding authors: salvatore.daniello@szn.it, filomena.ristoratore@szn.it

Background:

The regulation of cellular membrane trafficking in all eukaryotes is a very complex mechanism, mostly regulated by Rab family proteins. Among all membrane-enclosed organelles, melanosomes are the cellular site of synthesis, storage and transport of melanin granules, therefore they represent an excellent model for studies on organelle biogenesis and motility. Specific Rab proteins, Rab32 and Rab38, have been shown to play a key role in melanosome biogenesis. We analysed all the genes belonging to Rab32 and Rab38 subfamily in a teleost fish model (zebrafish) and in the basal chordate (amphioxus) in order to gain insight on the evolutionary history of these genes following gene and whole genome duplications.

Results:

Sequence-based phylogeny evidenced that the Rab32/38 subfamily is divided in three distinct branches: Rab32, Rab38 and Rab32LO. The Rab32 and Rab32LO proteins are present in all the animals from sponges to human, therefore highlighted as LECA; the latter was lost in olfactores. On the other hand, Rab38 is an evolutionary novelty of vertebrates, arisen from the *en bloc* genome duplication. Comparative expression pattern of Rab32/38 genes in zebrafish and amphioxus evidenced functional compartmentalization of all paralogues and a possible ancient function in notochord development, a function that has been lost in tetrapods. Synteny analysis showed that only one zebrafish Rab38 gene, the one expressed in pigmented cells, retained the linkage with tyrosinase while all other paralogues, not involved in pigmentation processes, lost it. Finally a genetic linkage of Rab32 or Rab38 and a GRM family gene has been conserved in all deuterostomes analysed, despite lack of conservation of any other surrounding gene.

Conclusions:

Phylogenetic analysis, synteny and expression pattern of Rab32/38 genes in representative chordate species allowed us to give insight on the evolutionary history of this gene family. The finding of chromosomal linkage among a Rab32/38 representative and a GRM gene open new perspectives on possible bystander gene regulation conserved across evolution.

Bibliography

Adolf, B., Chapouton, P., Lam, C. S., Topp, S., Tannhauser, B., Strahle, U., Gotz, M., Bally-Cuif, L., 2006. Conserved and acquired features of adult neurogenesis in the zebrafish telencephalon. Dev Biol. 295, 278-93.

Agapie, T., Suseno, S., Woodward, J. J., Stoll, S., Britt, R. D., Marletta, M. A., 2009. NO formation by a catalytically self-sufficient bacterial nitric oxide synthase from Sorangium cellulosum. Proceedings of the National Academy of Sciences. 106, 16221-16226.

Ahern, G. P., Klyachko, V. A., Jackson, M. B., 2002. cGMP and S-nitrosylation: two routes for modulation of neuronal excitability by NO. Trends Neurosci. 25, 510-7.

Alderton, W. K., Cooper, C. E., Knowles, R. G., 2001. Nitric oxide synthases: structure, function and inhibition. Biochem J. 357, 593-615.

Andreakis, N., D'Aniello, S., Albalat, R., Patti, F. P., Garcia-Fernandez, J., Procaccini, G., Sordino, P., Palumbo, A., 2011. Evolution of the Nitric Oxide Synthase Family in Metazoans. Molecular Biology and Evolution. 28, 163-179.

Andrew, P. J., Mayer, B., 1999. Enzymatic function of nitric oxide synthases. Cardiovasc Res. 43, 521-31.

Bardet, P.-L., Schubert, M., Horard, B., Holland, L. Z., Laudet, V., Holland, N. D., Vanacker, J.-M., 2005. Expression of estrogen-receptor related receptors in amphioxus and zebrafish: implications for the evolution of posterior brain segmentation at the invertebrate-to-vertebrate transition. Evolution & Development. 7, 223-233.

Barrington, E. J. W., 1965. biology of Hemichordata and Protochordata.

Benito-Gutierrez, E., 2006. A gene catalogue of the amphioxus nervous system. Int J Biol Sci. 2, 149-60.

Bertrand, S., Escriva, H., 2011b. Evolutionary crossroads in developmental biology: amphioxus. Development. 138, 4819-30.

Bertrand, S. p., Belgacem, M. R., Escriva, H., 2011a. Nuclear hormone receptors in chordates. Molecular and Cellular Endocrinology. 334, 67-75.

Bishop, C. D., Brandhorst, B. P., 2003. On nitric oxide signaling, metamorphosis, and the evolution of biphasic life cycles. Evolution & Development. 5, 542-550.

Bone, Q., 1958. Observations upon the living larva of amphioxus. Pubbl. Staz. Zool. Napoli. 30, 458-471.

Bone, Q., 1989. Evolutionary Patterns of Axial Muscle Systems in Some Invertebrates and Fish. American Zoologist. 29, 5-18.

Brooke, N. M., Garcia-Fernandez, J., Holland, P. W., 1998. The ParaHox gene cluster is an evolutionary sister of the Hox gene cluster. Nature. 392, 920-2.

Bryan, N. S., Bian, K., Murad, F., 2009. Discovery of the nitric oxide signaling pathway and targets for drug development. Front Biosci (Landmark Ed). 14, 1-18.

Bryan, N. S., Grisham, M. B., 2007. Methods to detect nitric oxide and its metabolites in biological samples. Free Radical Biology and Medicine. 43, 645-657.

Candiani, S., Moronti, L., De Pietri Tonelli, D., Garbarino, G., Pestarino, M., 2011. A study of neural-related microRNAs in the developing amphioxus. Evodevo. 2, 2041-9139.

Candiani, S., Moronti, L., Pennati, R., De Bernardi, F., Benfenati, F., Pestarino, M., 2010. The synapsin gene family in basal chordates: evolutionary perspectives in metazoans. BMC Evol Biol. 10, 1471-2148.

Candiani, S., Moronti, L., Ramoino, P., Schubert, M., Pestarino, M., 2012. A neurochemical map of the developing amphioxus nervous system. BMC Neuroscience. 13, 59.

Candiani, S., Pestarino, M., Cattaneo, E., Tartari, M., 2007. Characterization, developmental expression and evolutionary features of the huntingtin gene in the amphioxus Branchiostoma floridae. BMC Dev Biol. 7, 127.

Canestro, C., Yokoi, H., Postlethwait, J. H., 2007. Evolutionary developmental biology and genomics. Nat Rev Genet. 8, 932-42.

Castro, L. F. C., Rasmussen, S. L., Holland, P. W., Holland, N. D., Holland, L. Z., 2006. A Gbx homeobox gene in amphioxus: insights into ancestry of the ANTP class and evolution of the midbrain/hindbrain boundary. Developmental biology. 295, 40-51.

Chen, D., Lin, Y., Zhang, H., 2008b. Characterization and expression of two amphioxus DDAH genes originating from an amphioxus-specific gene duplication. Gene. 410, 75-81.

Chen, J. Y., Dzik, J., Edgecombe, G. D., Ramskold, L., Zhou, G. Q., 1995. A possible Early Cambrian chordate. Nature. 377, 720-722.

Chen, Y., Shin, P. K., Cheung, S. G., 2008a. Growth, secondary production and gonad development of two co-existing amphioxus species (Branchiostoma belcheri and B. malayanum) in subtropical Hong Kong. Journal of Experimental Marine Biology and Ecology. 357, 64-74.

Chin, T., 1941. Studies on the biology of the Amoy amphioxus Branchiostoma belcheri (Gray). Philipp J Sci. 75, 369-424.

Cho, H. J., Xie, Q. W., Calaycay, J., Mumford, R. A., Swiderek, K. M., Lee, T. D., Nathan, C., 1992. Calmodulin is a subunit of nitric oxide synthase from macrophages. J Exp Med. 176, 599-604.

Comes, S., Locascio, A., Silvestre, F., d'Ischia, M., Russo, G. L., Tosti, E., Branno, M., Palumbo, A., 2007. Regulatory roles of nitric oxide during larval development and metamorphosis in Ciona intestinalis. Dev Biol. 306, 772-84.

Conklin, E. G., 1932. The embryology of amphioxus. Journal of morphology. 54, 69-151.

Costa, O. G., 1834. Cenni zoologici ossia descrizione sommaria delle specie nuove di animali discoperti in diverse contrade del regno nell' anno 1834. Naples.

Courtney, W. A., The temperature relationships and age-structure of North Sea and Mediterranean populations of Branchiostoma lanceolatum. Symp zool Soc Lond, Vol. 36, 1975, pp. 213-233.

Crane, B. R., Sudhamsu, J., Patel, B. A., 2010. Bacterial nitric oxide synthases. Annu Rev Biochem. 79, 445-70.

Crawford, N. M., 2006. Mechanisms for nitric oxide synthesis in plants. J Exp Bot. 57, 471-8.

D'Aniello, S., Irimia, M., Maeso, I., Pascual-Anaya, J., Jimenez-Delgado, S., Bertrand, S., Garcia-Fernandez, J., 2008. Gene expansion and retention leads to a diverse tyrosine kinase superfamily in amphioxus. Mol Biol Evol. 25, 1841-54.

da Silva, L. F. B. d., Tavares, M., Soares-Gomes, A., 2008. Population structure of the lancelet Branchiostoma caribaeum (Cephalochordata: Branchiostomidae) in the Baìa de Guanabara, Rio de Janeiro, southeastern Brazil. Revista Brasileira de Zoologia. 25, 617-623.

Delsuc, F., Brinkmann, H., Chourrout, D., Philippe, H., 2006. Tunicates and not cephalochordates are the closest living relatives of vertebrates. Nature. 439, 965-8.

Desdevises, Y., Maillet, V., Fuentes, M., Escriva, H., 2011. A snapshot of the population structure of Branchiostoma lanceolatum in the Racou beach, France, during its spawning season. PLoS One. 6, 0018520.

Donald, J. A., Forgan, L. G., Cameron, M. S., 2015. The evolution of nitric oxide signalling in vertebrate blood vessels. Journal of Comparative Physiology B. 185, 153-171.

Donoghue, P. C., Purnell, M. A., 2009. Distinguishing heat from light in debate over controversial fossils. Bioessays. 31, 178-189.

Dzik, J., 1995. Yunnanozoon and the ancestry of chordates. Acta Palaeontologica Polonica. 40, 341-360.

Ericson, L., Fredriksson, G., Ofverholm, T., 1985. Ultrastructural localization of the iodination centre in the endostyle of the adult amphioxus (Branchiostoma lanceolatum). Cell and tissue research. 241, 267-273.

Fange, R., 2005. Discovery and early studies of the lancelet "Amphioxus". Sven Med Tidskr. 9, 83-93.

Feelisch, M., Martin, J. F., 1995. The early role of nitric oxide in evolution. Trends Ecol Evol. 10, 496-9.

Fehsel, K., Jalowy, A., Qi, S., Burkart, V., Hartmann, B., Kolb, H., 1993. Islet cell DNA is a target of inflammatory attack by nitric oxide. Diabetes. 42, 496-500.

Feinberg, T. E., Mallatt, J., 2013. The evolutionary and genetic origins of consciousness in the Cambrian Period over 500 million years ago. Frontiers in psychology. 4.

Ferrier, D., Brooke, N. M., Panopoulou, G., Holland, P., 2001. The Mnx homeobox gene class defined by HB9, MNR2 and amphioxus AmphiMnx. Development genes and evolution. 211, 103-107.

Foresi, N., Correa-Aragunde, N., Parisi, G., Calo, G., Salerno, G., Lamattina, L., 2010. Characterization of a nitric oxide synthase from the plant kingdom: NO generation from the green alga Ostreococcus tauri is light irradiance and growth phase dependent. Plant Cell. 22, 3816-30.

Förstermann, U., Closs, E. I., Pollock, J. S., Nakane, M., Schwarz, P., Gath, I., Kleinert, H., 1994. Nitric oxide synthase isozymes. Characterization, purification, molecular cloning, and functions. Hypertension. 23, 1121-31.

Förstermann, U., Sessa, W. C., 2012. Nitric oxide synthases: regulation and function.

Fredriksson, G., Ericson, L. E., Olsson, R., 1984. Iodine binding in the endostyle of larval Branchiostoma lanceolatum (Cephalochordata). General and Comparative Endocrinology. 56, 177-184.

Fuentes, M., Benito, E., Bertrand, S., Paris, M., Mignardot, A., Godoy, L., Jimenez-Delgado, S., Oliveri, D., Candiani, S., Hirsinger, E., D'Aniello, S., Pascual-Anaya, J., Maeso, I., Pestarino, M., Vernier, P., Nicolas, J. F., Schubert, M., Laudet, V., Geneviere, A. M., Albalat, R., Garcia Fernandez, J., Holland, N. D., Escriva, H., 2007. Insights into spawning behavior and development of the European amphioxus (Branchiostoma lanceolatum). J Exp Zool B Mol Dev Evol. 308, 484-93.

Fuentes, M., Schubert, M., Dalfo, D., Candiani, S., Benito, E., Gardenyes, J., Godoy, L., Moret, F., Illas, M., Patten, I., Permanyer, J., Oliveri, D., Boeuf, G., Falcon, J., Pestarino, M., Fernandez, J. G., Albalat, R., Laudet, V., Vernier, P., Escriva, H., 2004. Preliminary observations on the spawning conditions of the European amphioxus (Branchiostoma lanceolatum) in captivity. J Exp Zool B Mol Dev Evol. 302, 384-91.

Futch, C. R., Dwinell, S. E., 1977. Nearshore marine ecology at Hutchinson Island, Florida: 1971-1974: IV. lancelets and fishes.

Garcia-Fernandez, J., Benito-Gutierrez, E., 2009. It's a long way from amphioxus: descendants of the earliest chordate. Bioessays. 31, 665-75.

Garcia-Fernàndez, J., Jimènez-Delgado, S., Pascual-Anaya, J., Maeso, I., Irimia, M., Minguillòn, C., Benito-Gutièrrez, E., Gardenyes, J., Bertrand, S., D'Aniello, S., 2009. From the American to the European amphioxus: towards experimental Evo-Devo at the origin of chordates. International Journal of Developmental Biology. 53, 1359.

Gerstein, M., Zheng, D., 2006. The real life of pseudogenes. Scientific American. 295, 48-55.

Ghosh, D. K., Salerno, J. C., 2003. Nitric oxide synthases: domain structure and alignment in enzyme function and control. Front Biosci. 8, d193-209.

Godoy, L., Gonzàlez-Duarte, R., Albalat, R., 2006. S-nitrosogluthathione reductase activity of amphioxus ADH3: insights into the nitric oxide metabolism. International journal of biological sciences. 2, 117.

Gonzalez-Domenech, C. M., Munoz-Chapuli, R., 2010. Molecular evolution of nitric oxide synthases in metazoans. Comp Biochem Physiol Part D Genomics Proteomics. 5, 295-301.

Goretski, J., Hollocher, T. C., 1988. Trapping of nitric oxide produced during denitrification by extracellular hemoglobin. J Biol Chem. 263, 2316-23.

Gosselck, F., 1975. The distribution of Branchiostoma senegalense (Acrania, Branchiostomidae) in the off-shore shelf region off North West Africa. Internationale Revue der gesamten Hydrobiologie und Hydrographie. 60, 199-207.

Gosselck, F., Spittler, P., 1979. Age Structure, Growth, and Weight of Branchiostoma senegalense (Acrania, Branchiostomidae). off North-West Africa. Internationale Revue der gesamten Hydrobiologie und Hydrographie. 64, 541-550.

Gouge, R. C., Marshburn, P., Gordon, B. E., Nunley, W., Huet-Hudson, Y. M., 1998. Nitric oxide as a regulator of embryonic development. Biol Reprod. 58, 875-9.

Green, L. C., Wagner, D. A., Glogowski, J., Skipper, P. L., Wishnok, J. S., Tannenbaum, S. R., 1982. Analysis of nitrate, nitrite, and [15 N] nitrate in biological fluids. Analytical biochemistry. 126, 131-138.

Griffith, O. W., Kilbourn, R. G., 1996. Nitric oxide synthase inhibitors: amino acids. Methods in enzymology. 268, 375-392.

Griffith, O. W., Stuehr, D. J., 1995. Nitric oxide synthases: properties and catalytic mechanism. Annu Rev Physiol. 57, 707-36.

Gu, X., 1998. Early metazoan divergence was about 830 million years ago. J Mol Evol. 1998 Sep;47(3):369-71.

Haberling, W., 1924. Johannes Mùller: das Leben des rheinischen Naturforschers auf Grund neuer Quellen und seiner Briefe dargestellt. Akademische Verlagsgesellschaft.

Hatschek, B., 1893. The amphioxus and its development. Swan, Sonnenschein & Company.

Hecht, M., Wallace, B., Prance, G., Schaeffer, B., Deuterostome Monophyly and Phylogeny. Evolutionary Biology. Springer US, 1987, pp. 179-235.

Hecht, M. K., MacIntyre, R. J., Clegg, M. T., 1998. Evolutionary Biology. Springer US.

Hirakow, R., Kajita, N., 1994. Electron microscopic study of the development of amphioxus, Branchiostoma belcheri tsingtauense: the neurula and larva. Kaibogaku Zasshi. 69, 1-13.

Holland, L. Z., Albalat, R., Azumi, K., Benito-Gutièrrez, E., Blow, M. J., Bronner-Fraser, M., Brunet, F., Butts, T., Candiani, S., Dishaw, L. J., 2008. The amphioxus genome illuminates vertebrate origins and cephalochordate biology. Genome research. 18, 1100-1111.

Holland, L. Z., Holland, N. D., 1996. Expression of AmphiHox-1 and AmphiPax-1 in amphioxus embryos treated with retinoic acid: insights into evolution and patterning of the chordate nerve cord and pharynx. Development. 122, 1829-1838.

Holland, L. Z., Holland, N. D., 1999. Chordate origins of the vertebrate central nervous system. Current Opinion in Neurobiology. 9, 596-602.

Holland, L. Z., Holland, N. D., 2007. A revised fate map for amphioxus and the evolution of axial patterning in chordates. Integr Comp Biol. 47, 360-72.

Holland, L. Z., Onai, T., 2012. Early development of cephalochordates (amphioxus). Wiley Interdiscip Rev Dev Biol. 1, 167-83.

Holland, L. Z., Yu, J.-K., Charles A. Ettensohn, G. A. W., Gary, M. W., Cephalochordate (Amphioxus) Embryos: Procurement, Culture, and Basic Methods. Methods in Cell Biology, Vol. Volume 74. Academic Press, 2004, pp. 195-215.

Holland, N. D., Chen, J., 2001. Origin and early evolution of the vertebrates: new insights from advances in molecular biology, anatomy, and palaeontology. Bioessays. 23, 142-151.

Holland, N. D., Holland, L. Z., 2010. Laboratory spawning and development of the Bahama lancelet, Asymmetron lucayanum (cephalochordata): fertilization through feeding larvae. Biol Bull. 219, 132-41.

Holland, N. D., Paris, M., Koop, D., 2009. The club-shaped gland of amphioxus: export of secretion to the pharynx in pre-metamorphic larvae and apoptosis during metamorphosis. Acta Zoologica. 90, 372-379.

Holmqvist, B., Ellingsen, B., Alm, P., Forsell, J., Oyan, A.-M., Goksoyr, A., Fjose, A., Seo, H.-C., 2000. Identification and distribution of nitric oxide synthase in the brain of adult zebrafish. Neuroscience letters. 292, 119-122.

Holmqvist, B., Ellingsen, B., Forsell, J., Zhdanova, I., Alm, P., 2004. The early ontogeny of neuronal nitric oxide synthase systems in the zebrafish. Journal of experimental biology. 207, 923-935.

Hu, T.-M., Chiu, S.-J., Hsu, Y.-M., 2014. Nitroxidative chemistry interferes with fluorescent probe chemistry: Implications for nitric oxide detection using 2, 3-diaminonaphthalene. Biochemical and biophysical research communications. 451, 196-201.

Huelsenbeck, J. P., Ronquist, F., 2001. MRBAYES: Bayesian inference of phylogenetic trees. Bioinformatics. 17, 754-5.

Imai, J. H., Meinertzhagen, I. A., 2007a. Neurons of the ascidian larval nervous system in Ciona intestinalis: I. Central nervous system. The Journal of Comparative Neurology. 501, 316-334.

Imai, J. H., Meinertzhagen, I. A., 2007b. Neurons of the ascidian larval nervous system in Ciona intestinalis: II. Peripheral nervous system. The Journal of Comparative Neurology. 501, 335-352.

Imamura, M., Yang, J., Yamakawa, M., 2002. cDNA cloning, characterization and gene expression of nitric oxide synthase from the silkworm, Bombyx mori. Insect Mol Biol. 11, 257-65.

Jackman, W. R., Kimmel, C. B., 2002. Coincident iterated gene expression in the amphioxus neural tube. Evolution & Development. 4, 366-374.

Jackman, W. R., Langeland, J. A., Kimmel, C. B., 2000. Islet reveals segmentation in the Amphioxus hindbrain homolog. Developmental biology. 220, 16-26.

Janvier, P., 2003. Vertebrate characters and the Cambrian vertebrates. Comptes Rendus Palevol. 2, 523-531.

Jiang, Q., Zhou, Z., Wang, L., Wang, L., Yue, F., Wang, J., Song, L., 2013. A scallop nitric oxide synthase (NOS) with structure similar to neuronal NOS and its involvement in the immune defense. PLoS One. 8, e69158.

Kaji, T., Hoshino, Y., Henmi, Y., Yasui, K., 2013. Longitudinal Observation of Japanese Lancelet, Branchiostoma japonicum, Metamorphosis. Dataset Papers in Biology. 2013, 6.

Kaji, T., Shimizu, K., Artinger, K. B., Yasui, K., 2009. Dynamic modification of oral innervation during metamorphosis in Branchiostoma belcheri, the oriental lancelet. The Biological Bulletin. 217, 151-160.

Kan, L., Israsena, N., Zhang, Z., Hu, M., Zhao, L.-R., Jalali, A., Sahni, V., Kessler, J. A., 2004. Sox1 acts through multiple independent pathways to promote neurogenesis. Developmental biology. 269, 580-594.

Kellicott, W. E., 1913. Outlines of chordate development. H. Holt and Company.

Kim, P. K., Zamora, R., Petrosko, P., Billiar, T. R., 2001. The regulatory role of nitric oxide in apoptosis. International immunopharmacology. 1, 1421-1441.

Kishi, M., Mizuseki, K., Sasai, N., Yamazaki, H., Shiota, K., Nakanishi, S., Sasai, Y., 2000. Requirement of Sox2-mediated signaling for differentiation of early Xenopus neuroectoderm. Development. 127, 791-800.

Kojima, H., Urano, Y., Kikuchi, K., Higuchi, T., Hirata, Y., Nagano, T., 1999. Fluorescent indicators for imaging nitric oxide production. Angewandte Chemie International Edition. 38, 3209-3212.

Kon, T., Nohara, M., Yamanoue, Y., Fujiwara, Y., Nishida, M., Nishikawa, T., 2007. Phylogenetic position of a whale-fall lancelet (Cephalochordata) inferred from whole mitochondrial genome sequences. BMC Evolutionary Biology. 7, 127.

Koshland, D. E., Jr., 1992. Editorial: The Molecule of the Year. Science. 258, 1861.

Kovalevsky, A., 1867. On the development of Amphioxus lanceolatus. Journal of Natural History. 19, 69-70.

Kozmikova, I., Candiani, S., Fabian, P., Gurska, D., Kozmik, Z., 2013. Essential role of Bmp signaling and its positive feedback loop in the early cell fate evolution of chordates. Developmental biology. 382, 538-554.

Kuo, R. C., Baxter, G. T., Thompson, S. H., Stricker, S. A., Patton, C., Bonaventura, J., Epel, D., 2000. NO is necessary and sufficient for egg activation at fertilization. Nature. 406, 633-636.

Kuzin, B., Roberts, I., Peunova, N., Enikolopov, G., 1996. Nitric oxide regulates cell proliferation during Drosophila development. Cell. 87, 639-649.

Lacalli, T. C., 1996. Frontal eye circuitry, rostral sensory pathways and brain organization in amphioxus larvae: evidence from 3D reconstructions. Philosophical Transactions of the Royal Society B: Biological Sciences. 351, 243-263.

Lacalli, T. C., 2002. The dorsal compartment locomotory control system in amphioxus larvae. J Morphol. 252, 227-37.

Lacalli, T. C., 2006. Prospective protochordate homologs of vertebrate midbrain and MHB, with some thoughts on MHB origins. Int J Biol Sci. 2, 104-9.

Lacalli, T. C., Hou, S., 1999. A reexamination of the epithelial sensory cells of amphioxus (Branchiostoma). Acta Zoologica. 80, 125-134.

Lacalli, T. C., Kelly, S. J., 2000. The infundibular balance organ in amphioxus larvae and related aspects of cerebral vesicle organization. Acta Zoologica. 81, 37-47.

Lee, H. J., Zheng, J. J., 2010. PDZ domains and their binding partners: structure, specificity, and modification. Cell Commun Signal. 8, 8-8.

Leise, E. M., Thavaradhara, K., Durham, N. R., Turner, B. E., 2001. Serotonin and Nitric Oxide Regulate Metamorphosis in the Marine Snail Ilyanassa obsoleta. American Zoologist. 41, 258-267.

Lepiller, S., Laurens, V. r., Bouchot, A., Herbomel, P., Solary, E., Chluba, J., 2007. Imaging of nitric oxide in a living vertebrate using a diaminofluorescein probe. Free Radical Biology and Medicine. 43, 619-627.

Lin, Y., Chen, D., Zhang, W., Cai, Z., Chen, Z., Zhang, N., Mao, B., Zhang, H., 2011. Characterization of the immune defense related tissues, cells, and genes in amphioxus. Sci China Life Sci. 54, 999-1004.

Liu, Q., Gross, S. S., 1996. Binding sites of nitric oxide synthases. Methods Enzymol. 268, 311-24.

Mallatt, J., Chen, J. y., 2003. Fossil sister group of craniates: predicted and found. Journal of morphology. 258, 1-31.

Martínez-Ruiz, A., Lamas, S., 2009. Two decades of new concepts in nitric oxide signaling: From the discovery of a gas messenger to the mediation of nonenzymatic posttranslational modifications. IUBMB Life. 61, 91-98.

Meulemans, D., Bronner-Fraser, M., 2007. The amphioxus SoxB family: implications for the evolution of vertebrate placodes. International journal of biological sciences. 3, 356.

Miles, A. M., Wink, D. A., Cook, J. C., Grisham, M. B., 1996. Determination of nitric oxide using fluorescence spectroscopy. Methods in enzymology. 268, 105-120.

Moore, P., Al-Swayeh, O., Chong, N., Evans, R., Gibson, A., 1990. l-NG-nitro arginine (l-NOARG), a novel, l-arginine-reversible inhibitor of endothelium-dependent vasodilatation in vitro. British journal of pharmacology. 99, 408-412.

Moroz, L. L., Kohn, A. B., Bruno, T., Barry, T., On the comparative biology of Nitric Oxide (NO) synthetic pathways: Parallel evolution of NO-mediated signaling. Advances in Experimental Biology, Vol. Volume 1. Elsevier, 2007, pp. 1-44.

Morris, S. C., Caron, J. B., 2012. Pikaia gracilens Walcott, a stem-group chordate from the Middle Cambrian of British Columbia. Biological Reviews. 87, 480-512.

Moshage, H., KoK, B., Huizenga, J. R., Jansen, P., 1995. Nitrite and nitrate determinations in plasma: a critical evaluation. Clinical Chemistry. 41, 892-896.

Nelson, G., 1969. Amphioxus in old Tampa Bay, Florida. QJ Fl Acad Sci. 31, 93-100.

Nishida, C. R., Ortiz de Montellano, P. R., 1999. Autoinhibition of endothelial nitric-oxide synthase. Identification of an electron transfer control element. J Biol Chem. 274, 14692-8.

Ohno, S., 1970. Evolution by gene duplication. London: George Alien & Unwin Ltd. Berlin, Heidelberg and New York: Springer-Verlag.

Olsson, R., 1963. Endostyles and endostylar secretions: a comparative histochemical study. Acta Zoologica. 44, 299-328.

Pallas, P. S., 1774. Limax lanceolatus: descriptio Limacis lanceolaris. Spicilegia Zoologica, quibus novae imprimus et obscurae animalium species iconibus, descriptionibus. 10, 19.

Paris, M., Escriva, H., Schubert, M., Brunet, F. d. r., Brtko, J., Ciesielski, F., Roecklin, D., Vivat-Hannah, V. r., Jamin, E. L., Cravedi, J.-P., 2008. Amphioxus postembryonic development reveals the homology of chordate metamorphosis. Current Biology. 18, 825-830.

Paris, M., Hillenweck, A., Bertrand, S. p., Delous, G., Escriva, H., Zalko, D., Cravedi, J.-P., Laudet, V., 2010. Active metabolism of thyroid hormone during metamorphosis of amphioxus. Integrative and comparative biology. 50, 63-74.

Pascual-Anaya, J., Adachi, N., Alvarez, S., Kuratani, S., D'Aniello, S., Garcia-Fernàndez, J., 2012. Broken colinearity of the amphioxus Hox cluster. Evodevo. 3, 28.

Pascual-Anaya, J., D'Aniello, S., Garcia-Fernandez, J., 2008. Unexpectedly large number of conserved noncoding regions within the ancestral chordate Hox cluster. Dev Genes Evol. 218, 591-7.

Pascual-Anaya, J., D'Aniello, S., Kuratani, S., Garcia-Fernandez, J., 2013. Evolution of Hox gene clusters in deuterostomes. BMC Developmental Biology. 13, 26.

Peunova, N., Scheinker, V., Ravi, K., Enikolopov, G., 2007. Nitric oxide coordinates cell proliferation and cell movements during early development of Xenopus. Cell Cycle. 6, 3132-3144.

Piazza, M., Futrega, K., Spratt, D. E., Dieckmann, T., Guillemette, J. G., 2012. Structure and dynamics of calmodulin (CaM) bound to nitric oxide synthase peptides: effects of a phosphomimetic CaM mutation. Biochemistry. 51, 3651-61.

Pollock, V. P., McGettigan, J., Cabrero, P., Maudlin, I. M., Dow, J. A., Davies, S. A., 2004. Conservation of capa peptide-induced nitric oxide signalling in Diptera. J Exp Biol. 207, 4135-45.

Putnam, N. H., Butts, T., Ferrier, D. E. K., Furlong, R. F., Hellsten, U., Kawashima, T., Robinson-Rechavi, M., Shoguchi, E., Terry, A., Yu, J.-K., Benito-Gutierrez, E., Dubchak, I., Garcia-Fernandez, J., Gibson-Brown, J. J., Grigoriev, I. V., Horton, A. C., de Jong, P. J., Jurka, J., Kapitonov, V. V., Kohara, Y., Kuroki, Y., Lindquist, E., Lucas, S., Osoegawa, K., Pennacchio, L. A., Salamov, A. A., Satou, Y., Sauka-Spengler, T., Schmutz, J., Shin-I, T., Toyoda, A., Bronner-Fraser, M., Fujiyama, A., Holland, L. Z., Holland, P. W.

H., Satoh, N., Rokhsar, D. S., 2008. The amphioxus genome and the evolution of the chordate karyotype. Nature. 453, 1064-1071.

Rebrikov, D., Trofimov, D. Y., 2006. Real-time PCR: a review of approaches to data analysis. Applied Biochemistry and Microbiology. 42, 455-463.

Rees, D., Palmer, R., Schulz, R., Hodson, H., Moncada, S., 1990a. Characterization of three inhibitors of endothelial nitric oxide synthase in vitro and in vivo. British journal of pharmacology. 101, 746-752.

Rees, D. D., Schulz, R., Hodson, H. F., Palmer, R., Moncada, S., 1990b. Identification of some novel inhibitors of the vascular nitric oxide synthase in vivo and in vitro. Nitric oxide from L-arginine: a bioregulatory system. Elsevier, Amsterdam. 485-487.

Regehr, W. G., Carey, M. R., Best, A. R., 2009. Activity-Dependent Regulation of Synapses by Retrograde Messengers. Neuron. 63, 154-170.

Robinson, L. J., Michel, T., 1995. Mutagenesis of palmitoylation sites in endothelial nitric oxide synthase identifies a novel motif for dual acylation and subcellular targeting. Proc Natl Acad Sci U S A. 92, 11776-80.

Rodrigo, J., Springall, D., Uttenthal, O., Bentura, M., Abadia-Molina, F., Riveros-Moreno, V., Martinez-Murillo, R., Polak, J., Moncada, S., 1994. Localization of nitric oxide synthase in the adult rat brain. Philosophical Transactions of the Royal Society of London. Series B: Biological Sciences. 345, 175-221.

Ronquist, F., Huelsenbeck, J. P., 2003. MrBayes 3: Bayesian phylogenetic inference under mixed models. Bioinformatics. 19, 1572-4.

Schubert, M., Escriva, H., Xavier-Neto, J., Laudet, V., 2006. Amphioxus and tunicates as evolutionary model systems. Trends Ecol Evol. 21, 269-77.

Shu, D.-G., Morris, S. C., Han, J., Zhang, Z.-F., Yasui, K., Janvier, P., Chen, L., Zhang, X.-L., Liu, J.-N., Li, Y., 2003. Head and backbone of the Early Cambrian vertebrate Haikouichthys. Nature. 421, 526-529.

Shu, D., Zhang, X., Chen, L., 1996. Reinterpretation of Yunnanozoon as the earliest known hemichordate. Nature. 380, 428-430.

Snyder, S. H., Bredt, D. S., 1992. Biological roles of nitric oxide. Sci Am. 266, 68-71, 74-7.

SoRelle, R., 1998. Nobel Prize Awarded to Scientists for Nitric Oxide Discoveries. Circulation. 98, 2365-2366.

Stamler, J. S., Singel, D. J., Loscalzo, J., 1992. Biochemistry of Nitric Oxide and Its Redox-Activated Forms. Science. 258, 1898-1902.

Stokes, M., 1996. Larval settlement, post-settlement growth and secondary production of the Florida lancelet (= amphioxus) Branchiostoma floridae. Mar Ecol Prog Ser. 130, 71-84.

Stokes, M. D., Holland, N. D., 1995. Embryos and larvae of a lancelet, Branchiostoma floridae, from hatching through metamorphosis: growth in the laboratory and external morphology. Acta Zoologica. 76, 105-120.

Stricker, N. L., Christopherson, K. S., Yi, B. A., Schatz, P. J., Raab, R. W., Dawes, G., Bassett, D. E., Jr., Bredt, D. S., Li, M., 1997. PDZ domain of neuronal nitric oxide synthase recognizes novel C-terminal peptide sequences. Nat Biotechnol. 15, 336-42.

Sun, J., Zhang, X., Broderick, M., Fein, H., 2003. Measurement of nitric oxide production in biological systems by using Griess reaction assay. Sensors. 3, 276-284.

Takahashi, T., Holland, P. W., 2004. Amphioxus and ascidian Dmbx homeobox genes give clues to the vertebrate origins of midbrain development. Development. 131, 3285-94.

Takatori, N., Butts, T., Candiani, S., Pestarino, M., Ferrier, D. E., Saiga, H., Holland, P. W., 2008. Comprehensive survey and classification of homeobox genes in the genome of amphioxus, Branchiostoma floridae. Dev Genes Evol. 218, 579-90.

Tamura, K., Peterson, D., Peterson, N., Stecher, G., Nei, M., Kumar, S., 2011. MEGA5: molecular evolutionary genetics analysis using maximum likelihood, evolutionary distance, and maximum parsimony methods. Mol Biol Evol. 28, 2731-9.

Thompson, J. D., Higgins, D. G., Gibson, T. J., 1994. CLUSTAL W: improving the sensitivity of progressive multiple sequence alignment through sequence weighting, position-specific gap penalties and weight matrix choice. Nucleic acids research. 22, 4673-4680.

Titheradge, M., Hemmens, B., Mayer, B., Enzymology of Nitric Oxide Synthases. Nitric Oxide Protocols, Vol. 100. Humana Press, 1998, pp. 1-32.

Tung, T. C., U, S. C., Yeh, Y. F., 1961. Experimental studies on neural induction in Amphioxus. Shi Yan Sheng Wu Xue Bao. 7**,** 263-70.

Ulett, M. A., 2010. Kovalevsky, Alexander Onufrevitch. eLS.

Urata, M., Yamaguchi, N., Henmi, Y., Yasui, K., 2007. Larval development of the oriental lancelet, Branchiostoma belcheri, in laboratory mass culture. Zoolog Sci. 24**,** 787-97.

Vìtecek, J., Lojek, A., Valacchi, G., Kubala, L., 2012. Arginine-based inhibitors of nitric oxide synthase: therapeutic potential and challenges. Mediators of inflammation. 2012.

Wada, H., Garcia-Fernandez, J., Holland, P. W., 1999. Colinear and segmental expression of amphioxus Hox genes. Dev Biol. 213**,** 131-41.

Webb, J., 1971. Seasonal changes in the distribution of Branchiostoma lanceolatum (Pallas) at Helgoland. Vie et Milieu. 22**,** 827-839.

Webb, J. E., 1956a. A note on the lancelets of Singapore, with a description of a new species of Branchiostoma. Proceedings of the Zoological Society of London. 127**,** 119-123.

Webb, J. E., 1956b. On the populations of *Branchiostoma lanceolatum* and their relations with the west African Lancelets. Proceedings of the Zoological Society of London. 127**,** 125-140.

Webb, J. E., Hill, M. B., 1958. The Ecology of Lagos Lagoon. IV. On the Reactions of Branchiostoma nigeriense Webb to Its Environment.

Wells, M. M., 1926. Collecting amphioxus. Science. 64**,** 187-188.

Whittaker, J., 1997. Cephalochordates, the lancelets. Embryology: Constructing the Organism. 365-381.

Wicht, H., Lacalli, T. C., 2005. The nervous system of amphioxus: structure, development, and evolutionary significance. Canadian Journal of Zoology. 83**,** 122-150.

Wickstead, J. H., Bone, Q., 1959. Ecology of Acraniate Larvae. Nature. 184**,** 1849-1851.

Williams, N. A., Holland, P., 1996. Old head on young shoulders. Nature. 383**,** 490-490.

Wink, D. A., Kasprzak, K. S., Maragos, C. M., Elespuru, R. K., Misra, M., Dunams, T. M., Cebula, T. A., Koch, W. H., Andrews, A. W., Allen, J. S., et al., 1991. DNA deaminating ability and genotoxicity of nitric oxide and its progenitors. Science. 254, 1001-3.

Wlllcy, A., 1891. The later larval development of amphioxus. Quarterly Journal of Microscopical Science. 32, 183.

Wray, G. A., Levinton, J. S., Shapiro, L. H., 1996. Molecular Evidence for Deep Precambrian Divergences Among Metazoan Phyla. Science. 274, 568-573.

Wu, X.-H., Zhang, S.-C., Wang, Y.-Y., Zhang, B.-L., Qu, Y.-M., Jiang, X.-J., 1994. Laboratory observation on spawning, fecundity and larval development of amphioxus (Branchiostoma belcheri tsingtaunese). Chinese Journal of Oceanology and Limnology. 12, 289-294.

Xu, L., Yuan, S., Li, J., Ruan, J., Huang, S., Yang, M., Huang, H., Chen, S., Ren, Z., Xu, A., 2011. The conservation and uniqueness of the caspase family in the basal chordate, amphioxus. BMC biology. 9, 60.

Yarrell, W., 1841. A history of British fishes. John Van Voorst.

Yu, J. S., Holland, L. Z., 2009. Cephalochordates (amphioxus or lancelets): a model for understanding the evolution of chordate characters. Cold Spring Harbor Protocols. 2009, pdb. emo130.

Yue, J. X., Yu, J. K., Putnam, N. H., Holland, L. Z., 2014. The transcriptome of an amphioxus, Asymmetron lucayanum, from the Bahamas: a window into chordate evolution. Genome Biol Evol. 6, 2681-96.

Zhou, L., Zhu, D. Y., 2009. Neuronal nitric oxide synthase: structure, subcellular localization, regulation, and clinical implications. Nitric Oxide. 20, 223-30.